Dynamic Polydimethylsiloxane based Polymer Composites for Functional Materials

Dissertation

zur Erlangung des Grades

des Doktors der Naturwissenschaften

der Naturwissenschaftlich-Technischen Fakultät

der Universität des Saarlandes

von

Xiaozhuang Zhou

Saarbrücken

2020

Tag des Kolloquiums: 08. 10. 2020

Dekan: Prof. Dr. Guido Kickelbick

Berichterstatter:

Prof. Dr. Aránzazu del Campo Bécares

Prof. Dr. -Ing. Markus Gallei

Vorsitz: Prof. Dr. David Scheschkewitz

Akad. Mitarbeiter: Dr. Lola González-García

Dynamic Polydimethylsiloxane based Polymer Composites for Functional Materials

Xiaozhuang Zhou

geb. in Anqing, China

DISSERTATION

INM-Leibniz Institut für neue Materialien, Saarbrücken

《面朝大海，春暖花开》

作者:海子

从明天起，做一个幸福的人

喂马，劈柴，周游世界

从明天起，关心粮食和蔬菜

我有一所房子，面朝大海，春暖花开

从明天起，和每一个亲人通信

告诉他们我的幸福

那幸福的闪电告诉我的

我将告诉每一个人

给每一条河每一座山取一个温暖的名字

陌生人，我也为你祝福

愿你有一个灿烂的前程

愿你有情人终成眷属

愿你在尘世获得幸福

我只愿面朝大海，春暖花开

Acknowledgments

Nothing can compare with the family in the world, and I would like to first express my love and thanks to my family members, especially to my father and mother, father-in-law, and mother-in-law for shouldering my responsibility all the time. I would like to thank my beautiful and gentle wife for her continuous efforts, especially for giving birth to my lovely son. Thanks to my brother, sister, and sister-in-law for the encouragement all the time when I felt frustrated.

Without proper sculpture, a stone will never be an artwork. And without proper instruction and guidance, a student could not become a doctor. Thank Dr. Jiaxi Cui for offering the opportunity to study in the Switchable Microfluidic group and this means a lot for one layman to cross the door. During a 4-year study, I would thank for his guidance to be a pure scientist and I will continue to work in the way that you taught me.

As a Chinese old saying that friends are like the brothers and sisters when you are away from home. For me, the Switchable Microfluidic group is like a family and all the lab members are my brothers and sisters. Dr. Huaixia Zhao is my elder sister that help me to grow up during the last four years. I must say that I have changed a lot in the talking and thinking way under her impression. Mostly, I have grown from a naive boy to be a mature man, though this is mainly attributed to the time. Thank to Dr. Baiju Krishnan, Mr. Guoqiang Ma, and Ms. Li Zhang for the cooperation. It was a pleasant time to work with you due to your working enthusiasm and inclusive characters.

Also, many thanks for Dr. Lizbeth Ofelia Prieto López and Dr. Dan Yu for your instructions when I felt confused since both you are wise people. I could always get

inspiration by talking with you. However, I hope I could have less this kind of talking with you, meaning l will feel less confused in the future.

Thanks to all group members for spending this wonderful four years with you. I wish you all the best in the future.

Abstract

Polymer networks with dynamic covalent bonds show properties and functions not achievable with covalently crosslinked systems. Among of the different polymers connected by dynamic covalent bonds, this Thesis is based on polydimethylsiloxane (PDMS) elastomers prepared via acid-catalyzed ring-opening polymerization of cyclic monomer and cross-link. This reaction presents different dynamic equilibrium reactions, such as polymer-oligomer equilibrium and bond exchange reaction. In this Thesis, I have developed three different functional materials based on acid-catalyzed PDMS. In **Chapter 1**, the basic concepts of dynamic bond chemistry and the state-of-the-art of dynamic covalent polymer networks are described. In **Chapter 2**, a new PDMS-based elastomer that can self-grow and self-degrow is presented. **Chapter 3** describes how the acid-catalyzed PDMS was used to fabricate a strain sensor that could flexibly post-tailor the sensor properties. In the last part (**Chapter 4**), a gas-flow enhanced relaxation behavior observed in CB/dPDMS composite is described.

Zusammenfassung

Polymernetzwerke mit dynamischen kovalenten Bindungen zeigen besondere Eigenschaften und Funktionen, die mit kovalent vernetzten Systemen nicht erreichbar sind. Diese Arbeit befasst sich mit Polydimethylsiloxan (PDMS) -Elastomeren, die durch säurekatalysierte Ringöffnungspolymerisation von cyclischem Monomer und Quervernetzung hergestellt werden. In dieser Reaktion sind verschiedene dynamische Gleichgewichte beteiligt z.B. das Polymer-Oligomer-Gleichgewicht und die Bindungsaustauschreaktion. In dieser Arbeit wurden drei verschiedene funktionelle Materialien auf der Basis von säurekatalysiertem PDMS entwickelt. In **Kapitel 1** werden die Grundkonzepte der dynamischen Bindungschemie und der Stand der Technik dynamischer kovalenter Polymernetzwerke beschrieben. In **Kapitel 2** wird ein neues PDMS-basiertes Elastomer vorgestellt, das Selbstwachstum und Selbstabbau zeigt. **Kapitel 3** beschreibt, wie ein säurekatalysierte PDMS verwendet wurde, um einen Dehnungssensor herzustellen, dessen Sensoreigenschaften nachträglich flexibel anpassbar sind. Im letzten Teil (**Kapitel 4**) wird eine Verbesserung des Relaxationsverhaltens durch einen Gasfluss beschrieben, das in CB/dPDMS-Verbundwerkstoffen beobachtet wird.

Contents

Motivation and Scope of this Thesis

Introducing dynamic covalent bonds into polymer materials has become an indispensable approach to fabricate functional materials, such as intrinsic self-healable materials, solid-state recyclable materials, and controlled degradable materials. All of these characteristics and functionalities are impossible to achieve with covalent polymers, but become possible by introducing dynamic covalent bonds in the polymer chains, owing to their reversible breaking and reforming property. The development of dynamic covalent polymer materials has shed the possibility for the real application on the industrial scale. However, the methodologies proposed for their commercialization still need to overcome some major challenges, for example, the lower mechanical properties compared with the typical covalent-bond crosslinked polymers imposed by lower bonding energy from most reversible bonds. It is believed that polymer scientists and manufacturing industries will be more confident in promoting the dynamic covalent polymers if more and more examples of functional materials and advanced manufacturing process technologies based on dynamic covalent bonds are put in practice. Therefore, the pursuit of functional materials based on dynamic covalent chemistry is still necessary.

Silicone rubber has broad applications in diverse fields such as construction and restoration, electronics, aviation, and healthcare.[1-10] However, functional materials based on dynamic Si-O bonds are scarcely reported in the literature, except for the self-healing ability. Considering the importance of the silicone rubber in polymeric materials, it is truly believed developing functional materials based on dynamic Si-O bonds would not only broaden the current applications of silicone rubber but also

enrich the current proof-of-concept application of dynamic covalent polymers that could promote the commercialization of dynamic covalent polymer materials; and these are the inspirations for the research work completed in this thesis. Herein, functional materials based on dynamic Si-O bonds will be investigated in this Thesis.

The fundamentals of dynamic covalent chemistry and the current functional materials from the dynamic covalent chemistry are reviewed in **Chapter 1**. Also, the equilibrium reactions in the acid-catalyzed ring-opening polymerization of cyclodimethylsiloxane and the functional materials made from the dynamic Si-O bonds are introduced. In **Chapter 2**, a bio-inspired polymeric material based on dynamic PDMS with self-adaptive, self-growing and de-growing properties is presented. These materials could decrease the sizes when the oligomers are evaporated (self-degrow) and increase the sizes when the nutrients are given (self-grow). During the self-degrowing and self-growing processes, the size, shape, structure, mechanical property, optical property, and surface topography could be flexibly programmed. In **Chapter 3**, an on-demand strain sensor was prepared using a mechano-force to alter the sensor property. These conductive dynamic PDMS composites could be used as strain sensors at the high strain rates due to their solid-like behavior; while at the low strain rates, the polymer matrix retained its liquid-like behavior allowing the rearrangement of the conductive fillers within the matrix. In **Chapter 4**, the gas-flow responsive character of the dynamic PDMS composites was reported. The presence of a gas-flow accelerated the Si-O bond exchange and the mechanism for this phenomenon was investigated.

Chapter 1

1. Background and Introduction

Polymer materials containing dynamic covalent bonds (DCBs) constitute an emerging research field. DBCs have endowed materials with unprecedented properties and expand material applications beyond the scope of traditional polymers.[11] For example, the rapid growth of the polymer industry leads to the urgency for recycling due to their harm to the environment. It is easy to reprocess and reshape thermoplastics at elevated temperatures since the polymer chains are connected by physical intermolecular interactions. However, recycling thermosets for making new products is difficult since they are intractable when the shapes are permanently defined by the covalently crosslinked three-dimensional polymer networks.[12] The traditional strategy that depolymerizes at high temperatures is environmentally unfriendly and energy-intensive. Incorporation of DCBs into polymer could ease the recycling of thermosets at mild conditions by reversibly breaking and reforming the covalent bonds. Instead of simply breaking and reforming the dynamic covalent bonds, currently, scientists are also paying attention to the equilibrium nature of such processes. The equilibrium nature of the dynamic covalent bonds allows the polymer network to rearrange the topology while maintaining the integrity of a three-dimensional architecture, which

could be used for the intrinsic self-healing materials and shape-shifting materials.

In this introductory chapter, examples of different kinds of dynamic covalent bonds and the corresponding synthesis methods were first introduced. Then, functional polymeric materials containing dynamic covalent bonds were summarized. At last, dynamic Si-O equilibrium reactions initiated by acid and the functional materials made from the Si-O equilibrium reactions were introduced.

1.1 Dynamic Covalent Bonds

Dynamic covalent bonds are reversible covalent bonds that can break and reform in response to stimuli. They are normally stable at the ambient condition but display dynamic property under stimuli via the bond exchange. Generally speaking, the exchange of dynamic covalent bonds occurs by either associative or dissociative pathways.[11, 13-15] In a dissociative pathway, chemical bonds first break and then reform at other sites (**Fig.1A**), whereas, in an associative pathway, the breaking of a chemical bond and the reforming of a new chemical bond happen at the same time (**Fig.1B**). In the following parts, dynamic covalent bonds will be introduced according to the exchange mechanisms, e.g. associative dynamic covalent bonds or dissociative dynamic covalent bonds.

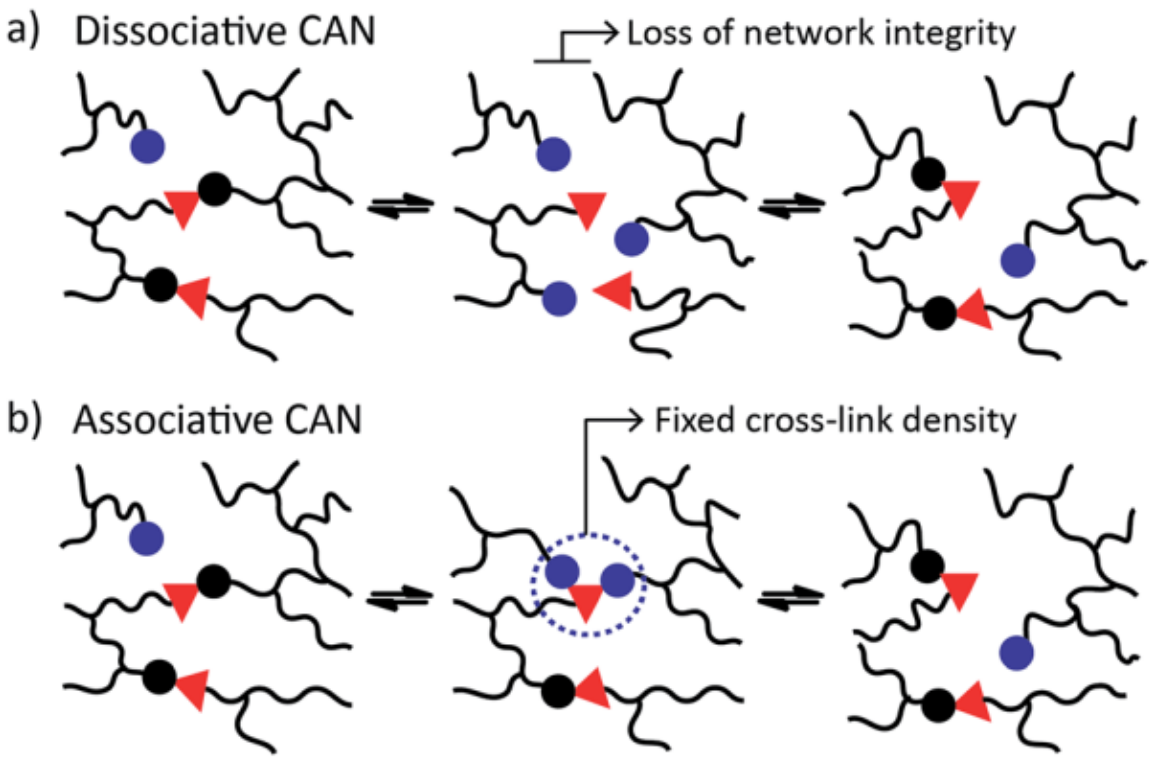

Figure 1. Different categories of covalent adaptable networks (CANs) based on the bond exchange mechanisms. **a)** Dissociative CANs. **b)** Associative CANs. Adapted with permission from respective publisher.[15]

1.1.1 Associative Dynamic Covalent Bonds

Associative dynamic covalent bonds break and reform covalent bonds concurrently, meaning that the cross-link density remains constant. Examples of this kind of dynamic covalent bonds include dynamic S-S bond, C-O bond, C=C, and C-N bonds.[16]

1.1.1.1 Dynamic S-S Bonds

The research of dynamic S-S bonds could date back to early 1940s when Tobolsky observed the stress-relaxation in polysulfide rubbers and they attributed the phenomenon to the disulfide interchange in the presence of a catalyst.[17] Nowadays, it has been shown that disulfide bonds can undergo exchange under different kinds of

stimuli, such as heat, light or external radicals. It has constituted a powerful building block to design various dynamic bonded polymer networks. For example, Norvez et. al prepared a thermal malleable epoxidized natural rubber by using the dithiodibutyric acid (DTDB) as the cross-link (**Figure 2a**).[18] In this way, the natural rubber can reshape at higher temperatures (above 150 ^{o}C) because of the disulfide exchange. Takahara et. al investigated the dynamic behavior of the disulfide bonds via the photoirradiation of a disulfide-containing polyester (DSPES) (**Figure 2b**).[19] Bowman and Anseth fabricated thiol functionalized poly(ethylene glycol) hydrogels, which can self-heal by introducing external radicals (**Figure 2c**).[20] After being synthesized, the hydrogels are swollen in a solution containing lithium acylphosphinate (LAP), which generates radicals upon exposure to light. The generated radicals cleave the disulfide bonds, producing the thiyl radicals. The thiyl radicals allow the exchange of the disulfide bonds and the self-healing property is achieved if the concentrations of thiyl radicals are appropriate.

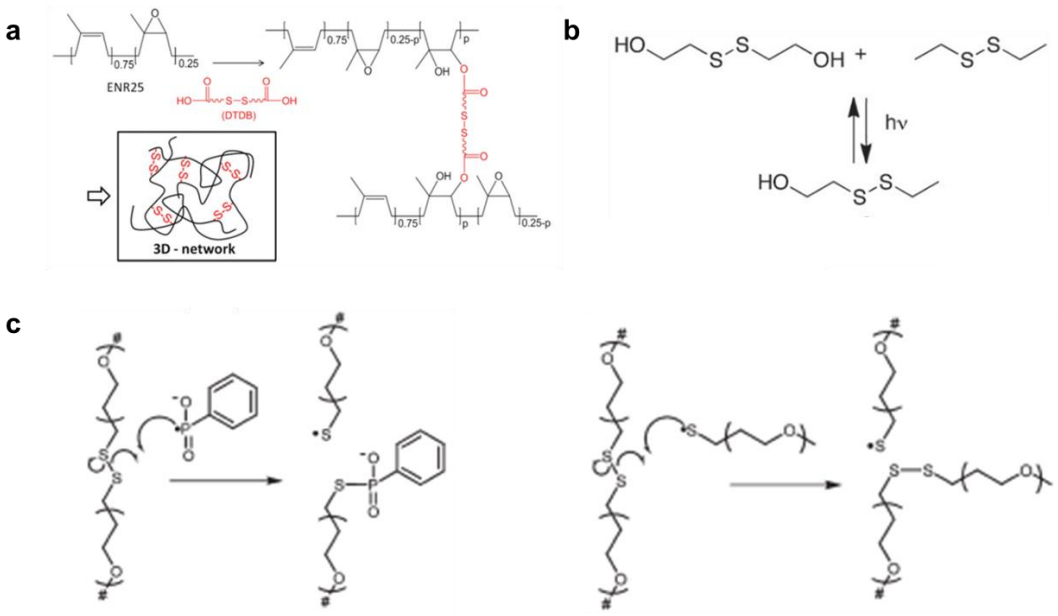

Figure 2. Dynamic disulfide bonds under different kinds of external stimuli. **a)** Heat, **b)** Light, **c)** Radicals. Adapted with permission from respective publisher.[18-20]

In addition to dynamic disulfide bonds, other sulfur derivatives have demonstrated the potential for designing dynamic materials, such as an allyl sulfide-based addition-fragmentation reaction. For example, Bowman et. al have shown the possible rearrangement of materials without any concomitant change in their properties by using alternative radical cleavage and reforming; during these processes, the topology of the network is reconfigured while the polymer chemistry and network connectivity remain unchanged (**Figure 3a**).[21] The radicals are introduced by photoinitiators and transferred by the reversible addition-fragmentation reaction (allyl sulfides). Though the excellent material plasticity achieved in this system, a major drawback in the synthesis is the requirement of external initiators to provide the starting radicals. The radicals could be easily annihilated and this means that the external photoinitiators were depleted continuously when the system is exposed to light to provide new starting radicals to reorganize the polymer network. Repeatedly reorganization of the polymer network would be a challenge because the photoinitiaotrs would be completely depleted. To improve the system, Matyjaszewski utilized trithiocarbonate (TTC, **Figure 3b**) to replace allyl sulfide since TTC could simultaneously work as the internal radical source and chain shuffling agent, which allows the repeated shuffling.[22] Despite the progress, the TTC system has the disadvantage of requiring an inert atmosphere or solvent since the radicals are easy to die in addition of requiring UV light which is harmful to the environment. Therefore, to further improve the system, Matyjaszewski and co-workers replaced the TTC with thiuram disulfide (TDS, **Figure 3c**). The TDS system containing disulfide bonds exhibites better bond-exchange ability under visible light even in the presence of oxygen.[23]

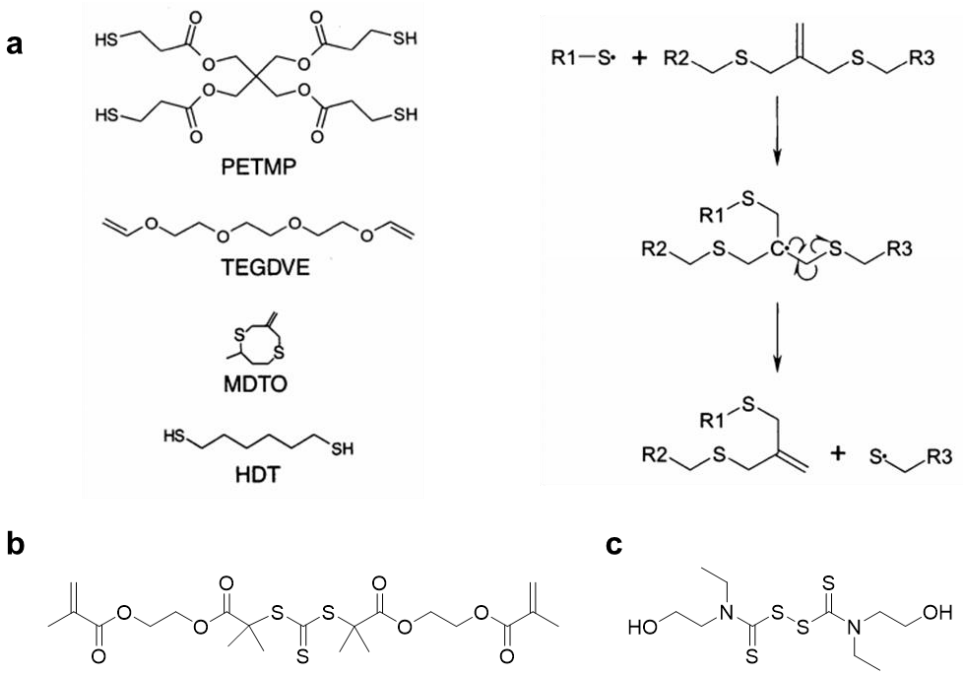

Figure 3. a) Allyl sulfide based network synthesis via thiol-ene chemistry and exchange of allyl sulfide derived from dithiacylooctane. **b)** TTC cross-link, **c)** TDS cross-link. Adapted with permission from respective publisher.[21-23]

1.1.1.2 Dynamic C-O Bonds

1 Transesterification

In 2011, Leibler and co-workers pioneered the dynamic covalent materials for recycling and reprocessing epoxy-based polyester.[24] They utilized the diglycidyl ether of bisphenol A (DGEBA) and a mixture of fatty dicarboxylic and tricarboxylic acids as the monomers, which could copolymerize with zinc acetate [$Zn(ac)_2$] as the catalyst. The resulting polymer behaves like a traditional epoxy but could flow like the liquid at high temperature (150 ^oC), due to the transesterification reaction. The viscosity of the system above the viscous flow temperature T_f shows a broad Arrhenius-like variation, similar to silica glass. They termed this kind of material as “Vitrimer” with the feature that is insoluble in a good, non-reactive solvent. By using the dynamic covalent

chemistry (transesterification), they achieved the rearrangement of the polymer network at the solid-state **(Figure 4a**).

Regardless of the great impact of vitrimer on polymer chemistry, the requirements of β-hydroxyl esters and external catalysts limit their application. In the past several years, vitrimers based on transesterifications have been widely improved, not only in terms of the transesterification chemistry but also of the catalysts. For example, both Xie and Hillmyer's groups suggested that ample hydroxyl groups are not necessary for the transesterification, which highly broadens the potential applications.[25, 26] As for the catalysts, various catalysts including organic bases compatible with polymer matrix were reported effective for the transesterification.[27] Recently, an interesting work by Du Prez reported that the neighboring group participation speed up the transesterification greatly, which could, in turn, be used as an internal catalyst.[28]

2 Transcarbamoylation

Due to the great success of vitrimer in recycling and reprocessing thermoset materials, scientists searched to expand the vitrimer concept to other dynamic covalent bonds. For example, Cramer and Hillmyer reported a polyhydroxyurethanes (PHUs) vitrimer using the transcarbamoylation chemistry.[29] Cross-linked PHUs prepared from the reaction of bis (cyclic carbonate) and triamines can be reprocessed at elevated temperature without external catalysts (**Figure 4b**). However, the hydroxyl groups are necessary for the transcarbamoylation. Later on, Xie's group demonstrated rapid transcarbamoylation in the absence of the hydroxyl groups. The polyurethane network synthesized from hexamethylene diisocyanate and glycerol in the presence of a catalyst could fully relax and reorganize within twenty minutes at 130 ^{o}C (**Figure 4c**).[30]

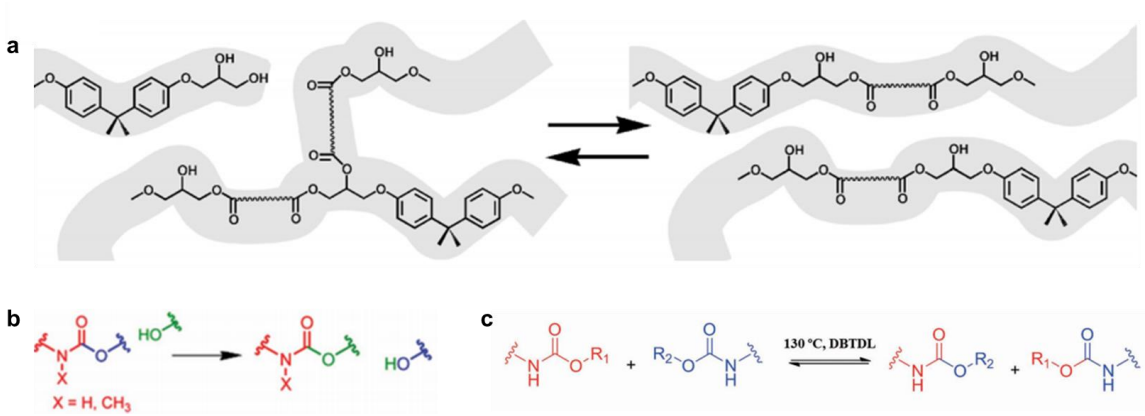

Figure 4. Associative dynamic C-O bonds. **a)** Transesterification based on *β*-hydroxyl ester. **b)** Hydroxyl mediated transcarbamoylation. **c)** Non-hydroxyl mediated transcarbamoylation. Adapted with permission from respective publisher.[29, 30]

1.1.1.3 Dynamic C=C

Due to the wide presence of carbon-carbon bonds in polymeric materials, it is of interest to exploit the dynamic properties of carbon-carbon bonds. However, carbon-carbon bonds are normally highly stable, which is difficult to be dynamic. Though chemists have designed some specific molecular structures, such as the vinylogous urethane or Diels-Alder cycloaddition to solve the issue, specifically designed polymers and high input external energy are generally required to trigger the dynamic character of carbon-carbon bonds. In order to produce the self-healing at ambient conditions of polymers containing carbon-carbon bonds without specific molecular design, Guan's group introduced one simple strategy employing the transition-metal-catalyzed olefin metathesis for reversible C-C double bond exchange. By introducing a very low level of Grubb's second-generation Ru metathesis catalyst into a readily crosslinked polybutadiene (PBD), the materials could self-heal efficiently under mild conditions (**Figure 5**).[31, 32] This strategy could be a powerful approach for designing self-healing materials given the effective polymer network reconfiguration efficiency

under the mild conditions as well as the abundance choice of the olefin-containing polymers.

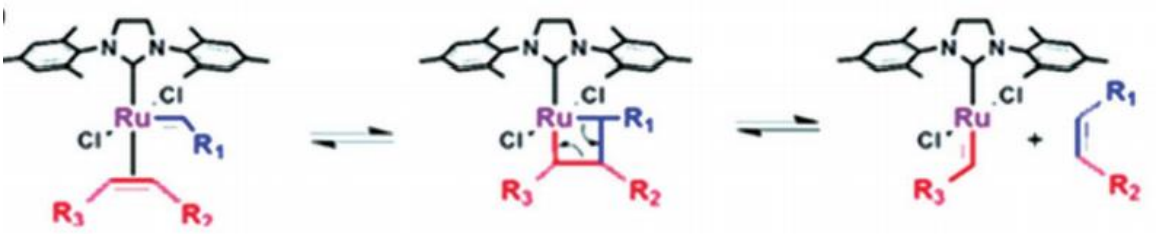

Figure 5. Associative dynamic C=C bonds in the presence of catalyst. Adapted with permission from respective publisher.[32]

1.1.1.4 Dynamic C-N Bonds

1 Transamination

Transamination is a chemical reaction in which amide reacts with amine to generate a new amide and amine. The reaction is typically slow since amides are much less reactive than esters, and transamination can only be carried out by air- and moisture-sensitive catalysts that are also incompatible with many other functional groups. However, compared to esters, polyamides require an easier synthesis and are less susceptible to hydrolysis since amide groups are thermodynamically favored, which could offer new applications for vitrimer materials. In order to take the advantages and avoid the disadvantages, Du Prez et al replaced amide groups by vinylogous amide groups to fabricate the dynamic polymers.[33-35] The resulting vinylogous urethane vitrimer maintains the thermodynamic and hydrolytic stability of amides advantages while they are more susceptible to bond exchange through the facile conjugate nucleophilic addition of an amine group at the elevated temperature. For example, dynamic vinylogous urethane network prepared from the condensation of bisacetoacetates, diamines, and triamines can be reprocessed at 170 ^{o}C within 85s

without any catalyst (**Figure 6a**). The bond exchange kinetics could also be influenced by the combination of various additives.[36] The availability of free amines is crucial to a fast reorganization process.

2 Transalkylation

Montarnal and Drockenmuller et al prepared the first conductive vitrimer based on poly(1,2,3-trizonium) ion liquids (PTILs).[37] The PTILs are obtained easily via one-step polyaddition of α-azide-ω-alkyne monomer and simultaneous alkylation of the resulting poly(1,2,3-triazole)s with difunctional 1,6-dibromohexane as cross-linkers in the absence of solvent and catalysts. The conductive vitrimer can be reprocessed by the transalkylation of C-N bonds between the 1,2,3-triazolium crosslinks and the halide-functionalized dangling chains (**Figure 6b**). The recycling of the polymers is possible with an appropriate solvent such as 1-bromopentane, in which they could be completely dissolved because of the displacement of transalkylation equilibrium. Functionalized vitrimers have significant potential applications in batteries, supercapacitors, or membranes for fuel cells and CO_2 recovery, applications where the excellent mechanical properties and facile processing of solid electrolytes are required.

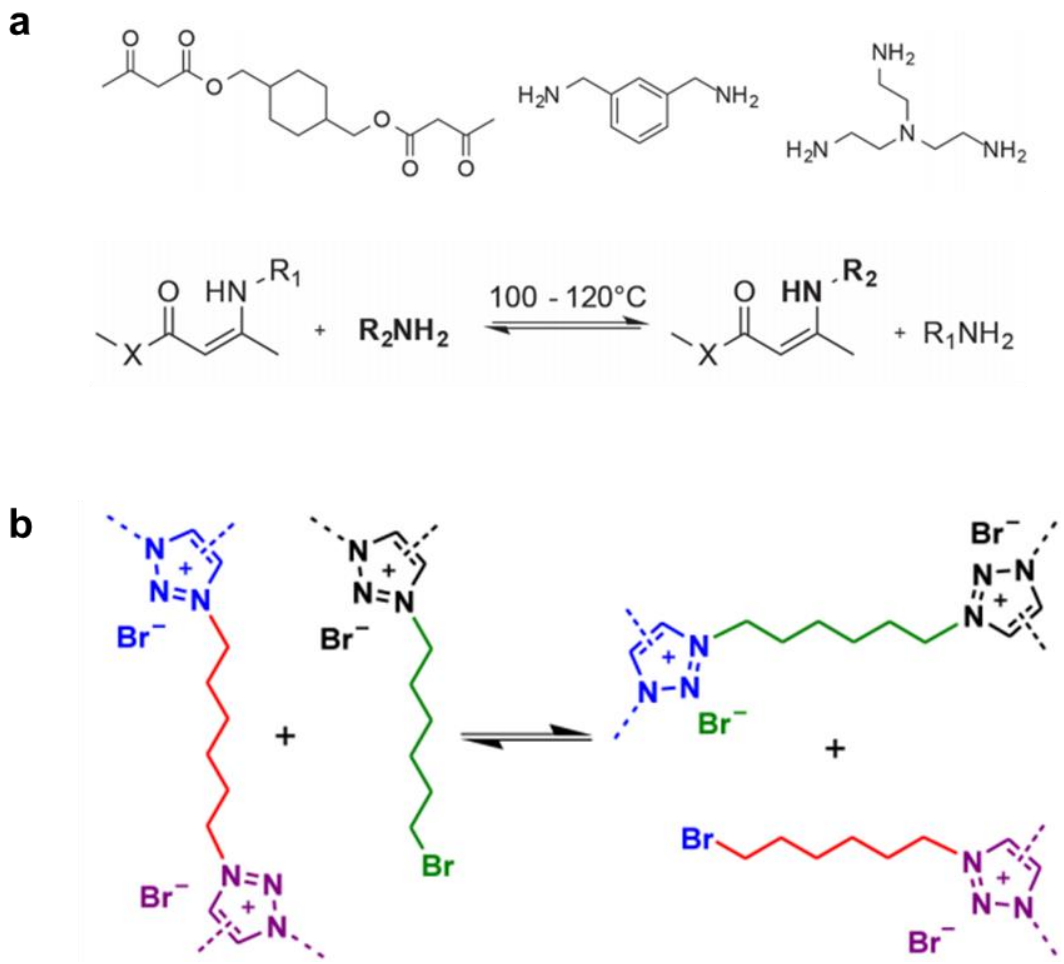

Figure 6. Associative dynamic C-N bonds. **a)** Synthesis of crosslinked poly(vinylogou urethane) and transamidation of PHU. **b)** Transalkylation of poly(1,2,3-trizonium ion liquid)s. Adapted with permission from the respective publisher.[36, 37]

1.1.2 Dissociative Dynamic Covalent Bonds

Dissociative dynamic covalent bonds first break the chemical bonds at a specific condition and then form new chemical bonds under another different stimulus. The polymer network will lose integrity during the breaking and reforming process.

1.1.2.1 Diels-Alder Reaction based Dynamic Covalent Bonds

Dynamic covalent bond based on DA (Diels-Alder) chemistry is one of the typical dissociative dynamic covalent bonds. The research of DA chemistry could date back

to 1928 and since then it has been one of the most powerful tools in organic chemistry.[38-40] The classical DA reaction is the [4+2] adduction reaction between conjugated diene (e.g. furan) and substituted alkene (termed dienophile, e.g. maleimide) to form the substituted cyclohexene derivatives. The DA reactions are reversible, and the typical stimuli to trigger the equilibrium between the reagents and adducts is temperature. To be specific, the equilibrium lies far towards adducts at a lower temperature while towards the reactants at a higher temperature (retro-DA reaction). Despite the long history of the DA reaction, it was until 2002 that Wudl et al. first employed the DA reaction for self-healing materials.[41] They used multi-furan and multi-maleimide to prepare a polymeric material, which could be fully polymerized at 75 ^{o}C for 3h (**Figure 7**). The re-mendability is accomplished via the retro-DA reaction at higher temperatures (120 ^{o}C-150 ^{o}C) and subsequent cooling. Though the viscosity of this polymer also follows the Arrhenius-law, it is a dissociative dynamic exchange. Since the first paper in 2002, the DA reaction has been extended to different kinds of re-mendable materials, such as epoxy resin,[42] polycaprolactone,[43] polyurethane,[44] polyketones[45] and so on.

Except for the diene and dienophile, reactants containing carbonyls and imines can be also applied to heterocycle DA reactions.[46] The normally heterocycle DA reactions include aza-DA reactions that convert imines and dienes to tetrahydropyridines; oxo DA reactions that convert aldehyde and diene into dihydropyran ring; and imine DA reactions that replace dienophiles as imines. One of the interesting examples of the heterocycle DA reaction was reported by Du Prez et al, in which 1,2,4-triazoline-3,5-dione (TAD) molecule was employed as an alternative dienophile.[47] Although DA reactions between TAD and dienes could proceed very quickly even at room

temperature, the retro-DA reaction ability is lost. However, replacing dienes with indoles to react with TAD, could again enable a reversible reaction and give a TAD-indole adduct. Also, the addition of a diene to this reversible TAD-indole adduct would result in a new and irreversible click reaction with the formation of a new Diels–Alder adduct. The introduction of such unique dynamic chemistry (TAD-indole reaction) to polyurethane and polymethacrylate materials allows the self-healing, reshaping, and recycling of polymeric materials.

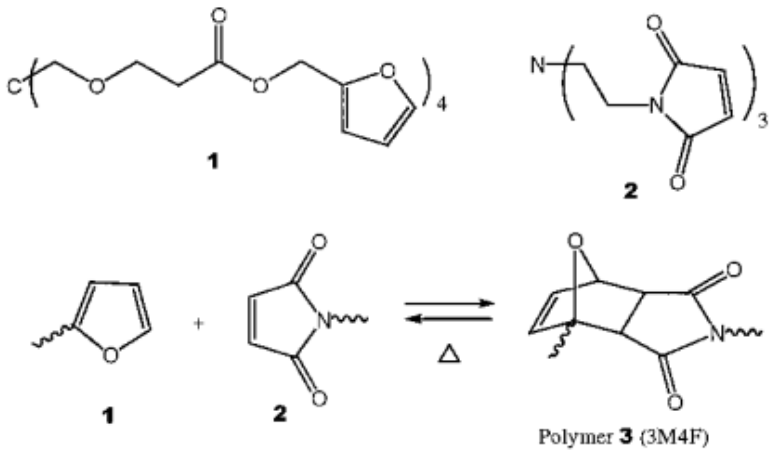

Figure 7. Diels-Alder reaction and retro-DA for multi-furan and multi-maleimide system. Reproduced with permission.[41]

1.1.2.2 Dynamic C-N bond

Chen's group reported one type of dynamic hindered urea bonds that could reversibly break and reform according to the equilibrium between isocyanate, bulky amines, and corresponding urea bonds (**Figure 8)**.[48] Isocyanate and amines could form the urea bonds and the urea bonds could also dissociate into isocyanate and amines. In the paper, they pointed out that the reversible dissociation of urea bonds is attributed to the bulky substituent of a urea bond on the nitrogen atom as it can weaken the carbonyl-amine interactions. The resulting polymer materials bearing the dynamic

hindered urea bonds are malleable and recyclable, and the conditions required to trigger the dynamic property of the materials are related to the substituents. For example, 1-(tert-butyl)-1-ethylurea (TBEU) substituted poly(urea-urethane), has been shown suitable for making dynamic polymers even at room temperature without catalysts, while 2-(tertbutylamino)ethanol (TBAE) substituted poly(urea-urethane) can be malleable only at a higher temperature (> 100 °C).[49]

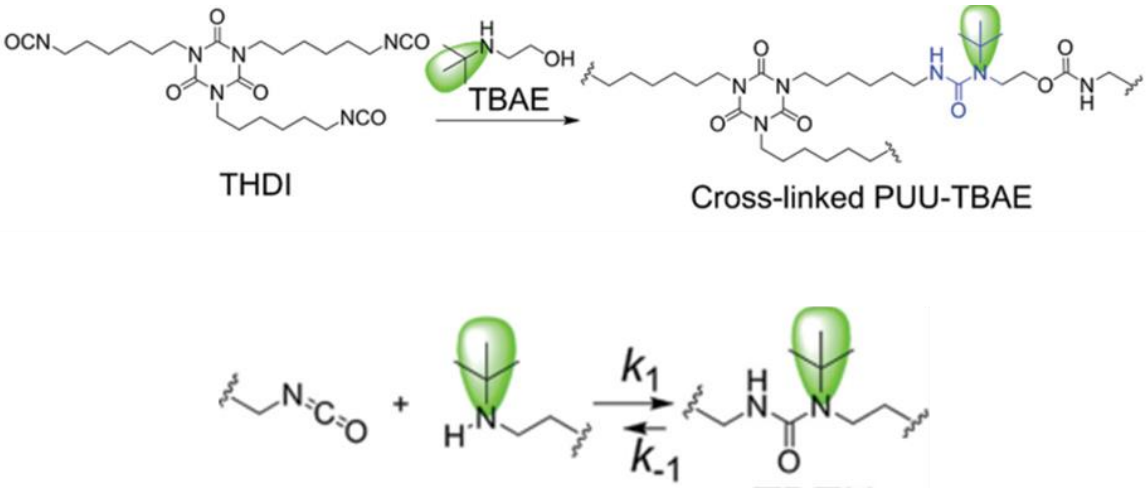

Figure 8. Synthesis of crosslinked poly (urea-urethane) and dynamic bond exchange of HUB. Reproduced with permission.[49]

1.2 Functional Materials based on Dynamic Covalent Chemistry

Polymer materials containing dynamic covalent bonds have been demonstrated to have unprecedented properties that are impossible in traditional thermosets, such as intrinsic self-healing and solid-state recycling. In this section, the main advances that are enabled by dynamic covalent chemistry for polymer materials will be introduced.

1.2.1 Intrinsic Self-healing Materials

In nature, the ability to self-heal is intrinsic to all multicellular organisms.[50] For example, in a healthy body human skin can fully recover its mechanical properties and the

functionalities a few days after being damaged, even without special care. Self-healing is also important in materials since traditional healing methods such as welding or patching are impossible for invisible microcracks which lead to material failure. The automatic recovery of properties would prolong the life service and decrease the fabrication cost. It was not until White et al exploiting microencapsulated healing agents in 2001 when automatic healing was realized **(Figure 9a)**.[51] However, automatic healing is not intrinsic self-healing but rather than extrinsic healing, since it sequestered healing agents from the embedded containers in the matrix. Intrinsic self-healing driven by the dynamic chemical bonds of the polymer matrix can be repeated infinitely in principle and has been one of the main applications for the dynamic chemistry. Depending on the bond breaking and reforming pathways, e.g. associative or dissociative, the healing process could be classified into one-step fashion and two-step fashion.

Two-step fashion is normally binder to the dissociative pathway. Dynamic covalent chemistry contributing to this two-step fashion self-healing includes DA reaction, triazolinedione chemistry, and anthracene dimerization. DA reaction plays the key role in this kind of healing and the healing mechanism lies in the disconnection of covalent bonds through the retro-DA reaction at higher temperatures, followed by the reconnection of the bonds via DA reaction at lower temperatures, as shown in **Figure 9b**. DA reaction is very general and can be incorporated into different kinds of polymer systems, such as epoxy, polyamide, polyurethane, polymethylacrylate, polyimide, carbon fiber, glass fiber, and silica nanoparticles. Besides using heating as the stimuli, light can also be used to heal the materials. Different to [4+2] cycloaddition by heat, the chemical systems for photo-induced healing materials are normal [4+4] and [2+2]

cycloadditions. The reversion of resultant polymers to starting materials (reagents) can readily take place in solid-state. The first example of crack healing of a rigid and transparent polymer via photocycloaddition reaction was proposed by Chung and co-workers.[52] They used a photo-curable cinnamate monomer, 1,1,1-tris-(cinnamoyloxymethyl)ethane (TCE) to prepare the transparent film, which could exclusively reverse to original cinnamoyl structure upon crack formation and propagation. The re-irradiation of the cracked samples at 280 nm allows the recovery of the crosslinked network within 10min (**Figure 9c**).

As for one-step fashion healing, it normally involves the associative dynamic covalent bonds. Various exchangeable bonds could contribute to this kind of self-healing, such as disulfide exchange, transesterification, and siloxane exchange. The advantage of one-step healing is its simplicity and its load-bearing capacity during the healing process due to the integrity of the polymer network.

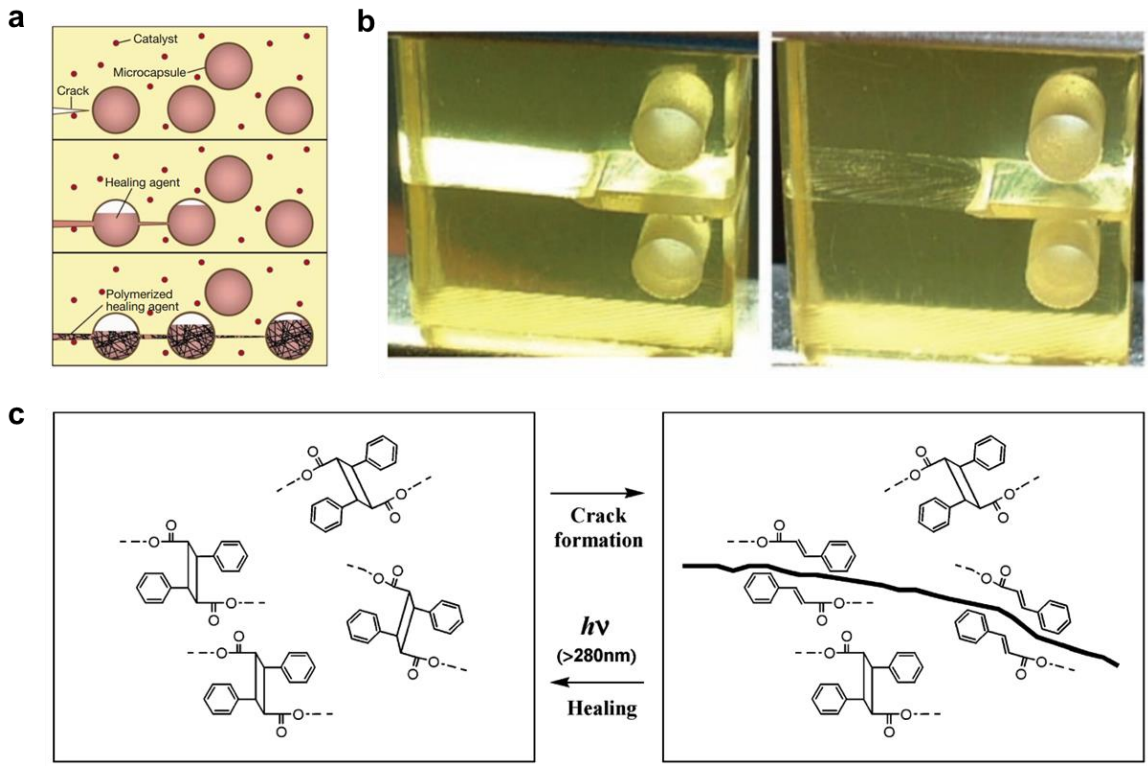

Figure 9. Materials healing. **a)** Automatically of the polymer materials using a microencapsulated healing agent. **b)** Thermal triggered-self-healing. **c)** Light-triggered self-healing. Adapted with permission from the respective publisher.[41, 51, 52]

1.2.2 Improvement of Processability

The viscosity of dynamic covalent polymers above the flowing temperatures offers diverse approaches for polymer processing. In the following section, the incorporation of dynamic covalent chemistry into the crosslinked polymers for improved polymer processing will be discussed.

1.2.2.1 Photo-Induced Shape-Shifting

The mechanism for the photo-induced shape-shifting lies in the manipulation of internal stress distribution within the materials. To be specific, gradient stress is introduced to the pre-stretched materials via the non-uniform stress relaxation in-plane

or out-of-plane, which would reshape the materials when they are released from the pre-stretched states to redistribute the gradient stress.[22] For example, Bowman and co-workers flexibly controlled the shapes of a dynamic polymer system (the mechanism of the dynamic chemistry is shown in **Figure 3a**) by introducing uneven internal stress to the samples via light.[53] Out-of-plane gradient stress is introduced to the pre-stretched samples by photo-irradiating the samples on one side only (**Figure 10a**). Upon releasing the stretched samples, the dynamic polymer would bend away from the light irradiation side since the irradiated side would like to maintain the stretched state while the unirradiated side would like to contract to recover to the original state (unstretched state). The bending angles depend on the value of the gradient stress and can be reprocessed into more shapes by post-irradiation. The authors further applied the photo-induced shape-shifting dynamic polymer materials to fabricate origami that requires bending and folding the materials many times.

In addition to introducing out-of-plane gradient stress, Bowman and co-workers also introduced in-plane gradient stress to manipulate the material shape (**Figure 10b**), which is called “mechanophotopattering (MPP)”.[54] The main protocol is to photo-irradiate a pre-stretched elastomer with a mask. The uncovered regions would experience plastic deformation because of the light-induced rearrangement of the dynamic polymers while the recovered regions are still elastic. The stress inhomogeneity buckles the materials when they are released from the stretching. Unlike the traditional photolithographic approaches, MPP avoids the usage of any wet chemistry or surface deposition/modification process.

Despite the uniqueness of the photo-induced shape-shifting through the manipulation of stress distribution in-plane and out-of-plane, the requirement of an external force

during the photoirradiation limits its applications. Considering the disadvantage, Qi et al used a composite laminate strategy to overcome this (**Figure 10c**).[55] They inserted one pre-stretched elastomer film between two stress-free light activate polymer (LAP) films. Light exposure on one side would lead the laminated film to bend towards the light irradiation source because of the forming compressive stress within the laminate film. The compressive stress is formed since the elastic energy stored in the intermediate film would transfer to the LAP film on the light-irradiated side while the elastic energy remained unchanged on the un-irradiated side.

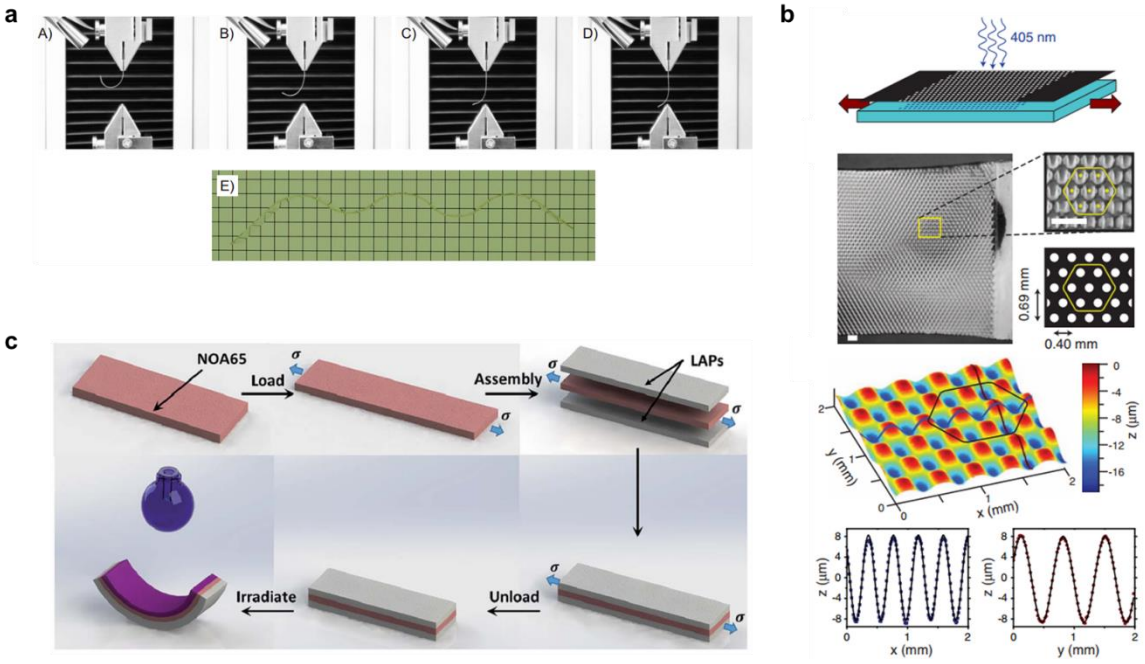

Figure 10. Light-induced shape shifting for dynamic polymer network. **a**) Actuation of a dynamic polymer by introducing out-of-plane gradient stress to the pre-stretching dynamic polymer. **b)** Mechnophotopattering of a dynamic polymer by introducing the in-plane gradient stress to the pre-stretching polymer. **c)** Actuation of a laminated polymers without the requirement of pre-stretching. Adapted with permission from the respective publisher.[53-55]

1.2.2.2 Thermadaptive Shape Memory

Shape memory polymers (SMPs) are polymeric smart materials that could recover

from a temporal deformed shape to the original shape via an external stimulus, such as heating.[56-61] The mechanism behind this phenomenon is the conformational entropy. There is more and more evidence showing that the combination of dynamic covalent bonds into the SMPs would favor the processing of complex geometrical configurations.[62] For example, Xie et al synthesized an SMP containing dynamic covalent bonds by radical polymerization of PCL-diacrylate (PCLDA), using tetrathiol as the cross-link.[26] The crosslinked polymer has two characteristics, one is the thermally-induced elasticity inherited from SMPs (the shape is temporarily fixed and later recovered on demand) and the other one is plasticity enabled by the dynamic covalent bonds (the shape is permanently fixed). These two kinds of properties are independent with each other since the temperature to trigger the plasticity is much higher than the temperature to trigger the elasticity. The cumulative ability of the plasticity simplifies the formation of the complex shapes and the thermally-induced elasticity enables the shape memory behavior (**Figure 11a**). Polymers with both plasticity and shape-induced elasticity pave a new way to fabricate geometrically complex multifunctional devices and can be expanded to other polymer systems. Recently, the same group prepared a dynamic thermoset shape-memory polyurethane with both elasticity and plasticity and observed unexpected shape-shifting versatility by employing Jianzhi's technique (**Figure 11b**).[30]

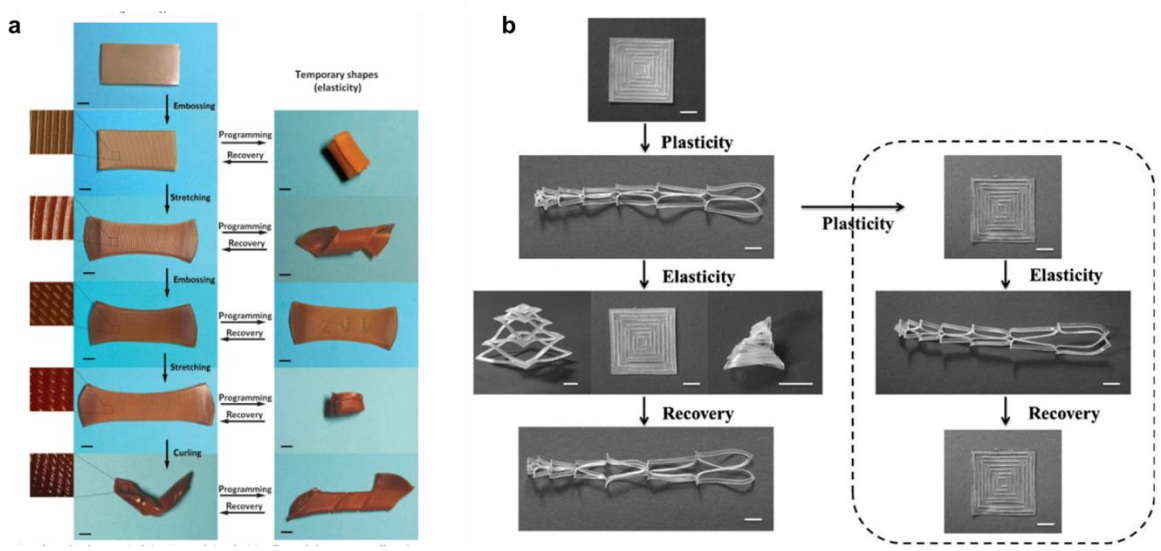

Figure 11. Thermadaptive shape memory polymers. **a)** The cumulative effect in plasticity. **b)** Origami shape memory circle with complex shapes using heat as the stimuli. Adapted with permission from the respective publisher.[26, 30]

1.2.2.3 Orientation of Liquid Crystalline Elastomers

Liquid crystalline elastomers (LCEs) are a class of highly active moving polymers and have remarkable practical applications for actuators, which convert external stimuli into mechanical energy.[63, 64] The normally used two-step crosslinking method for fabricating LCE actuators involves the alignment of the mesogens induced by mechanical stretching in the partially crosslinked network and subsequent further crosslinking to fix the alignment.[65] The two-step method has an inherent contradiction that the mesogen formation in the first step by mechanical stretching requires a robust network to sustain the mechanical stretching disorder, which would increase the disorder in the second step to fix the alignment. A pioneered work reported by Yan Ji and co-workers successfully tackled the problem by introducing dynamic covalent bonds into the LCE network.[66] Stretching the liquid-crystal elastomers with exchangeable links (xLCE) at a temperature higher than the topology-freezing

transition temperature T_v induces the mono-domain formation and the cooling below the isotropic transition temperature T_i preserves the alignment, which will not interrupt with each other (**Figure 12**). The easy processing and alignment, and the ability to mold xLCEs into any dimension and shapes open the way to industry the LCEs for actuators and artificial muscles. Later on, Yan Ji and co-workers further improved the system by incorporating CNTs into the xLCE network to locally control the domain orientation for the complex movement.[67, 68]

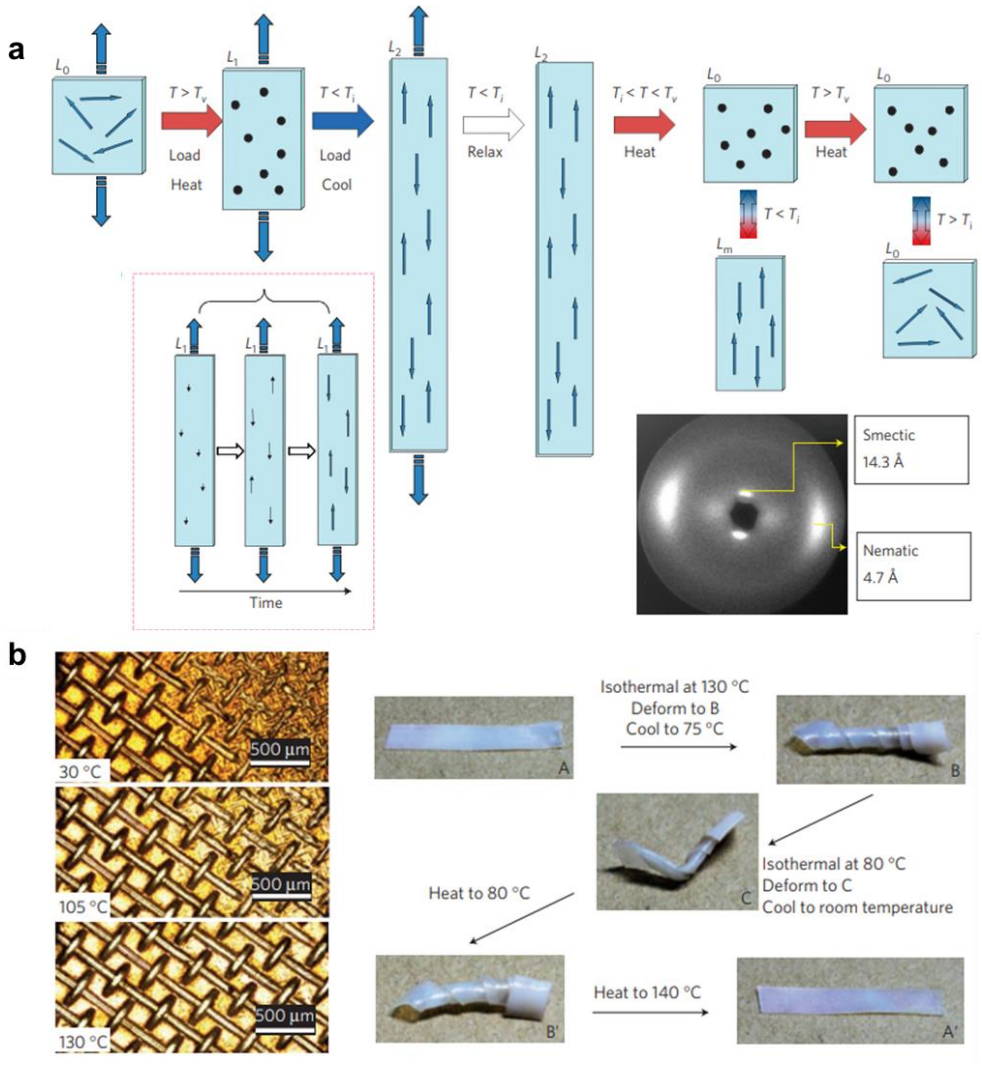

Figure 12. Orientation of liquid crystalline elastomers within the dynamic polymers. **a)** Schematic diagram showing the method for reversibly aligning the LCE. **b)** Triple shape-memory effects in a non-aligned polydomain xLCE. Adapted with permission from respective publisher.[66]

1.2.3 Property Regulation

Generally speaking, it is difficult to modify material properties after the synthesis, especially for thermosets. However, the dynamic nature of the reversible covalent bonds offers the chance to post-tune the material properties for different applications, e.g. structural and functional materials.

1.2.3.1 Property of Structural Materials

Mechanical property is one of the most important factors that determine the applications of structural materials. Polymers are macromolecules built from repeating units. Not only the molecular weight and chain structure account for the polymer properties but also the higher-level organization, such as morphology. Any change of the molecular weight, chain structure, and morphology would alter the mechanical properties. In the following part, strategies employing the dynamic covalent bonds to tune the mechanical property will be introduced.

Yoshie and co-workers prepared a pre-polymer of furyl-telechelic poly(1,4-butylene succinate-co-1,3-propylene succinate) ($PBPSF_2$), which is then polymerized with tris-maleimide (M_3) linker in the bulk state below 100 ^oC (retro-DA reaction temperature) (**Figure 13**).[69] The resulting polymers ($PBPSF_2M_3$) exhibit different mechanical properties depending on the heat-treating history. For example, polymerization at a temperature (70 ^oC) above the $PBPSF_2$ crystal melting point (52-64 ^oC) and subsequent heating at 25 ^oC gave a soft polymer network while polymerization at the temperature below the melting point (25 ^oC) gives a hard polymer network. The different mechanical properties are attributed to different crystallite sizes. Polymerization at 70 ^oC and subsequent crystallization at 25 ^oC renders small size

crystallites because the first crosslinked polymer network formed at 70 °C disturbs the subsequent growth of the $PBPSF_2$ crystallites at 25 °C. In contrast, polymerization at 25 °C provides large size crystallites since the polymerization rate is so low that large crystallites formed earlier than the crosslinked polymers. Combining the crystals and DA reactions, the system could easily convert back and forth between hard and soft properties. Later on, the same group demonstrated that the molecular weight and substituents of the pre-polymer affect the hard-soft conversion greatly.[70, 71]

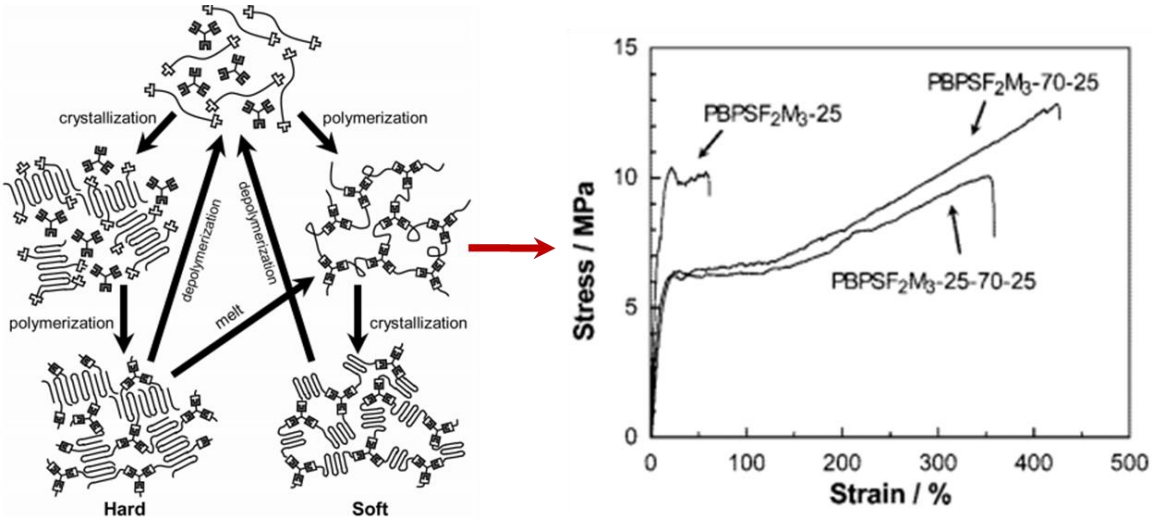

Figure 13. DA covalent bonds to regulate the mechanical property of $PBPSF_2M_3$ polymer. Adapted with permission from the respective publisher.[69]

1.2.3.2 Property of Functional Material

The dynamic covalent chemistry can be used not only to tune the mechanical properties, but also the functional properties. For example, Lehn et al developed one optodynamer based on the hydrazone bond exchange reaction (**Figure 14**).[72] Two kinds of different polyhydrazone films are superimposed and heated. The color and fluorescence are altered with the hydrazine bond exchange reaction proceeded within superimposed films.[73] In addition to utilizing the intrinsic properties of the dynamic

covalent polymer, dynamic chemistry is also combined with the block polymers to control the dispersion and migration of nanoparticles within the polymer matrix, and eventually the properties of the polymer composites.[74, 75] For example, PEG-*b*-PS block copolymers containing DA bond functionalized Au particles (1-DA-3-Au) are mixed with PS-*b*-PMMA block polymers in CH_2Cl_2 and the solvent evaporation at room temperature leads to the phase separation. The 1-DA-3-Au particles would be dispersed homogeneously within the PS-*b*-PMMA block polymers. However, subsequent annealing at 120 ^oC would drive the movement of Au particles from PMMA domains to PS domains since heating cleaves the PEG shell from the particles and the residual PS functionalized Au tends to aggregate in the PS domain to reduce the surface energy. Using the strategy, Beyer et al controlled the dispersion of SiO_2 particle within the PMMA matrix and regulated the optical property of the PMMA film (from transparent to opaque when being heated.[74]

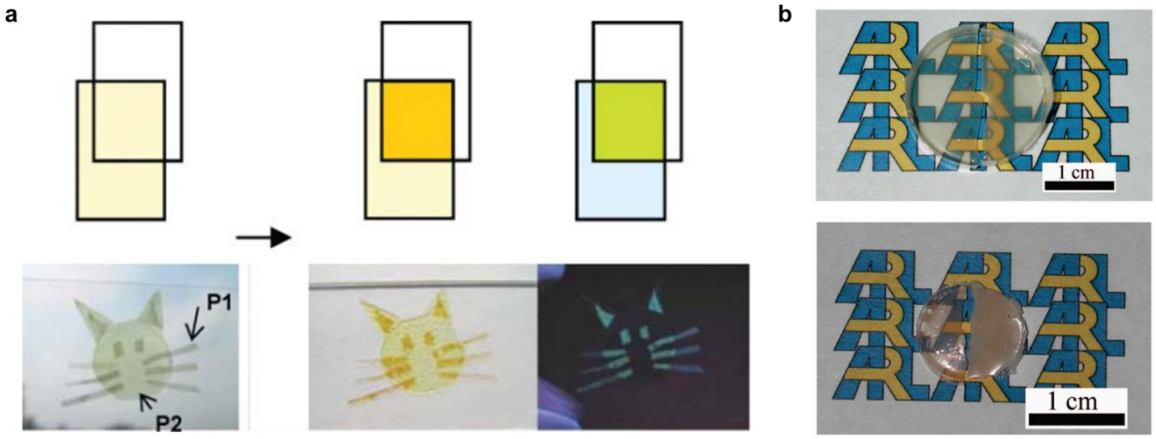

Figure 14. Regulation of functional property using the dynamic covalent bonds. **a)** Color and fluorescence emergence using polyacylhydrazone. **b)** Optical property change using DA bonds. Adapted with permission from the respective publisher.[73, 75]

1.2.4 Recycling of Thermosets at Solid-state

Due to the significant environmental pollution caused by plastics, there is a great need

to recycle them. Generally speaking, current plastic recycling methods could be referred to as “primary”, “secondary”, “tertiary” or “energy recovery”.[12, 76] Primary recycling refers to mechanical reprocessing of waste plastic to give a product that is used for the same purpose as the original plastic. Examples of this kind of recycling include the production of plastic bottles from the blend of the recycled PET (rPET) and the virgin PET. Secondary recycling also refers to the mechanical reprocessing of waste plastic to give a product. However, the recycled product normally has a lower value and different use as the original plastic, which is often called “downgrading” or “downcycling”. Tertiary (chemical) recycling uses a chemical process to recover the chemical constituents. An example of this kind of recycling is pyrolysis, in which the plastics are subjected to high temperatures in the presence of catalysis. This method requires sizable energy input, which limits its implementation on an industrial scale. However, if pure monomers could be recovered from waste polymers via chemical recycling, the price of the polymers would be decoupled from the oil price. This motivates the research of the controlled degradation of polymers to monomers or macromolecule under mild situations in the presence of catalysts. The controlled degradation will be discussed in more detail in the following section (**section 1.2.5**). Energy recovery means the incineration of plastics, during which process energy stored in the polymer will be released in the form of heat. However, the burning of plastics normally originates green gases and toxins and the energy generated from this method is substantially less than the energy conserved by primary and secondary recycling (e.g. the heating value for plastics is about 36,000kJ/kg, whereas mechanical recycling conserves 60,000–90,000kJ/kg), making it unsuitable for recycling plastics.[77] For these reasons, it is preferred to use mechanical processing to recycle the plastics.

However, the traditional recycling method for thermosets is chemical recycling (depolymerization) since it is not possible to use mechanical processing to recycle them. The covalently crosslinked polymer network makes them unable to be reshaped and reprocessed under heat and force. The introduction of dynamic covalent chemistry into polymeric networks sheds light on the recycling of thermosets. In 2011, Leibler et. al introduced transesterification into an epoxy network and achieved the recycling of epoxy at the solid-state without depolymerization, as like the mechanical processing of thermoplastics.[24] Later on, different kinds of dynamic covalent chemistries discussed above have been incorporated into polymer networks to make the thermosets mechanically recyclable, which is undoubtedly an important advance towards the development of environmentally friendly, energy-saving, and cost-effective technology.

1.2.5 Controlled Degradation

For sustainable development, it is preferred to convert the waste polymers to reusable raw substances (original reactants) under relatively mild conditions. However, conventional high-temperature degradation of polymers involves random chain scission and the degradation products are difficult to control, which hinders the reuse of the polymers.[78-80] Controlled degradation of polymers to monomers or macromolecular pre-polymers follows “cradle to cradle” philosophy. The processing method should be simple and not energy-intensive, with monomers easily isolable and highly efficient reversions. Crucially, the materials made from the recycled monomers must possess both mechanical and thermal properties necessary for the targeted applications. It is clear that dynamic covalent chemistry is an ideal candidate. In this section, examples of controlled degradation via dynamic covalent chemistry are

discussed.

Epoxy is one of the widely used engineering plastics thanks to its excellent inherent strength and chemical stability. But for the same reason, the degradation of epoxy under mild condition is not an easy task. To solve the problem, the incorporation of dynamic covalent bonds to epoxy could be one effective solution. Dynamic covalent bonds such as disulfide bond, acetal bond, and DA bonds have been introduced into the crosslinked epoxy network and the resulting epoxy could undergo degradation under the mild conditions due to the reversible breaking and reforming of the dynamic covalent bonds.[81-84]

Polyurethane is another kind of plastic that has wide applications in engineering. The repeating units in the backbone such as urethane and urea are cleavable in principle, therefore, it is possible to degrade the polyurethane into small molecules and oligomers.[85] However, traditional degradation of polyurethane normally requires harsh conditions due to the chemical stability of the urethane bonds. Therefore, new strategies are required for controlled degradation. Since now, polyurethane containing acetal bond was developed to chemical-recycle the polyurethane elastomer.[86] Other engineering plastics such as polyethylene materials have been chemically recycled by tandem catalytic cross alkane metathesis under mild conditions. Another interesting chemistry for recycling is the equilibrium polymerization of spiroorthoester (SOE) derivative, which consists of cationic single ring-opening polymerization and the reverse depolymerization of poly(SOE) (PSOE).[87, 88]

In addition to its use as the engineering plastic, cross-linked polymers could also work as a rubber. Vulcanized rubber is one of the widely applied rubbers while the vulcanized three-dimensional polymer network precludes recycling and degradation.

Introducing disulfide bonds into the rubber offers a solution due to the dynamic nature of the disulfide bonds. Currently, supercritical CO_2 (ss CO_2) has been successfully used for the degradation of the vulcanized rubber in the presence of devulcanizing reagent via the bond exchange reaction between the disulfide bonds and the small devulcanized reagent.[89-92] In this way, the cross-linked vulcanized rubber could be degraded into sol fractions and be recycled.

1.3 Dynamic Si-O Covalent Bonds and derived Functional Materials

The investigation of dynamic siloxane chemistry could date back to the 1950s. Silicone rubber in the presence of either a strong acid (pK_a < -9) or a strong base (i.e. tetramethylazanium hydroxide) was demonstrated to undergo a reorganization of cross-links and to maintain the equilibrium between the cyclic oligomers and the linear polymer.[93] Since then, much attention has been paid to the polymerization mechanism of cyclodimethylsiloxane but little attention has been paid to prepare materials based on the dynamic Si-O bonds. In this Thesis, the possibility to apply acid-catalyzed silicone rubber to develop Si-O based dynamic functional materials at room temperature will be explored, in contrast to silicone rubber in the presence of a strong base which requires heating to behave as a dynamic covalent network. Relevant literature is reviewed in the next sections.

1.3.1 Polymerization of Cyclodimethylsiloxane

Many chemical reactions are reversible. When the reaction rate of the forward reaction is equal to that of backward one, the reaction is in a dynamic equilibrium state (**reaction 1**), displaying constant concentrations of the reactants and the products and showing no property change of the system. The thermodynamic equilibrium constant,

$K_c = k_+/k_-$, where k_+ and k_- are the forward reaction rate constant and reverse reaction rate constant, respectively. K_c changes with temperature.

$$aA + bB \underset{k_-}{\overset{k_+}{\rightleftharpoons}} cC + dD \qquad (1)$$

The equilibrium state could be disturbed by changing the reaction conditions, such as the reactant concentrations, product concentrations, temperature, pH, and stress. According to the Le Châtelier's principle, when the reaction conditions are changed, the point of the equilibrium will move to partially counteract the change.[94, 95] For example, adding more A from the outside will increase the reactant concentrations and then the system will increase the forward reaction kinetic to counteract the effect, though the k_+, k_- and K_c will stay unchanged. The acid-catalyzed reactions of silicones are reversible and therefore, obtained silicone elastomers are in an equilibrium state.

1.3.1.1 Initiation

The initiation of the polymerization of cyclodimethylsiloxane starts from the electrophilic attack of the proton of trifluoromethanesulfonic acid on one oxygen of the siloxane ring and the opening of the ring, forming cationic species.[96, 97] The cationic species are not stable and will form silyl esters in the presence of acid. Since the silyl esters are demonstrated not able to open the siloxane bonds by themselves, the formation of the silyl esters from the cationic species is the deactivation process of the cationic species. Reversibly, the silyl esters could be re-activated to the active centers due to the hydrolysis of the silyl ester (**Figure 15**). That is to say, the deactivation and activation of the active centers are equilibrium reactions. The active centers are in equilibrium with the silanol end groups, silyl esters, and acid. The change of the

reaction conditions would move the point of the equilibrium to counter the change, and the proportion of the active centers, silanol end groups, and silyl esters will also be changed.

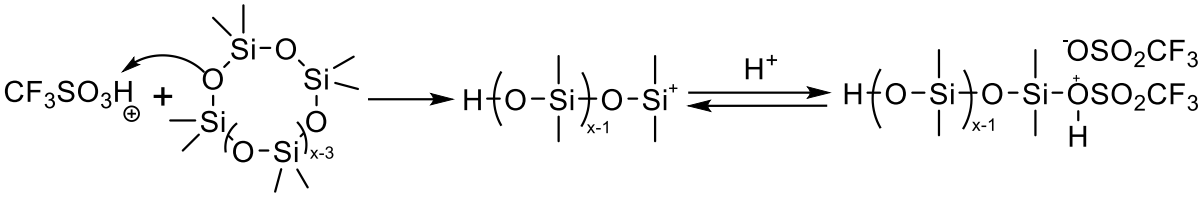

Figure 15. Equilibrium reaction of the active centers and the silyl esters.

1.3.1.2 Propagation

For the propagation, there are generally two possible mechanisms for the polymer chain to grow. One pathway involves the direct addition of monomers onto the active centers and the other pathway involves the acidolysis of the cyclosiloxane, followed by the end group condensation (**Figure 16**). In fact, neither of these two mechanisms could explain all the phenomena observed for the cationic polymerization of the cyclosiloxane.[97, 98] For example, the direct addition of monomers could not explain the formation of D_{3x} (multiples of D_3 like D_6, D_9 and so on) cycles and the accelerated propagation rate in the presence of water for the acid polymerization of D_3 while the acidolysis-condensation could not explain the absence of polymerization in the presence of disilanol for the acid-catalyzed polymerization of D_4. It is reasonable to hypothesize that linear growth may coexist with the acidolysis-condensation.

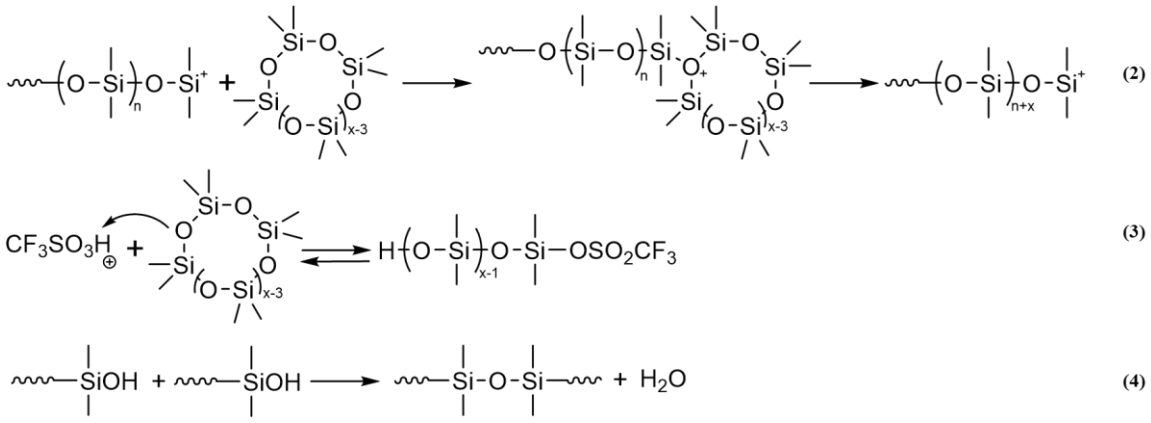

Figure 16. Mechanisms for the polymer chain growth. **(2)** Direct addition of monomers onto the active centers. **(3) & (4)** Acidolysis of monomers and end-group condensation to grow the polymer chain.

1.3.1.3 Ring-chain Equilibrium

A general feature of the cationic polymerization of cyclodimethylsiloxane to produce linear polymers is the formation of various cyclic oligomers. The fraction of cyclic oligomers can be high in some conditions. For example, the oligomer fraction can be 40%-50% in the cationic polymerization of D_3 in CH_2Cl_2 in the presence of CF_3SO_3H. Back-bite reaction is supposed to explain the formation of the cyclic oligomers (**reaction 5 in Figure 17**) while end-biting (end-to-end ring closure reactions, **reaction 6 in Fig. 17**) is believed to be the main reason for the formation of cyclic oligomers in the acid-catalyzed D_3.[99] The back-bite mechanism in acid-catalyzed D_4 is indicated by the descending proportions of the cyclooligomers when the cyclosizes increased ([D_5] < [D_6] < [D_7], …< [D_x]) and the final equilibrium of various oligomers. The polymerization and depolymerization occur together and the equilibrium point varies with reaction conditions. For the acid-catalyzed D_3, The end-to-end ring closure mechanism was proved by the correlation between the kinetically controlled concentrations of cyclic oligomers and the conformational properties of the open chains.

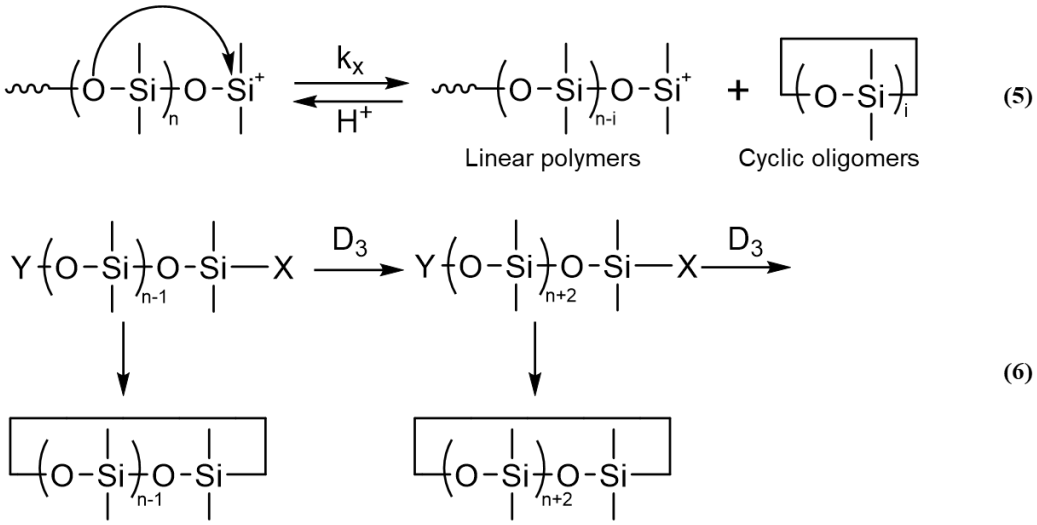

Figure 17. Mechanism for the formation of cyclic oligomers. **(5)** Back-bite reaction. **(6)** End-biting reaction.

1.3.1.4 Termination

Both direct addition of monomers onto the active centers and acidolysis-condensation pathways lead to chain growth without consuming the cationic species. A back-biting reaction would lead to the reformation of the cyclic monomers and the decrease in the molecular weight of the polymer chains. This reaction also does not lead to the deactivation of the cationic species. There are three kinds of termination reactions of the propagating silyl cations: with a counterion to form a silylester (**reaction 7 in Figure 18**) or with water to release a proton (**reaction 8 in Figure 18)**. This proton can initiate polymerization again while the ester chain can undergo condensation to extend or react with water to reform the trifluoromethanesulfonic acid.[96, 100, 101] The end-biting mechanism could also terminate the active silyl cations to release a proton (**reaction 6 in Fig. 17**).

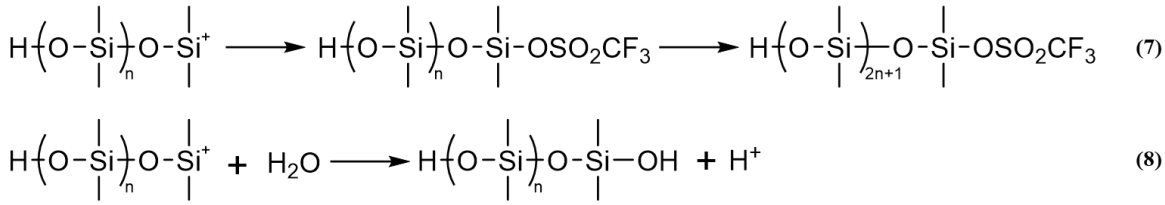

Figure 18. Termination of silyl cations

1.3.1.5 Dynamic Si-O Bond Exchange Reaction

The self-healing and reconfiguration of the polymer networks in silicone rubber is possible due to the exchange of the siloxane bond. It was suggested that either a strong acid having a pK_a of <-9 could trigger the rearrangement of siloxane materials.[93, 100] In the acid system, the acid also first reacts with the siloxane chain to form a silanol and a silyls ester. However, the silyls ester group is not active enough to cleave the siloxane bond. The reforming of the siloxane linkages is due to the condensation of two silanol groups, with the formation of water, which can be eliminated by the reaction with silyls ester to give an acid and a silanol group (**Fig. 19**).

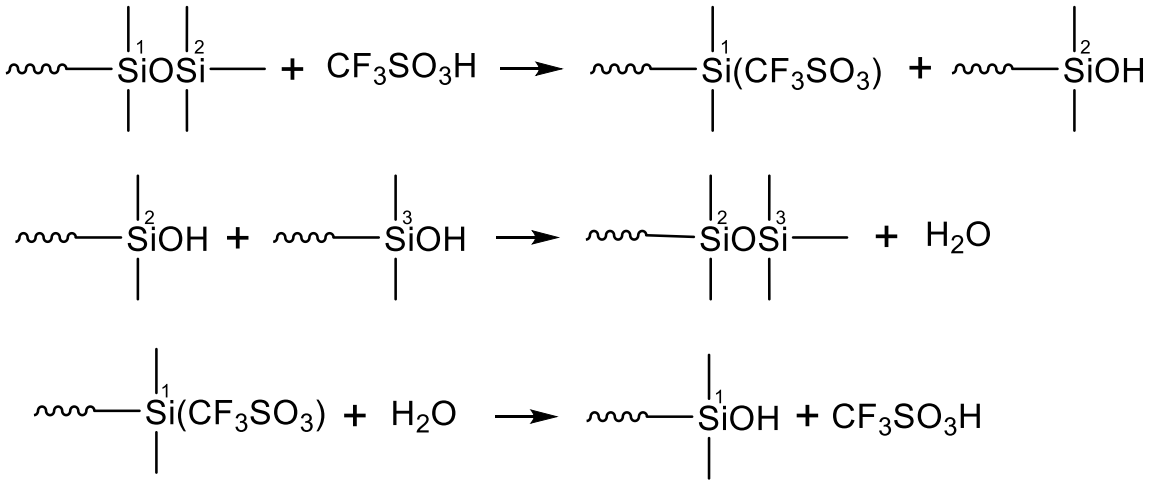

Figure 19. Acid-catalyzed chain exchange reactions

1.3.2 Functional Materials based on the Dynamic Si-O Bonds

Though much efforts have been made to discover the polymerization mechanism of

the cyclodimethlysiloxane, it was not until McGarthy's group in 2012 that employs this old chemistry for self-healing materials.[102] The crosslinked polymers are prepared by copolymerization of octamethylsiloxane (D_4) and bis(heptamethylcyclotetrasiloxanyl)-ethane (bis-D_4), using bis(tetramethylammonium)oligodimethylsiloxanediolate as the catalyst. The reactive tetramethylammonium dimethylsilanolate end groups render the siloxane rubbers as the "living rubber" since the reactive end groups could react with the network chains to reconstruct the network topography and catalyze the equilibration of oligomers with the network. The living rubbers show impressive self-healing performance that could fully recover the fracture toughness when the cracked materials are put together and heated at 90 ^{o}C for 24 hours. A later detailed study on the living PDMS rubbers reveal that the temperature for the appreciable stress relaxation and self-healing abilities could be tuned by adjusting the crosslinking density and catalyst concentration.[103]

Chapter 2

2. A Bio-inspired Self-adaptive, Self-growing and Degrowing Elastomer with Programmable Bulk Properties

Abstract: Planarians are able to resize (grow and degrow) the body to survive the harsh conditions.[104] Herein, a “living” polymeric material based on acid-catalyzed polydimethylsiloxane (PDMS) was prepared to mimic this self-growing and self-degrowing capability. The living PDMS elastomer could not only continuously self-grow by absorbing the nutrients (a mixture of monomers and cross-links), but also self-degrow by depolymerizing polymers into oligomers, which would escape from the materials via evaporation. The addition of particles having the protonatable groups into the living PDMS was demonstrated to be able to stabilize the acid, which could better maintain the dynamic property. The bulk properties such as size, shape, structure, mechanical property, optical property, and surface topography could be flexibly programmed by using the self-growing and self-degrowing technique. Because of the dynamic property and the ability to program the bulk properties of the materials, the potential of this self-growing and degrowing technique in self-healing materials, materials regeneration, and adaptive materials is therefore envisioned.

2.1 Introduction

Planarians of the Turbellaria class who live in both salt and fresh water can resize the body to maintain a functional and proportional body (**Figure 1a**). The mechanism for the body resize depends on the availability of food, i.e., they would grow the body when they are fed with abundant food and degrow by releasing the dead cells when they are in starvation (**Figure 1b**).[104-106] Introducing this kind of growth and degrowth behavior to materials would not only imparts them with programmable bulk properties such as size, composition, and physical properties but also self-adaptive property.[107-111] Recently, programmable polymeric materials have received considerable attention due to the important role of making static products reconfigurable, viable and adaptable.[112] However, despite advances in programmability, programmable polymeric materials employing liquid crystalline elastomers,[63, 113-118] and supramolecular polymer[119-121] remain limited to shape changes, reversible activation, volume changes, and morphological changes without preserving or controlling their properties. It is not yet possible to program a bulk size and property of a material into an intelligent material whose size, weight, composition, and properties can be changed at the macroscopic level as needed, as natural systems normally do for their existence and survival. To this issue, planarians might offer a resolution because of the unique growing and degrowing properties. Herein, a promising polymeric elastomer that exhibits unusual self-growing and self-degrowing phenomenon depending on the availability of feeding nutrients (a mixture of monomers and cross-links) is described. This phenomenon allows us to tune the bulk-size, shapes, mechanical properties, optical properties, and surface topology of the materials.

Figure 1c displays the detailed design for the self-growing and self-degrowing

polymeric materials. As inspired by the planarians, the polymeric materials would be able to self-grow if they could continuously incorporate nutrients from the environment into the polymer network while they would be able to degrow if they could release nutrients from the polymer network in the absence of nutrients. Within the general design, “living” polydimethylsiloxane (PDMS) made by acid initiated ring-opening polymerization of octamethylcyclotetrasiloxane (D_4) with 1,1,1-tri(2-heptamethylcyclotetrasiloxane-yl-ethyl)-methylsilane ($triD_4$) as the cross-link, is expected to meet all the requirements. The ionic propagating species in PDMS are known to retain the activity after polymerization. These ionic species are not only able to react with and incorporating monomers, but also to induce ongoing chain-exchange reactions keeping the PDMS networks in a dynamic state, making the self-growing possible. In addition, the cross-linked polymers are also possible to degrow if the oligomers are removed from the polymeric materials since the polymers would depolymerize into oligocyclosiloxane via the back-bite reaction to maintain the polymer-oligomer equilibrium. Since the self-growing behavior of the polymeric materials has been elaborately described by Cui et. al, this chapter focuses on the self-degrowing behavior of the materials.[122]

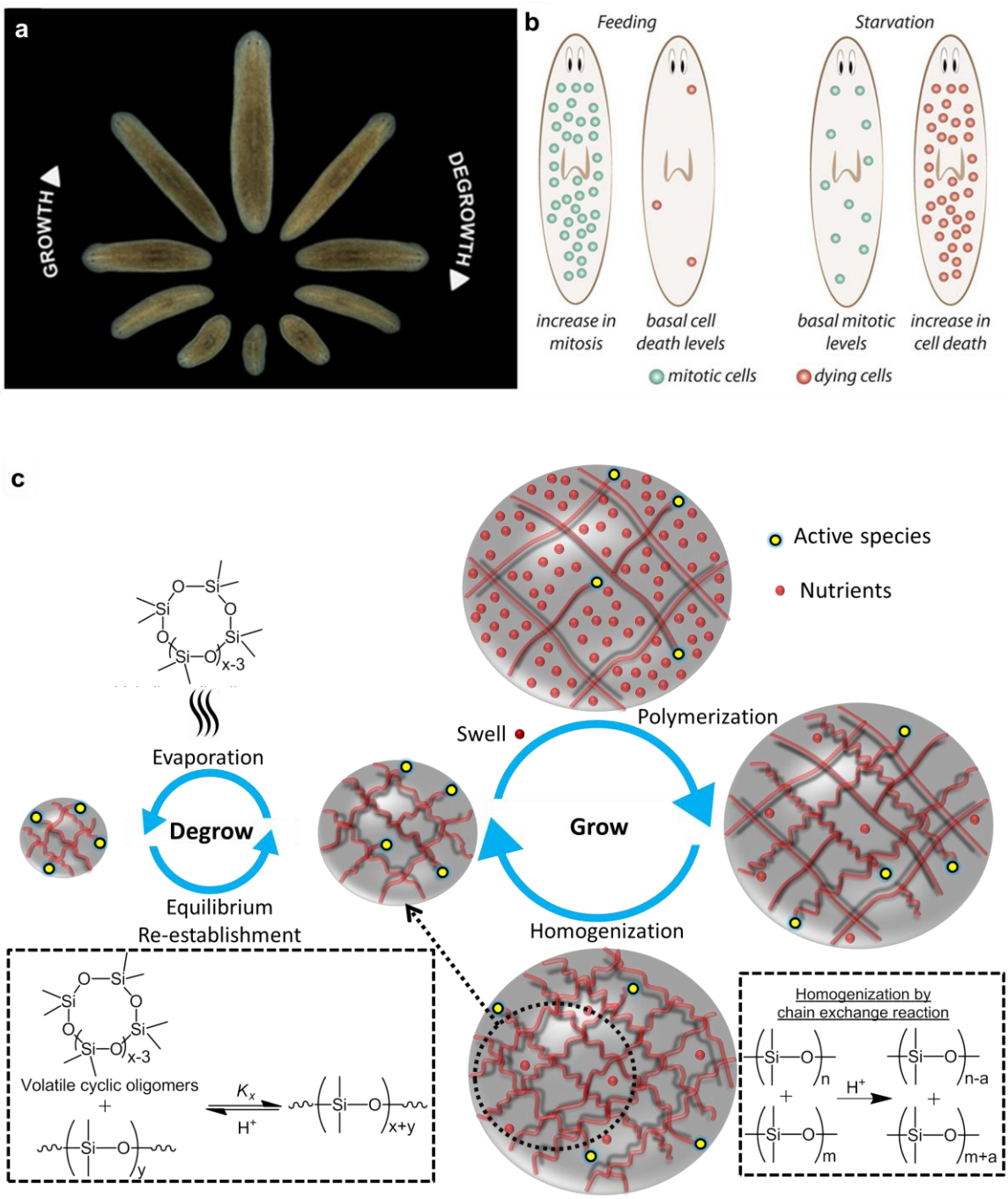

Figure 1 a) & b) Self-growing and self-degrowing behaviors of planarians in response to nutrient availability. Reprinted with permission.[123] **c)** A proposed strategy for imparting self-growing and self-degrowing behaviors to the polymeric system and the proposed regeneration process by synthetic materials.

2.2 Results and Discussion

2.2.1 Self-degrowing Behavior of the Acid-catalyzed PDMS Elastomer and the Mechanism Behind

According to the design, the removal of oligomers would cause the dynamic PDMS elastomers to self-degrow, providing oligomers to maintain the polymer-oligomer equilibrium. In this section, the self-degrowing behavior of the dynamic PDMS elastomer will be demonstrated and the mechanism will be also investigated.

Acid-catalyzed PDMS elastomer was selected to demonstrate the self-degrowing behavior. The samples were prepared by ring-opening polymerization of D_4 monomer with the triD_4 as the crosslinker in the presence of triflic acid, and the as-prepared PDMS elastomers are named as the "PDMS(*y*) living seeds", where *y* denotes the crosslinker content (%). The trilfic acid concentration is 5μl/1g D_4 for all the samples. A 2g circular PDMS(1) living seeds with a diameter of 32mm were put on the petri dish and stored in the hood. It is expected that the oligomers could escape the PDMS living seeds and evaporate away when the PDMS living seeds are put in the open environment, causing the living seeds to self-degrow. As shown in **Figure 2a**, the diameters of the PDMS(1) living seeds in the hood decreased with the time, showing a size reduction. The mass tracking indicated that the size reduction was attributed to the weight loss (**Figure 2b**). Actually, the PDMS(1) living seeds could lose about 60% of the initial weight when the incubation time reached 200 hours. The gradual decrease of materials' diameter and weight clearly demonstrated the PDMS living seeds could self-degrow when they are left in the open environment.

Then, the evaporation-induced depolymerization mechanism was investigated. A set

up shown in **Figure 2c** was built to collect the possible oligomers evaporated from the materials. The set up contains three components: a round bottle, a trap, and a vacuum pump. The round bottle was connected to a vacuum pump via a trap. The round bottle was used for placing the living seeds and the vacuum pump was used for sucking the oligomers to escape living seeds, which were collected by cooling with liquid nitrogen in the trap. To demonstrate the self-degrowth mechanism, PDMS(1) living seeds were placed in the round bottle and after being pumped for 3h, the liquid was collected in the trap (**Figure 2d**) and the PDMS(1) living seed lost about 25% weight. The composition of the collected liquid mixture wàs further analyzed by NMR (**Fig. 2d**) and gas chromatography-mass spectrometry (GC-MS, **Fig. 2e**). Using hexanmethylcyclotrisiloxane (D_3), D_4, and decamethylcyclopentasiloxanes (D_5) as standards, the composition of the collected liquid was unraveled as D_4 (80%) and D_5 (20%). The results from the GC-MS analysis (**Figure 2e**) were in agreement with the NMR results. Signal peaks for D_4 (85%) and D_5 (15%) were observed. Both the NMR and GC-MS demonstrated that the slow evaporation of D_4 compared to other oligomers that led to the PDMS living seed to self-degrow.

Though it was demonstrated that the self-degrowing of the PDMS living seeds was due to the oligomer evaporation, it is unclear whether the polymer has undergone depolymerization or not since the evaporated oligomers could either be provided by the polymer depolymerization or by the residual oligomers in the PDMS living seeds due to the polymer-oligomer equilibrium. To make it clear, PDMS(1) living seeds were washed by immersing them in a toluene solvent containing 1 wt% triethylamine and the samples were subsequently dried under vacuum after 2h-immersion. The triethylamine was used to kill the living species (trifilc acid) to stop the

depolymerization and toluene was supposed to carry away the unreacted reagents. A ~10% weight loss was observed, indicating the maximum amount of oligomers consisting of the polymer-oligomer equilibrium should be less than 10%. Since the weight loss during the 3h-pumping reached 25% of the weight, it is clear that the polymers should have undergone depolymerization when oligomers are removed from the PDMS(1) living seeds. In addition, the depolymerization produces small fragments (mainly D_4 and D_5 monomers), confirming the back-bite depolymerization mechanism. Next, it was also checked if the molecular weight changes during the depolymerization since depolymerization was supposed to decrease the molecular weight of the polymers. To confirm this, linear PDMS polymers created by triflic acid initiated ring-opening polymerization of D_4 without triD_4 were put on the surface of a petri dish and stored in the hood, the linear polymers could depolymerize in the open environment as the oligomers evaporate. After 9 days, the linear PDMS polymers lost about 50% weight, and the self-degrown linear polymers were named as the n-self-degrown linear PDMS polymers (n denotes the lost mass ratio compared to initial weight). As-prepared linear PDMS polymers were used as the control sample. Both the as-prepared and self-degrown linear polymers were deactivated before being subjected to GPC analysis by immersing the samples in triethylamine to kill the living species. The GPC results revealed that the molecular weight of the as-prepared PDMS linear polymers was the same as in the 50%-self-degrown linear PDMS polymers (**Figure 2f**), indicating that the polymer chain reorganizes during the self-degrowing process.

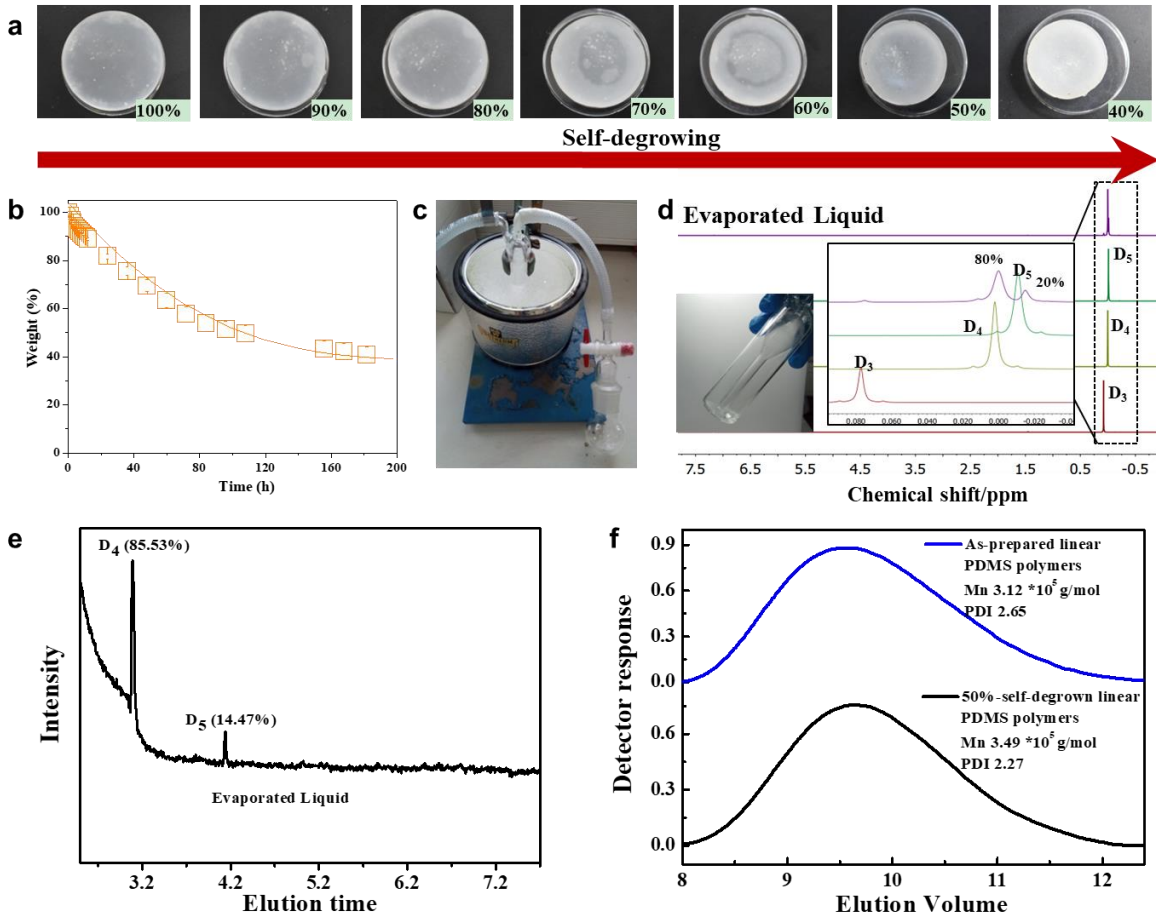

Figure 2. Characterization of the self-degrowing behavior. **a)** Photographs showing the diamater change of a circular PDMS(1) living seeds (initial diameter: 32mm) with increasing incubation time. **b)** Self-degrowing kinetic of the PDMS(1) living seeds measured by tracking the weight of the self-degrown PDMS elastomer. **c)** A set-up to collect the evaporated small molecules from the PDMS living seeds by vaccum pumping. **d**) ^{1}H NMR spectra of D_3, D_4, D_5 and the oligomer mixture collected from PDMS(1) living seeds in the trap after 3h-pumping. Inset shows the collected liquid. **e)** GC-MS chromatogramo of the oligomer mixture collected in the trap. **f)** GPC curve of the acid-catalyzed linear PDMS polymers and the 50%-self-degrown linear PDMS polymers.

2.2.2 Effect of the Particles on the Self-degrowing Polymer Materials

The living species in PDMS are critical to preparing self-degrowing polymeric materials. However, triflic acid can easily evaporate during treatment and this limits its application. A strategy to retain the acid would be advantageous. It is known that organic acids like

triflic acid firmly adsorb on particles whose surface has protonatable groups, such as -COOH, -OH, -OR, through electrostatic interactions (**Figure 3**).[124] Carbon black (CB) was selected to prove that such interactions could stabilize the acid in the dPDMS matrix. CB/dPDMS polymer composite was prepared by polymerization of CB, D_4 and triD_4 mixture solution in the presence of triflic acid, named as the CB(*x*)/dPDMS(*y*) living seeds, where *x* is the CB weight concentration (%) and *y* is the triD_4 contents (%). To confirm the electrostatic interactions between CB and triflic acid, CB(1)/dPDMS(1) living seeds and PDMS(1) living seeds were treated by three-time toluene swelling-evaporation cycles. The swelling and subsequent evaporation of toluene were supposed to be able to remove unadsorbed acid in the PDMS living seeds while the presence of CB would prevent the removal of the acid in the CB/dPDMS composites because of the electrostatic interactions. To confirm this, the treated CB(1)/dPDMS(1) living seeds and PDMS(1) living seeds were analyzed with EDX (**Figure 4**). EDX of treated CB(1)/dPDMS(1) living seeds (**Figure 4a**) showed the presence of the elements silicon, fluorine (of adsorbed triflic acid), apart from the signal of carbon, oxygen, and silicon, which is attributed to the siloxane network. The EDX spectrum of the treated PDMS(1) living seeds (**Figure 4b**) showed only carbon, oxygen and silicon, suggesting that the acid was completely leached away in the absence of CB due to lack of electrostatic interactions. These experiments revealed that the presence of CB could effectively stabilize the triflic acid via the electrostatic interactions between the protonatable groups such as -COOH, -OH, -OR, and triflic acid (counter anion).

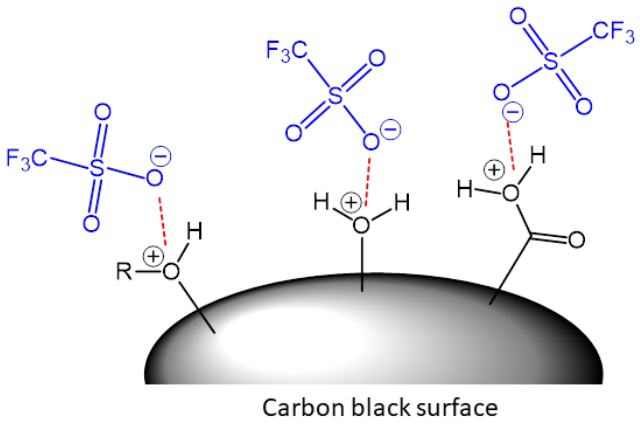

Figure 3. Possible electrostatic interactions between triflic acid and carbon black.

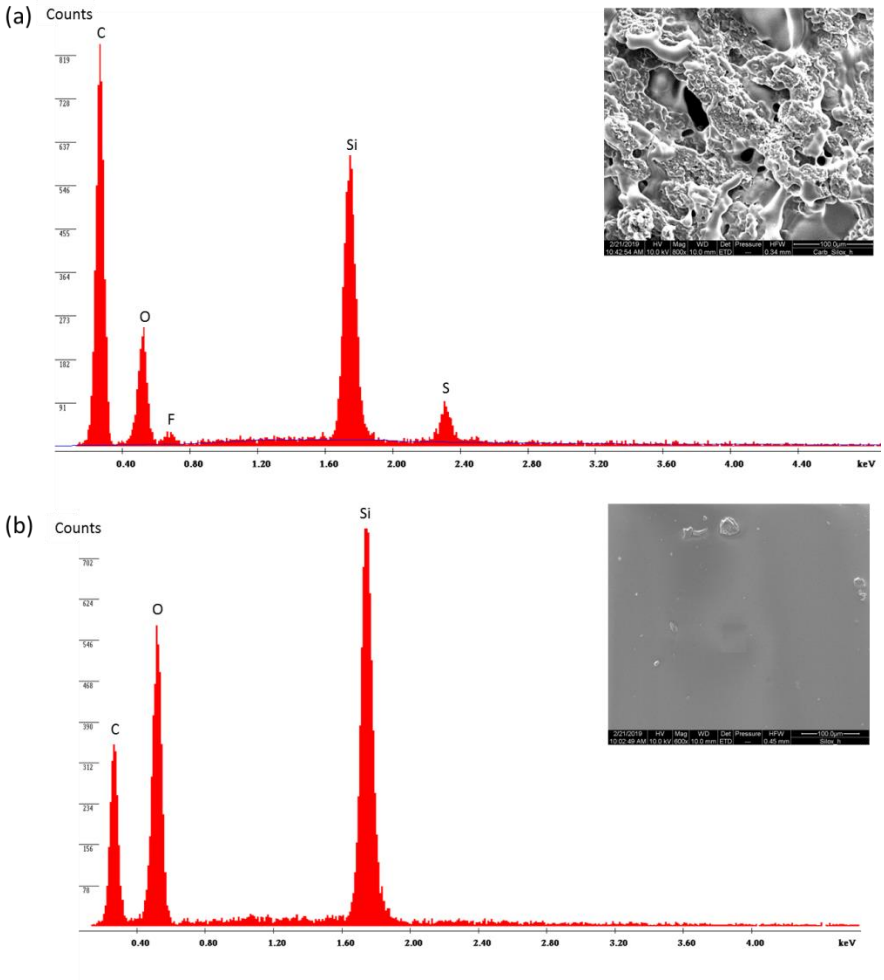

Figure 4. a) & b) EDX spectrums of treated CB(1)/dPDMS(1) living seeds and PDMS(1) living seeds.

To find further evidence of a strong interaction between CB and trifluoromethanesulfonic acid, the formation of elastomers using CB supported triflic

acid was demonstrated. To prepare the CB-supported acid, a dispersion of CB in toluene (0.02 g CB/10 g toluene) was prepared by sonicating for 10 minutes. To this dispersion, triflic acid was added slowly and sonicated for 20 minutes. The CB-supported acid was finally obtained by evaporation of toluene, followed by washing with toluene and drying. An elastomer was prepared when a solution of 1% triD_4 in D_4 (2g) was mixed with this CB-supported acid (0.02 g), indicating that acids on the surface of CB are active like free acids (**Figure 5**).

Figure 5. Formation of CB/dPDMS elastomer with the CB-supported acid as the initiator.

Then, the effect of particles on the self-degrowing kinetic was investigated. The kinetics of the self-degrowing materials with different carbon black contents was recorded. **Figure 6a** showed that the self-degrowing rate increased with increasing CB contents. The CB(1)/dPDMS(1) living seeds rapidly lost weight compared to CB(0.5)/dPDMS(1) living seeds and PDMS living seeds. Replacing carbon black powders with 10-20 nm silica particles, the obtained SiO2(*x*)/dPDMS(*y*) living seeds (named analog to the CB(*x*)/dPDMS(*y*) living seeds, where *x* is the SiO_2 weight percentage and *y* is the triD_4 contents by weight) showed the same trend as the CB/dPDMS living seeds: the self-degrowing rate increased when more silica particles were incorporated into the polymer composites (**Fig. 6b**).

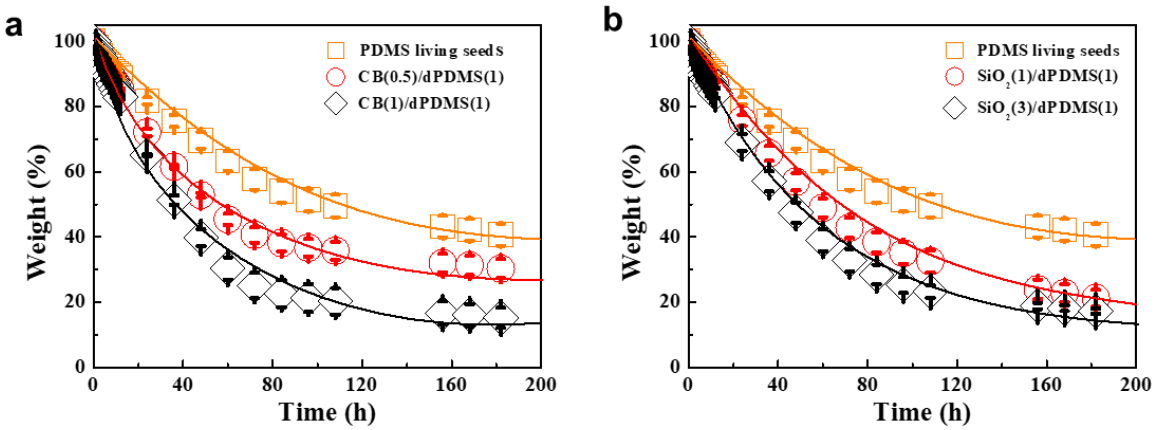

Figure 6. The self-degrowing rate of the living seeds with different powder contents. **a)** carbon black, **b)** SiO_2

The effect of particles on the depolymerized products was also analyzed to see if the presence of powders catalyzed the formation of different small molecules. 1g of CB(1)/dPDMS(1) living seed was placed in the setup shown in **Figure 2c** to collect the oligomers that evaporated from the sample due to the back-bite reaction. After 3h suction, the sample lost about 31% by weight, higher than 25% compared to the PDMS(1) living seeds. When the collected liquid was checked by NMR (blue line in **Figure 7a**) and GC-MS (**Figure 7b**, red line), however, no much difference was found to the oligomers collected from the sample without CB. Therefore, the presence of particles could not catalyze the formation of different oligomers.

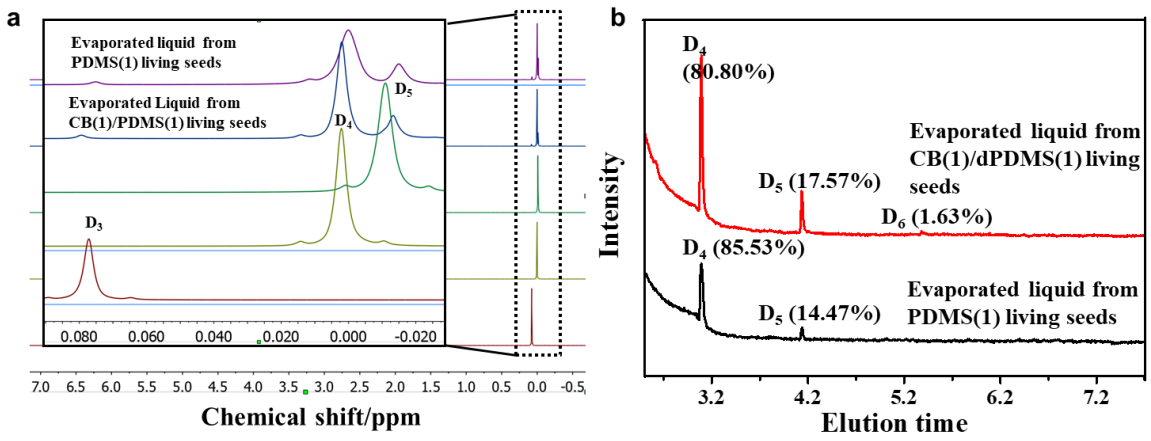

Figure 7. Effect of CB on the depolymerized products. **a)** ^{1}H NMR comparison of D_3, D_4, D_5 and the evaporated oligomer mixture from the PDMS(1) living seeds and CB(1)/dPDMS(1) living seeds. **b)** GC-MS comparison of the evaporated oligomer mixture from the PDMS(1) living seeds and CB(1)/dPDMS(1) living seeds.

At last, the effect of particles on acid-catalyzed ring-opening polymerization of D_4 was investigated to see if the presence of particles affects the polymerization. The molecular weight of the linear PDMS polymers catalyzed by the triflic acid from D_4 without crosslinker in the presence/absence of carbon black were analyzed. The composites obtained in the presence of CB were named as the linear CB(*x*)/dPDMS polymers and in the absence of CB were linear PDMS polymers, as shown above. The molecular weight of linear CB(1)/dPDMS polymer and linear PDMS polymers were measured by GPC to show the effect of CB on the polymerization. Before subjected to GPC, both linear PDMS polymers and linear CB(1)/dPDMS polymers were deactivated to kill the living species. As for linear CB(1)/dPDMS, CB was removed by the filter before the GPC measurement. The GPC analysis showed that both linear PDMS polymers, either polymerized in the presence of CB or the absence of CB, had a very similar molecular weight distribution (**Fig. 8**), which strongly showed the presence of CB does not affect the polymerization of D_4 monomers.

The more interesting thing here is that when putting the as-prepared linear PDMS polymers and as-prepared linear CB(1)/dPDMS polymers in the hood for self-degrowing, though the latter lost more weight (about 90%, and the obtained composites were named as self-degrown linear CB(1)/dPDMS polymers) than the former one (about 50%), the molecular weight of the self-degrown linear polymers is similar, even similar with the as-prepared linear polymers. This again demonstrates the chain exchange happened during the self-degrowing process, maintaining a similar polymer length at each stage of the depolymerization, otherwise, the molecular weight should decrease as the materials lost weight.

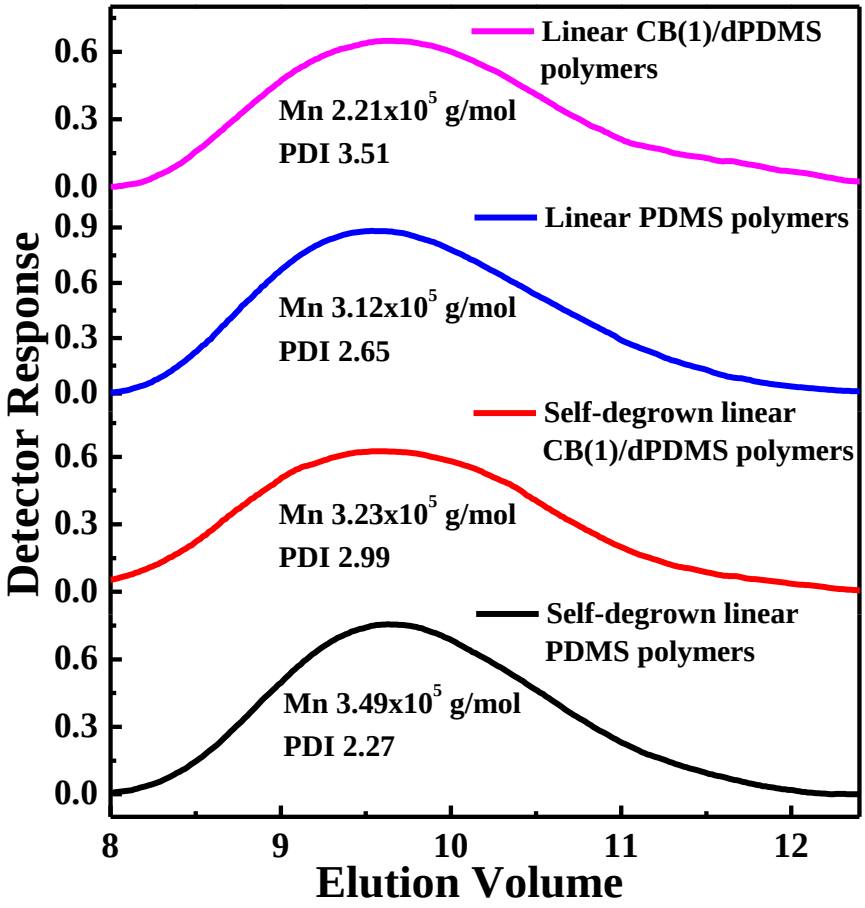

Figure 8. GPC of linear PDMS polymers, linear CB(1)/dPDMS polymers, self-degrown linear PDMS polymers, self-degrown linear CB(1)/dPDMS polymers.

2.2.3. Structure and Shape Control during Self-degrowing and Self-growing Process

Acid-catalyzed dynamic PDMS elastomers were able to retain the original shapes when they grow up because of the uniform distribution of the acid.[122] But for the self-degrowing materials, the driving force for the self-degrowth was the oligomer evaporation. The surface of the living seeds exposed to the open environment would self-degrow faster than the inside materials because the oligomer on the surface was easier to escape than the oligomers in the inside materials. The uneven de-growth of the materials would make the materials inhomogenous, which might alter the structure and shapes of the materials. Here, a ball representing particle/dPDMS composites was used to explain the structure evolution during self-degrowing and self-growing process (**Figure 9 & 10**), and then the shape control (**Figure 11 and Figure 12**) due to the structure change was also introduced. Particle/dPDMS living seeds were used in the following experiments since particles having protonatable groups could prevent the evaporation of the triflic acid. When the living seeds are self-degrowed and the obtained polymer composites are named as *n*-self-degrown particle/dPDMS composites, where *n* is the mass loss ratio compared to the mass of the living seeds.

2.2.3.1 Structure Control during Self-degrowing and Self-growing Process

As shown in **Figure 9a**, the oligomers on the surface escape faster than from the inside. When a ball-shape living seed was exposed to an open environment, the self-degrowth on the surface would be faster because of the easier escape of the oligomers. As the $triD_4$ was supposed not to degrade (will be discussed in **section 2.3.3.3**) during the self-growth process, the concentrations of $triD_4$ on the surface would be higher

than the inside materials since more polymers were depolymerized into oligomers. Therefore, the surface would be stiffer than the inside materials, giving a core-shell structure (**Figure 9b**). On the other hand, the higher triD$_4$ concentrations decrease the polymer chain mobility, which eventually reduces the self-degrowth kinetic. With increasing triD$_4$ concentrations in the shell materials, the degrowth kinetic becomes slower and slower, eventually reaching a critical point at which the self-degrowth kinetic is slower than the core materials. Then, the core materials degrow faster than the shell materials, and the materials finally become homogenous (**Figure 9c**). Generally speaking, the living seeds first self-degrow faster on the surface exposed to the open environment and form a core-shell structure. Then the core materials would self-degrow faster than the shell material, eliminating the core-shell structure and eventually forming a homogenous material. To confirm the assumption, a ball-shape CB(1)/dPDMS(1) living seed (14g) was fabricated by hand as a starting sample, which was put in the oven at 70 ^{o}C for the symmetric self-degrowth (**Figure 9f**). The symmetric degrowth means the surfaces exposed to the open environment were geometrically symmetric. The symmetric degrowth of the ball-shape samples was performed by putting the living seeds on a small open size bottle with the sample size is much larger than the open bottle size, so the contact area between the samples and the bottle was negligible (**Figure 9e).** The self-degrown CB(1)/dPDMS(1) was cut into two halves when it lost 30% of its initial weight, displaying a core-shell structure (**Figure 9g**). It was also noted that the material can self-heal when these halves were put together, which is supposed to have no effect on the following self-degrowth. As the self-degrowth progressed further, the core-shell structure disappeared when the materials lost 90% of its original weight (cut into halves, **Figure 9h**), indicating the

homogeneity of the materials. The formation of core-shell structure and final disappearance of the core-shell structure has clearly shown our assumption for self-degrowing process.

While the self-degrowing could form the core-shell structure in the ball shape materials, making the materials inhomogeneous, the effect of self-growing on the structure of the materials was also explored. Self-growing the 90%-self-degrown CB/dPDMS composites with monomers to the original weight, the materials will retain the shapes and the homogenous structure (**Figure 9i**). Moreover, self-growing the core-shell structure self-grown CB/dPDMS composites (**Figure 9g**) to original weight (14g) at 70 ^{o}C for 2 days, the core-shell structure disappeared and a homogenous material was observed by eyes (**Figure 9i**). The reason for the structural homogenization during self-growing might be either that the shell materials grow faster than the core materials because of the higher density of the living species or the bond exchange of the dynamic covalent polymers, which favors the homogenous structure.

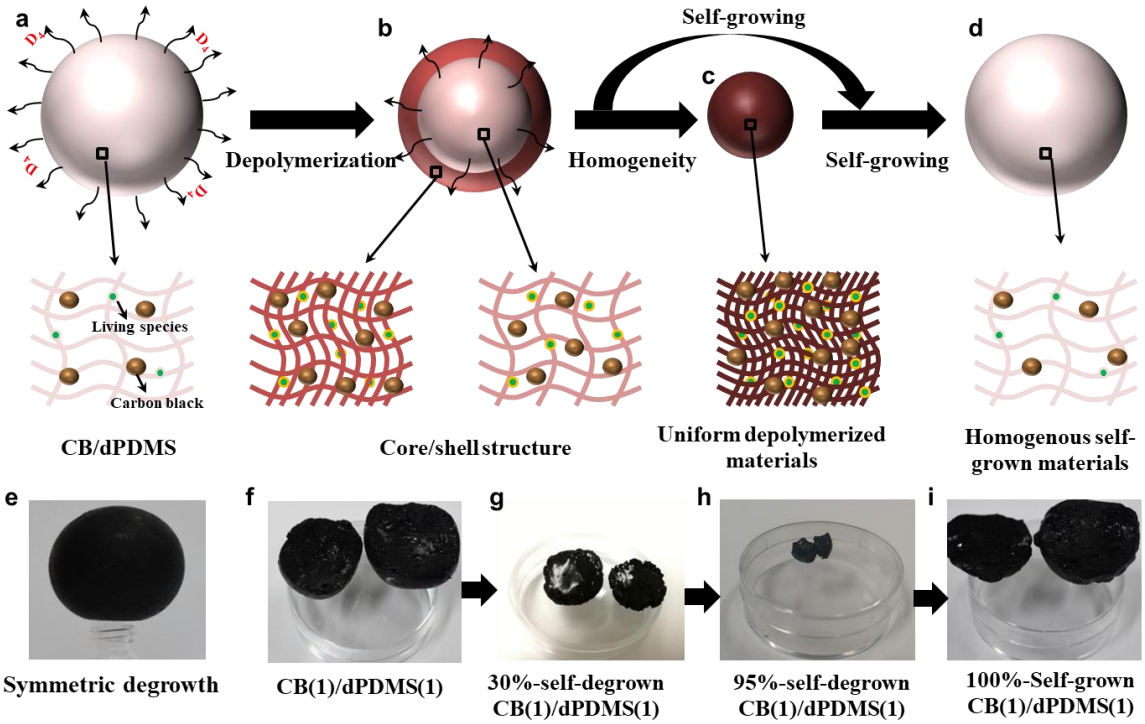

Figure 9. Structure evolutions of the polymer composites during self-degrowing and self-growing. **a)** Particle/dPDMS living seeds. **b)** Core-shell structure of the self-degrown particle/dPDMS composites. **c)** Homogenous structure of the self-degrown particle/dPDMS composites. **d)** Homogenous self-grown materials from the self-degrown composites (either core-shell structures or homogenous self-degrown materials). **e)** Pictures show the symmetric degrowth for the ball-shape living seeds. **f-i)** Demonstration of the structure change during the self-degowing using the CB(1)/dPDMS(1) living seeds.

The inhomogeneous structure appears to be inevitable during the self-degrowing, an attempt to introduce other methods to eliminate the gradient structure other than employing the self-growing was described. Self-degrowing forms the gradient structure within the materials because of the different self-degrowing kinetics controlled by the oligomer evaporation. But for the acid-catalyzed PDMS, the polymer chain could exchange with others, homogenizing the materials. The chain exchange happens all the time, even in the self-degrowing process, which contradicts with the formation of the gradient structure. This is probably because the chain exchange kinetic is slower than the self-degrowing kinetic, therefore, the gradient structure still

formed even the chain exchange reaction is present. But in principle, the gradient structure will disappear if the self-degrowing kinetic is slower than the chain exchange reaction kinetic. To confirm this, a 2 mm-thick film made of SiO_2(3)/dPDMS(1) living seeds (**Figure 10a**) was prepared and then asymmetrically self-degrowed which means the surfaces exposed to the open environment were asymmetric. The asymmetric degrowth of the rectangular shape materials was performed by putting the sample on the petri dish, with one surface exposed to an open environment and one surface exposed to a closed environment (**Figure 10d**). In this case, the self-degrowth kinetic is supposed to faster than the chain exchange rate, therefore, a gradient structure is expected. The film was found to become opaque (**Figure 10b**) when it lost 30% in weight. The opaque film was attributed to the porous SiO_2 when the polymers are self-degrowed. Cutting the samples and observing the cross-section of the samples, it was found that only the surface exposed to the open environment became porous and the rest parts are not, indicating the formation of the gradient structure (**Figure 10e**). Then the opaque material was sealed in a close petri dish and stored in an oven at 70 ^{o}C. In this case, the chain exchange rate is believed to be faster than the self-degrowth kinetic, a homogenous materials was expected. The film was found became translucent after 12 h heating (**Figure 10c**), which clearly demonstrated that the gradient structure can be eliminated if the chain exchange kinetic is faster than the self-degrowth rate.

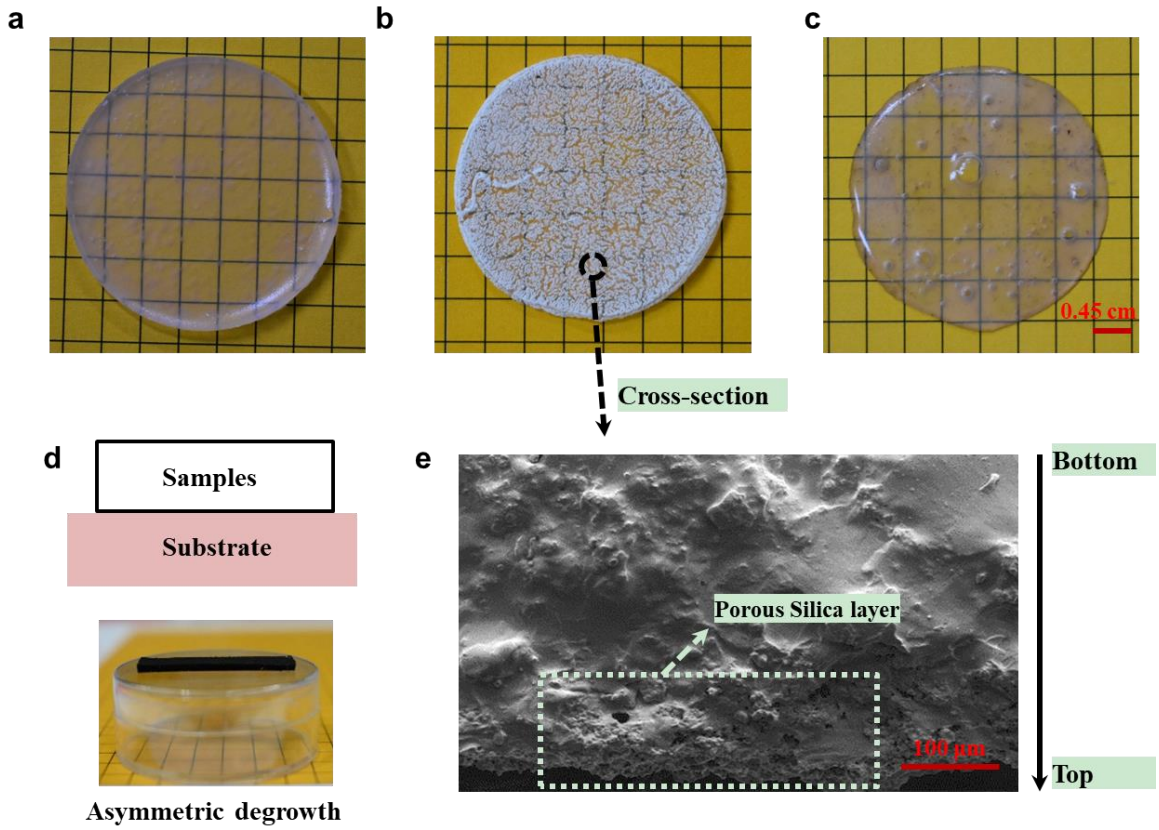

Figure 10. Gradient structure elimination by heating. **a)** SiO_2(3)/dPDMS(1) living seeds. **d)** Translucent SiO_2/dPDMS composites after heating opaque 30%-self-degrown SiO_2(3)/dPDMS(1) composites in a closed container at 70 °C for 12h. **c)** Opaque self-degrown SiO_2(3)/dPDMS(1) after being self-degrowed to 70% of the initial weight. **d)** Schematic and pictures show the aymmetric degrowth of the circular shape SiO_2(3)/dPDMS(1) living seeds. **e)** SEM of the cross-section of the opaque SiO_2/dPDMS composites.

2.2.3.2 Shape Control

The shape evolution during the self-degrowing process was dependent on the self-growing mode, i.e., symmetric degrowing or asymmetric degrowing. If the materials were self-degrowed symmetrically, no internal stress would be generated within the materials. Therefore, the materials would like to retain the original shapes (**Figure 11a**). To demonstrate this assumption, CB(1)/dPDMS(1) living seeds have been made into different kinds of shapes such as bone-like shape, circular shape, and ball for the

symmetric degrowth. While the symmetric degrowth of the ball-shape materials has been described above, the symmetric degrowth of the bone-like shape and circular shape was performed by penetrating a copper wire (d = 0.1mm) to hang them (**Figure 11b**). The results displayed that all the different shape materials retained the shapes well during the self-degrowing and self-growing process, demonstrating that the symmetric degrowth could maintain the original shapes well.

But if the materials were degrown asymmetrically, there would be internal stress within the materials, changing the original shapes. Rectangular shape materials were used for showing the mechanism (**Figure 12a**). When the rectangular shape materials were asymmetrically degrowed by exposing one surface to the open environment, and the other surface to the petri dish, the surface exposed to open environment would like to contract to decrease the volume while the surface exposed to a close environment would like to maintain the original shape. The asymmetric degrowth would introduce internal stress into the materials, causing the materials to reshape to redistribute the internal stress. The self-growing would eliminate the gradient structure, releasing the internal stress, making the reshaped materials recover to the original shape. To confirm this, a rectangular CB(1)/dPDMS(1) living seed was allowed to asymmetrically degrow. The materials bent to the open environment during the degrowing, and recovered to the original shape during the self-growing, which demonstrated the reshaping mechanism (**Figure 12b**). In summary, the shapes of the materials can be flexibly controlled by controlling the D_4 evaporation.

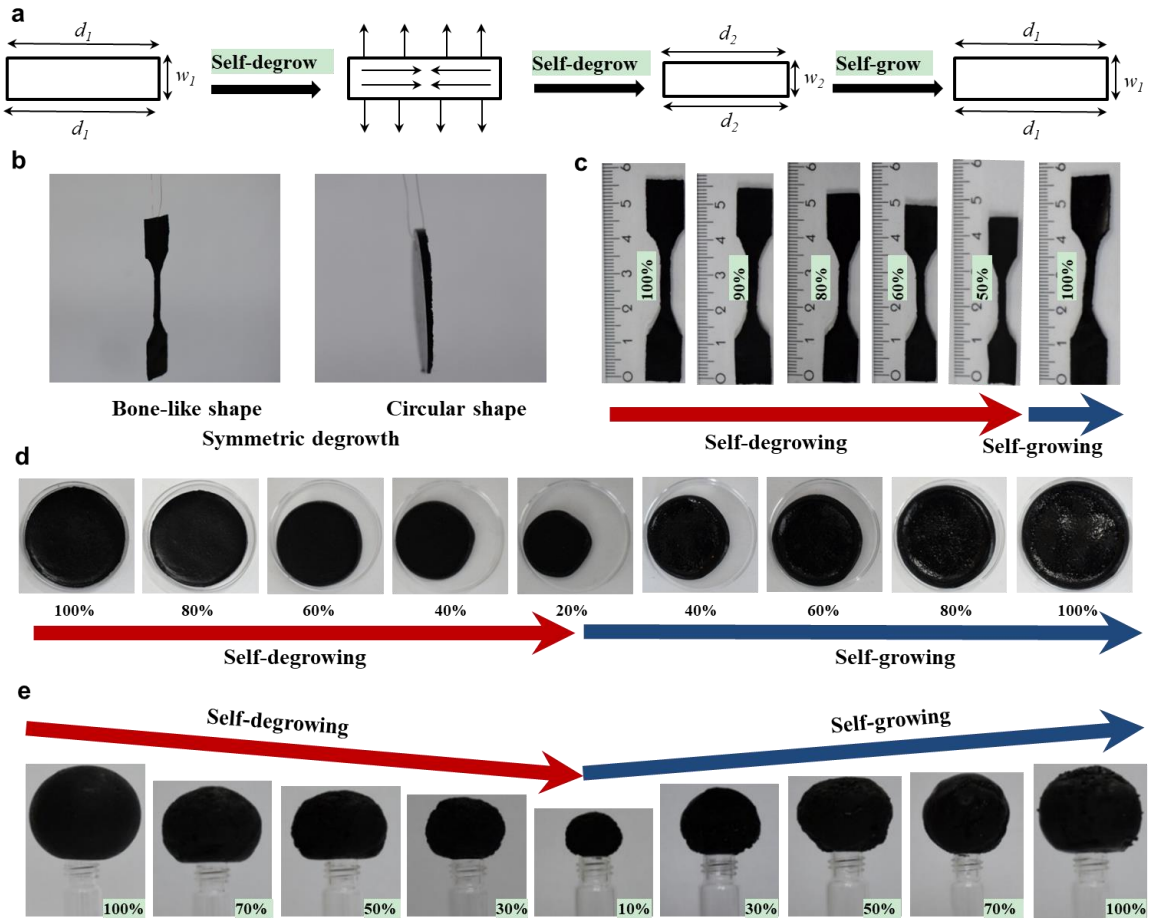

Figure 11. Shape maintenance during self-degrowing and self-growing process. **a)** Schematic diagram showing the mechanism to retain the original shapes during the self-degrowing and self-growing process. b) Pictures showing the method to symmetrically degrow the bone-like and circular shape materials. **c-e)** Demonstration of the shape maintenance ability of the CB(1)/dPDMS(1) livingseeds during the self-degrowing and self-growing process using **c)** A circular shape, **d)** A bone-like shape, **e)** A ball shape.

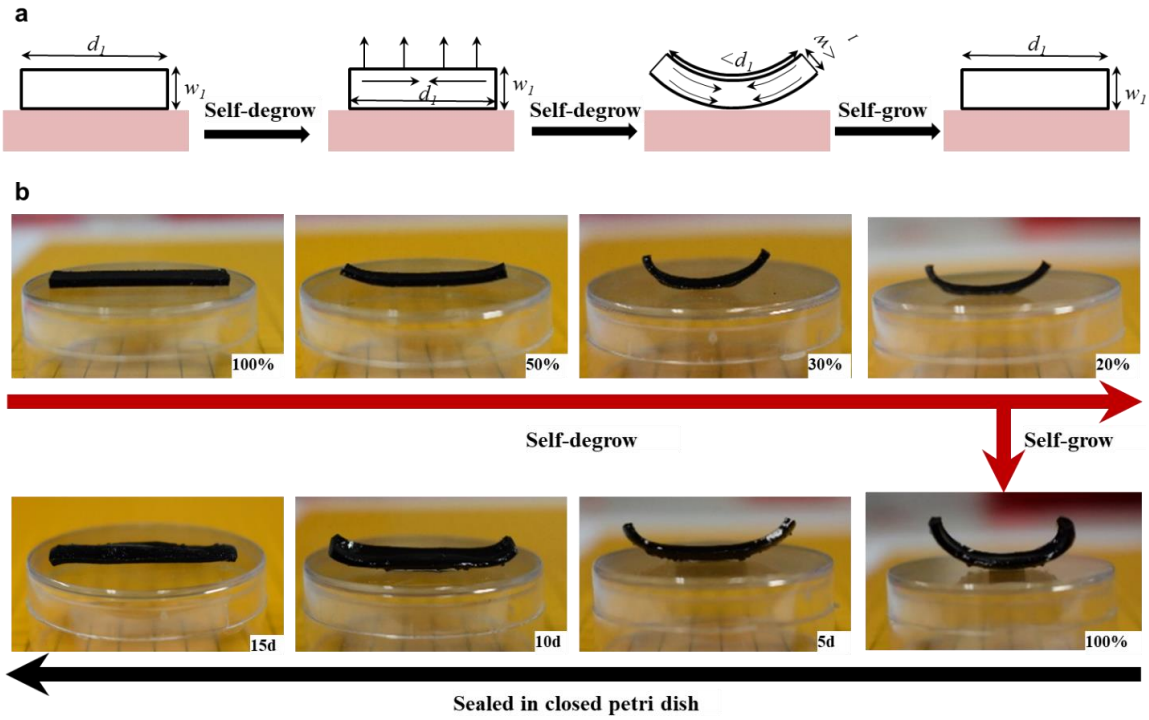

Figure 12. Reshaping of the materials during the self-degrowing process and subsequent recovery in the self-growing process. **a)** Schematic diagram showing the actuation mechanism of CB/dPDMS during self-degrowth and the recovery during self-growing. The surface exposed to the open environment tends to contract while the surface exposed to the petri dish tends to maintain the original state due to the different depolymerization rates, thus a stress gradient is introduced to the sample. In order to distribute the stress evenly within the sample, it will be bent. In the self-growing process, the sample will recover to the original state (no bending) **b)** Demonstration of the schematic diagram described by using the CB/dPDMS living seeds.

2.2.3.3 Mechanical Property Control during Self-growing and Self-degrowing Process

Bone-like CB(1)/dPDMS(1) living seeds were prepared with a thickness of approximately 2 mm. The living seeds were symmetric self-degrowed to 90%, 70%, 50% and 30% of the initial weight, respectively. The stress-strain curves were measured immediately after the materials were fabricated. A gradual increase in the E-modulus was found as the materials continued to degrow (**Figure 13a and Figue**

13b). To be specific, the E-modulus of the CB(1)/dPDMS(1) living seeds was 300 ± 19 KPa which increased to 875 ± 170 KPa for the 30%-self-degrown CB(1)/dPDMS(1) composites. The increase in E-modulus was attributed to the increase in crosslinker density since it was assumed that the crosslinker would not be degraded during the self-growing processing. To confirm this, a CB(1)/dPDMS(1) living seed self-degrowed to 70 wt.% of the initial weight, which was then fed to self-grow at room temperature for 7 days. The E-modulus of the self-grown composite was comparable to the CB(1)/dPDMS(1) living seeds (both are approximately 300 ± 19 KPa), demonstrating that the crosslinker should not be degraded during self-degrowing. Otherwise, the mechanical property could not recover. However, a decrease of the E-modulus was witnessed when the CB(1)/dPDMS(1) living seeds were first depolymerized to 30% of the initial weight and then self-growed to the original weight with D_4 monomers. The E-modulus decreased from 300 ± 19 KPa (CB(1)/dPDMS(1) living seeds) to 202 ± 11 KPa (self-grown material). This was mainly due to the lower crosslinker degree in the restricted space. Though there was a limitation, tuning the mechanical properties of the grown materials could be easily achieved by altering the crosslinker contents in the nutrients. To confirm this, the 70%-self-degrown CB(1)/dPDMS(1) composites were self-grown to 50%, 70%, 90% and 100% of the initial weight with D_4 monomer, D_4 monomer containing 1% triD_4, and D_4 monomer containing 2% triD_4, respectively. The E-modulus of each sample was checked (**Figure 13b**), and it increased with the higher triD_4 contents are incorporated, clearly demonstrating that the mechanical property could be tuned by altering the nutrients contents.

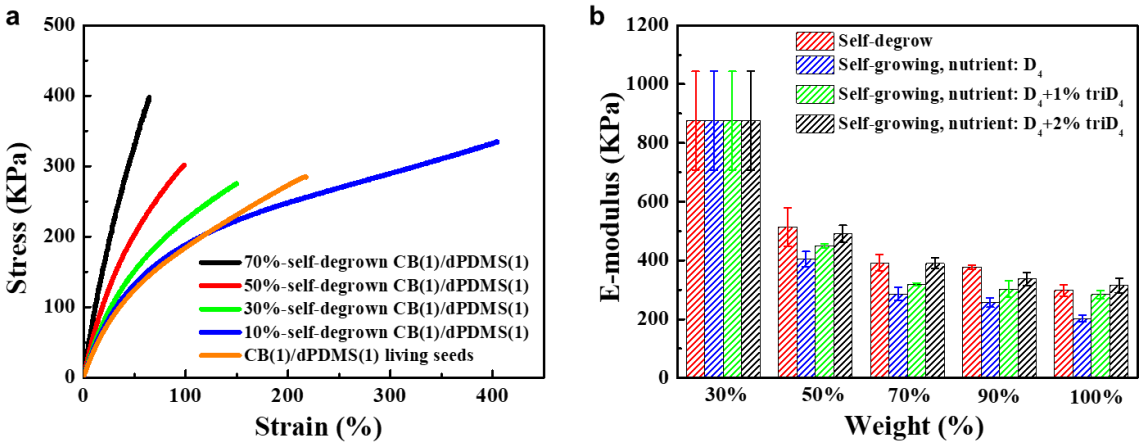

Figure 13. Mechanical property evolution of CB(1)/dPDMS(1) living seeds during self-degrowing and self-growing process. **a)** Stress-strain curves of the CB(1)/dPDMS(1) living seeds and the derived self-degrown CB(1)/dPDMS(1) composites. **b)** E-modulus of the CB(1)/dPDMS(1) composites during the self-degrowing process and self-growing process. For the self-growing, 70%-self-degrown CB(1)/dPDMS(1) composites were used as the starting material, and then grown up with different nutrients containing varying crosslinker contents.

2.2.4 Application of Self-degrowing and Self-growing Materials

2.2.4.1 Self-healing

In the presence of a strong acid/base, the dynamic nature of PDMS networks should lead to excellent self-healing ability. The self-healing behavior of the PDMS(1) living seeds was estimated both by macroscopic observation and by tensile tests. For macroscopic observation, the samples were cut into two pieces and then put together. After the samples were stored in an inert atmosphere for 12 hours, they were stretched. The self-healed samples could be stretched again, indicating they were well self-healed from the cut. The intact and healed samples were cut into typical "dog bone" shape and their mechanical properties were tested using a mechanical testing machine. **Figure 14** shows that the self-healed PDMS(1) living seeds having a self-healing efficiency of 96.5% by the rupturing energy, demonstrating the excellent self-

healing ability of the acid-catalyzed PDMS elastomer.

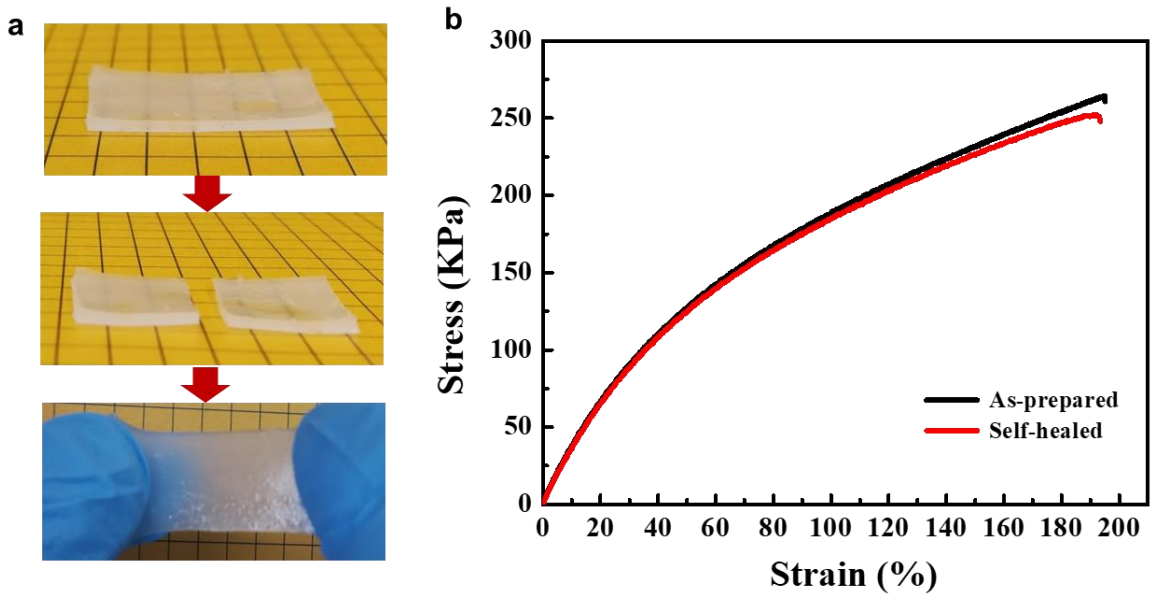

Figure 14. Demonstration of the self-healing ability of the PDMS(1) living seeds. **a) Pictures showing the** self-healing of PDMS(1) living seeds. The cut samples were put together for 12 h at room temperature without any stimuli. **b)** Mechanical tests for the intact and the self-healed PDMS(1) living seeds.

2.2.4.2 Regeneration

Regeneration is quite common in biology. For example, Geckos would detach their tails when grabbed by the predators and they can re-grow a new tail within 30 days.[125, 126] Stem cells in the human body also have the ability to regeneration.[127] When the Planarians are cut into pieces, each of the pieces could regenerate into a new body, as shown in **Figure 15a**. Herein, regeneration ability was also mimicked using the acid-catalyzed PDMS. First, one 8cmx7cmx6cm cubic PDMS(1) living polymer seed was fabricated and cut symmetrically into eight pieces with a uniformed size of 4cmx3.5cmx3cm. Feeding the small species in the nutrients (D_4 monomer with 1 wt.% crosslinker) until the weight recovered to the original weight and then took them out,

stored in a sealed petri dish for 7 days. It was found that each small species re-grows to a large cubic material (**Fig. 15b**), with the shapes being well controlled (**Figure 15c**).

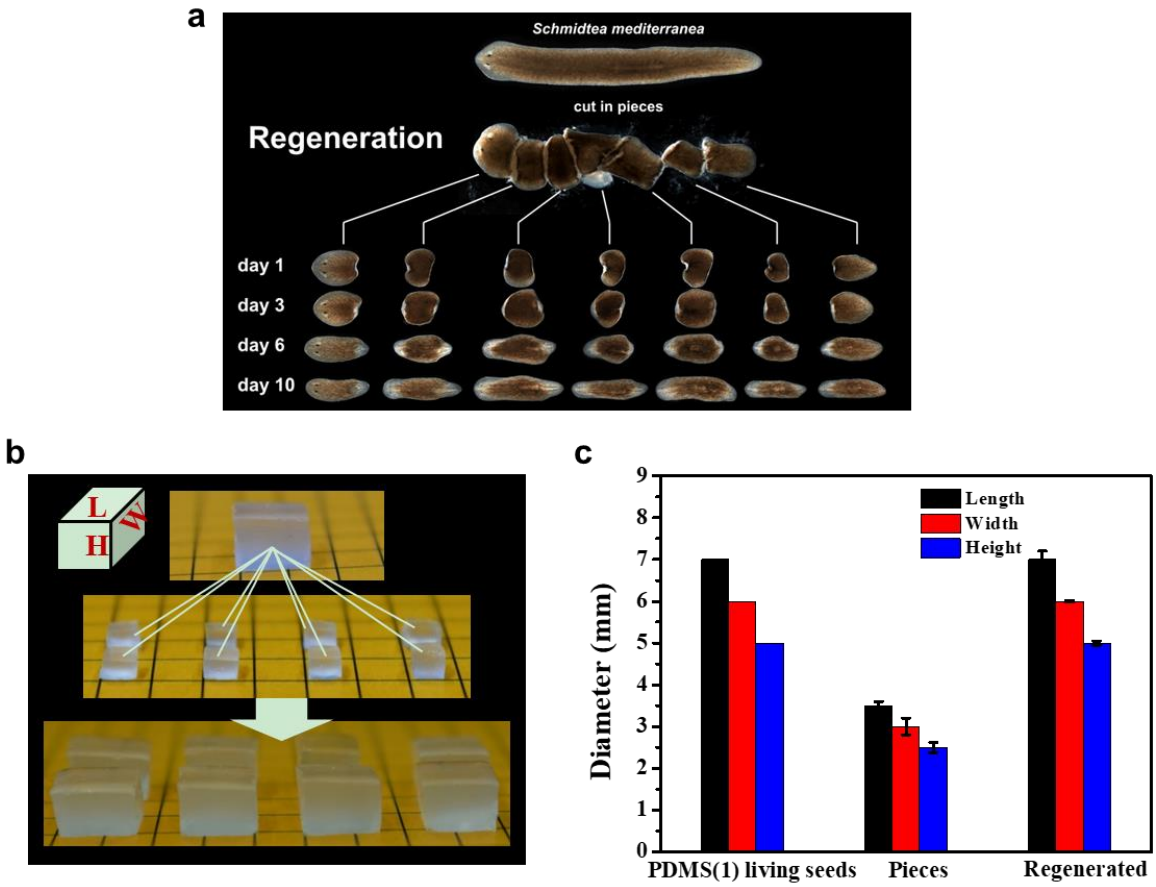

Figure 15. Bio-inspired regeneration ability of the acid-catalyzed PDMS. **a)** Regeneration ability of the planarian. **b)** The regeneration ability. A big PDMS(1) living seed was then cut into 8 small pieces, which could self-grow to 8 big samples as the same as the PDMS(1) living seed in size. **c)** Shape maintenance ability during regeneration.

2.2.4.3 Reconfigurable Surface Topography

Adaptive materials with reconfigurable surface topography in response to external stimuli have attracted considerable attention in various fields, such as switchable adhesion and friction and controlled droplet collection.[128-134] Currently, a reconfigurable topography surface could be achieved either by reconfiguring surface geometry or by reversibly altering physical and chemical properties.[135] Magnetic field,

heat, and light are commonly used stimuli to trigger the surface topography reconfiguration. Here, a new methodology employing only the flowing gas to reconfigure the surface topography using the self-growing and self-growing materials is presented. A SiO_2(3)/dPDMS(1) living seed was used to demonstrate the process and the mechanism to reconfigure the surface. The circular shape SiO_2(3)/dPDMS(1) living seed was allowed to asymmetrically degrow. The materials turned from translucent to opaque when the materials self-degrowed (**Figure 16a and Figure 16b**). The opaque composites were attributed to the formation of the porous SiO_2 aerogels which were caused by the removal of the polymers. The porous SiO_2 aerogels also changed the surface property, such as the hydrophobicity. The contact angle of the SiO_2(3)/dPDMS(1) living seed is about 117^o while it increases to 152^o for the 30%-self-degrown SiO_2(3)/dPDMS(1) composites (**Figure 16c and Figure 16d**). Self-growing of the 30%-self-degrown SiO_2(3)/dPDMS(1) composites with D_4 monomers for 1 day at 70^{o}C in the oven will transform opaque films to translucent again (**Figure 16b and Figure 16e**), with the contact angle recovering to 113^o for the self-grown SiO_2/dPDMS composites.

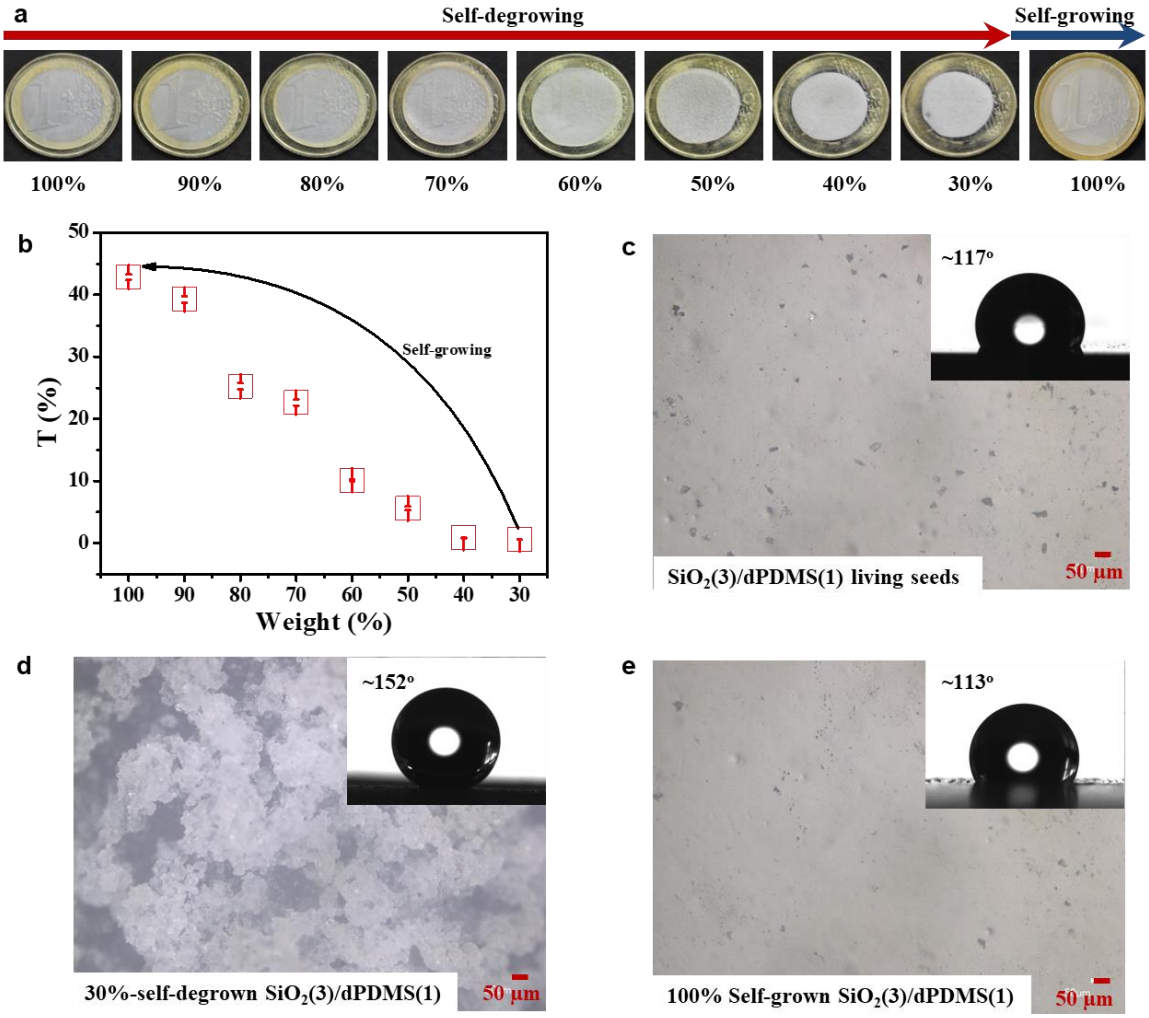

Figure 16. Reconfigurable surface topography. a) Pictures showing the transparency change during the self-degrowing and self-growing process for SiO_2(3)/dPDMS(1) living seeds (about 1mm in thickness, asymmetric self-degrowed). **b)** The transmittance change for the SiO_2(3)/dPDMS(1) living seeds during the self-degrowing and self-growing process. **c)** Optical images of the surface for the SiO_2(3)/dPDMS(1) living seeds. Inset shows the contact angle using 5µl water. **d)** Optical images of the surface for the 30%-self-degrown SiO_2(3)/dPDMS(1) composites. Inset shows the contact angle. **e)** Optical images of the surface for the self-grown SiO_2(3)/dPDMS(1) composites. Inset shows the contact angle.

In addition, the ability to localize the materials' degrowth by evaporation lithography was demonstrated. Evaporation lithography is a novel technique to pattern soft materials by controlling the migration of particles in the drying of a liquid phase. That

is to say, liquid phase is normally the starting materials and functionalized solid soft materials are prepared during the solvent evaporation. Currently, solid polymer composites were employed as the starting materials and patterned the materials using one simple method. A SiO_2(3)/dPDMS(1) living seed was packaged as shown in Figure 17, masks made of PTFE were put on the top of the surface, which was heated in the hood at 40 ^oC. After 12 hours, the polymer composites obtained in this way displayed patterned optical and hydrophobic properties. The covered regions remain translucent while the uncovered parts are opaque because of the depolymerization. The covered regions are hydrophobic whereas the uncovered regions are superhydrophobic. By changing the mask shapes, different kinds of patterns could be coated on the polymer composites, such as the rectangles and rounds (**Fig. 17**). More interestingly, these patterns could be easily erased during the self-growing process. In conclusion, we reversibly patterned the coating on the polymer composites by using the solid polymer as the starting materials, which can be applied to localize materials functions such as optical, and anti-fouling properties.

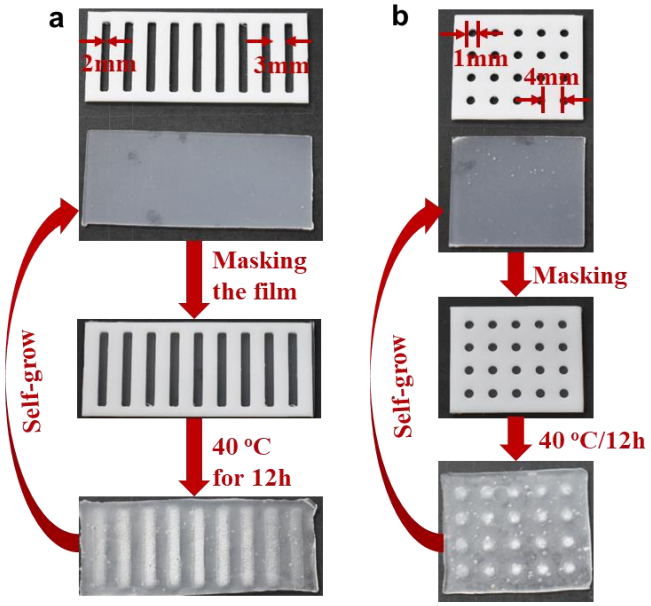

Figure 17. Local control of the self-degrowing with different masks using SiO_2(3)/dPDMS(1) living seeds.

2.3 Conclusion

In this chapter, a polymeric material that is able to grow and degrow in a controlled manner is described. The living PDMS elastomers self-degrow when they are put in the open environment and self-grow when they are given the nutrients and sealed in a closed environment. We have demonstrated that the self-degrowing is attributed to the oligomer evaporation-induced depolymerization. More interesting, the polymer chains maintain the molecular weight during the depolymerization.

We also have proved that the addition of particles with protonatable groups into the dynamic PDMS can accelerate the self-degrowing kinetics, which has been revealed by the polymer composites filled with carbon black and silica. The particles could stabilize the triflic acid and prevent its evaporation, therefore, the polymer composites maintain the dynamic property and depolymerize faster.

Using the self-growing and self-degrowing strategy, the structure, shape, mechanical property could be flexibly controlled during the self-growing and self-degrowing process.

- Structure control: During the self-degrowing process, the polymer composites normally first form a gradient structure, and finally form the homogenous structure. The gradient structure turns into a homogeneous structure during the self-growing process. Moreover, we can also eliminate the gradient structure by simply heating in a sealed container.
- Shape Control: The shapes of the materials could be controlled by changing the self-growing mode, i.e., asymmetric self-degrowth and symmetric degrowth. In the symmetric self-degrowth mode, the polymeric materials could retain the original shapes well and in the asymmetric self-degrowth mode, the elastomers could be reconfigured into 3D complex shapes.

- Mechanical property control: The elastomers become stiffer and stiffer during the self-degrowing process as the crosslinker content increases when the polymer matrix degrows, and the mechanical property could be flexibly controlled during the self-growing process by changing the nutrient component.

The self-degrowing and self-degrowing strategy has been used to reconfigure the surface topography of the polymeric materials. The SiO_2/dPDMS composites turned from hydrophobic (contact angle: 117^o) to superhydrophobic (contact angle:152 ^{o}) during the self-growing process, and recovered to hydrophobic (contact angle: 113^o) after self-growing to the original weight. In addition, we have proved that the self-degrowth can be controlled by using the masks and therefore, the polymeric materials can be patterned. Moreover, the patterns would disappear during the self-growing process, providing repeated performance.

2.4 Experiment Section

a. Materials and Methods

Octamethylcyclotetrasiloxane (D4, 98%,Gelest), trifluoromethanesulfonic acid (99%, Sigma-Aldrich), heptamethylcyclotetrasiloxane (tech-95, Gelest), trivinylmethylsilane (95%, Gelest), tetramethylammonium siloxanolate (Gelest), platinum(0)-1,3-divinyl-1,1,3,3-tertramethyldisiloxane in xylene (Pt catalyst, 2% of Pt, Sigma-Aldrich), perylene-3,4,9,10-tetracarboxylic dianhydride (97%, Sigma-Aldrich), 4,4'-dihydroxyazobenzene (97%, Synthon Chemicals GmbH) and solvents were used as purchased. Carbon black pearls 2000 (Carbot) was offered for experiment research. Solution ^{1}H spectra were measured in $CDCl_3$ solution at 25 ^{o}C using Varian M400 400 MHz or I500C 500 MHz spectrometer. The mechanical properties were tested on

Zwick. The solid samples were investigated using a FEI (Hilsboro, OR, USA) Quanta 400 FEG Scanning Electron Microscope (SEM) operating at 10 kV accelerating voltage. Secondary (SE) electron images were collected in high vacuum mode. X-Ray spectral (EDAX) analysis of the solid samples was performed using an EDAX Genesis V6.04 system. Gas chromatography–mass spectrometry (GC-MS) measurements were performed with a GC-MS Shimadzu QP 2010 using ZB-5HT-Inferno columns and NMR results were collected with a Bruker 300 MHz nuclear magnetic resonance equipment. The number-average molecular weight (Mn) and polydispersity index were measured with an Agilent HPC chromatography (GPC) system using a ZB-5HT-Inferno column with a series of silicone oils as standard samples. The concentrations for GS-MS and GPC were 1mg/ml in toluene. Carbon black/dynamic PDMS composites for ^{1}H NMR and GPC were first drawn into a syringe and filtered using a 0.45 μm syringe filter to remove the CB black powders before characterization.

b. Synthesis of 1,1,1-tri(2-heptamethylcyclotetrasiloxane-yl-ethyl)-methylsilane (triD$_4$)

To the mixture of heptamethylcyclotetrasiloxane (30 mmol, 8.46g) and trivinylmethylsilane (10 mmol, 1.24g) was added Pt catalyst xylene solution (10 ul) under stirring (**Figure 18**). The mixture became viscous and a yellow liquid was obtained after 30 min. The obtained product (a mixture of triD4 and its isomers) was used directly without any purification. ^{1}H NMR (400 MHz, $CDCl_3$, δ ppm): 0.500-0.342 (m, 12H, CH_2), 0.100 (s, 63H, CH_3), -0.076 (s, 3H, CH_3). The isomer shows peaks at 1.0 ppm (d, J = 12 Hz, $CHCH_3$ on isomer) and the integration of the peaks suggests that the isomer/triD$_4$ ratio is 0.23/1.

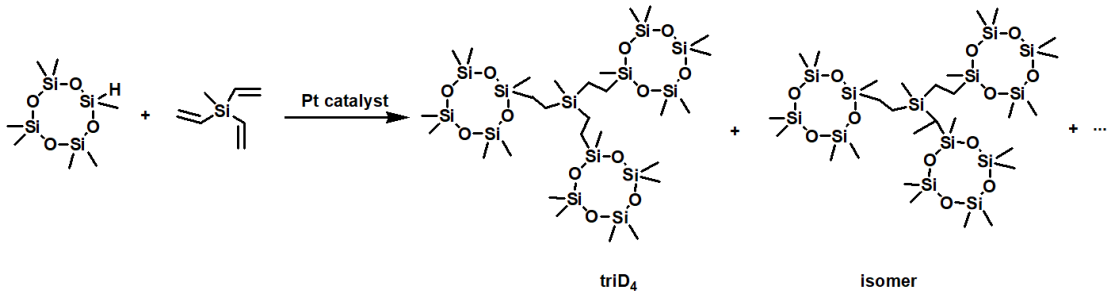

Figure 18. Synthesis of triD4. The products include triD4 and its isomers. All the isomers have similar branch structure and act as triD4.

c. Preparation of Living Seeds and Polymer Composites

PDMS living seeds: This refers to the as-prepared dynamic PDMS initiated by the triflic acid. To the solution (2~20 mL) of D4 and triD4 was added CF_3SO_3H. A highly viscous liquid formed immediately. After 5 min, an elastomer formed, which was sealed and stored for 12 hours before use. Typically, the living polymers made from a D4 solution containing 1 wt% triD4 and 1 wt% CF_3SO_3H.

Particle/dPDMS living seeds: This refers to the as-prepared particle/dynamic PDMS composites initiated by the triflic acid. For example, carbon black was first dispersed homogenously with D4 and triD4 mixture by sonification before the addition of CF_3SO_3H. The polymer composites were also sealed for 12 hours before use. Silica/dPDMS living seeds were prepared as the procedure.

d. Deactivation of PDMS and CB/dPDMS Living Seeds

PDMS living seeds and CB/dPDMS living seeds were immersed in triethylamine for 4 hours and then the absorbed triethylamine was removed under vacuum. After three swelling-drying cycles, the materials were fully deactivated. Another way to deactivate living materials is to coat magnesia powder on the surface of the materials and keep them coated for 10-15 hours (typically, overnight). This method was reported previously.

e. Washing

The PDMS and CB/dPDMS living seeds were immersed in a toluene solution containing 1 wt% triethylamine to stop the acid-catalyzed reactions and remove the unreacted reagents. After being immersed for two hours (this time proved sufficient for the samples to become fully swollen), the samples were dried under vacuum at room temperature. This washing process was repeated three times and the weights of the dried samples were recorded.

Chapter 3

3. Self-healable and Recyclable Tactile Force Sensors with Post-tunable Sensitivity

Note: This Chapter has been submitted as a manuscript: Self-healable and Recyclable Tactile Force Sensors with Post-tunable Sensitivity, Xiaozhuang Zhou, Xuan Zhang, Huaixia Zhao, Baiju P. Krishnan, Jiaxi Cui, 2020

Abstract: It is challenging to post-tune the sensitivity of a tactile force sensor. Herein, we report a facile method to tailor the sensing properties of conductive polymer composites by utilizing the liquid-like property of dynamic polymer matrix at low strain rates. The idea is demonstrated by dynamic polymer composites (CB/dPDMS) made via evaporation-induced gelation of the suspending toluene solution of carbon black (CB) and acid-catalyzed dynamic polydimethylsiloxane (dPDMS). The dPDMS matrices allow CB to redistribute to change the sensitivity of materials at the liquid-like state, but exhibit typical solid-like behavior and thus could be used as strain sensors at normal strain rates. We show that the gauge factor of the polymer composites can be easily post-tuned from 1.4 to 51.5. In addition, the dynamic polymer matrices also endow the composites interesting self-healing ability and recyclability. Therefore, we envision that this method could be useful in design of various novel tactile sensing

materials for many applications.

3.1 Introduction

Electronic skin (E-skins) is attracting more and more attention because of their potential applications in soft robotics,[136] prosthetics,[137, 138] health monitoring,[139, 140] and various wearable devices.[141] It is designed to mimic the human sophisticated somatosensory system by transducing external stimuli (such as light, mechano-force, heat and pH) into electrical signals. Essential to this transduction, flexible materials that could sense tactile force should be built into E-skin to mimic the force-sensing ability of the human skin. Human skin contains four kinds of mechanoreceptors to realize different characteristics of force perception, i.e. two slow adapting receptors (SA-I and SA-II) response to static force and two fast adapting receptors (FA-I and FA-II) measure the dynamic force.[142-144] This complex system allows the skin to tune its sensitivities to perceive a wide range of mechano-stimuli. To fully construct such capability of human skin for various applications, several strategies have been developed to fabricate flexible tactile force sensors with tunable sensitivity,[145-149] such as tailoring the material compositions of conductive polymer composites[145, 146, 149] or controlling the structure of the materials.[150-152] However, these strategies suffer from high costs, complicated fabrication processes, poor controllability, and limited tunable range of sensing force, making them difficult for practical applications.[153, 154] Therefore, a facile method to precisely tune the force-sensing property of flexible tactile force sensors in a large range is still desirable.

In addition to tunable sensitivity, the recoverability of sensing functions or even full recyclability after the tactile force sensor has been damaged is other important

properties for practical applications. Introducing these capabilities into flexible tactile force sensors can significantly elongate their service time and then reduce waste. To this end, both concepts of self-healing[155] and recycling[156] are applied to fabricate flexible tactile force sensors by using the composites made from dynamic polymer matrices (dynamic composites), leading to the creation of many self-healable or/and recyclable sensors. Despite this progress, it is still a challenge to combine these capabilities to force-sensing materials that could precisely tailor the sensitivity.

Here, a strategy for tuning the sensitivity of strain-sensing materials was reported. This strategy is based on the utilization of the unique mechanical properties of dynamic polymer networks (**Figure 1a**), i.e. showing liquid-like behavior (storage modulus, G'<G", loss modulus) at an extremely low strain rate due to the reconfiguration of polymer networks but solid-like behavior (G'>G") at a normal strain rate (5-400 Hz).[157, 158] In practical applications, the solid-like materials could fix conductive particles in them to show strain-sensitivity, i.e. reversibly breaking the conductive pathways under a strain (**Figure 1b, c**). In the liquid-like state, the polymer matrices would allow conductive particles entrapped in the matrices to move to re-distribute when the sample is deformed.[159-161] Since the conductivity of the composite depends on the arrangement of conductive particles in the matrices, we assume that such redistribution of conductive particles should lead to a significant change in the force sensitivity. A polymer composite consists of carbon black (CB) and dynamic covalent polydimethylsiloxane (dPDMS) elastomer (**Figure 1d**) is used to demonstrate this assumption. In the presence of the catalyst, the silicone is in an equilibrium state. Continuous chain exchange occurs at room temperature, which enables not only the reorganization of CB in a relaxation process but also self-healing behavior after

damage. The equilibrium of siloxane matrices can also be utilized to induce depolymerization for recycling the materials (**Figure 1e**).

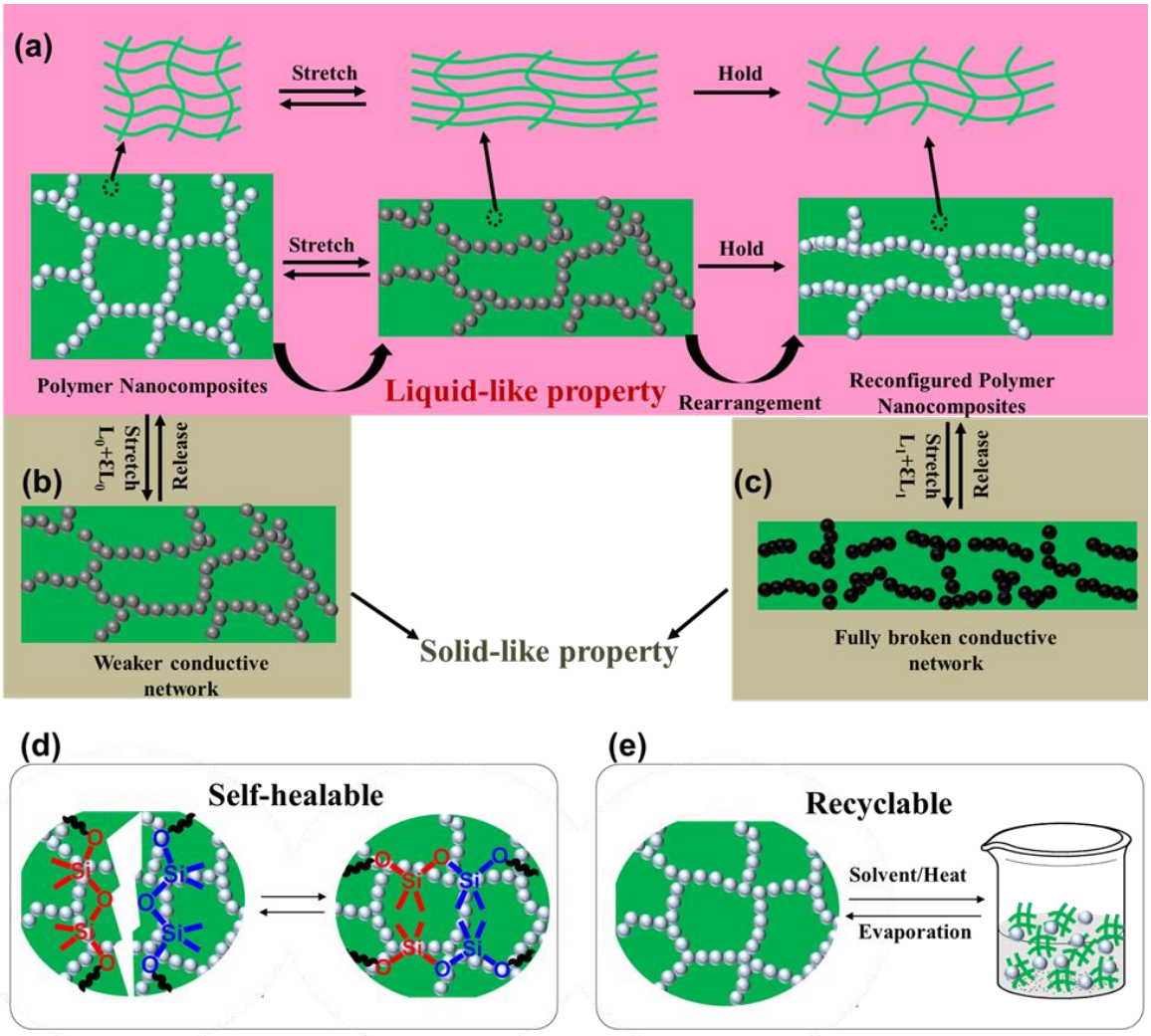

Figure 1. Schematic diagram showing the methodology for tailoring the sensitivity and sensing range by mechanical stretching **a)** Liquid-like property at a fixed strain: the reshuffle of the polymer chain and rearrangement of particle networks. **b)** The electrical response of sensors made from the composites versus strain at high strain rates, **c)** The electrical response of sensors made from the reconfigured polymer composites versus strain at high strain rates. **d)** The self-healing mechanism of the CB/dPDMS composites. **e)** Recycling mechanism of the CB/dPDMS composites.

3.2 Results and Discussion

3.2.1 Preparation of CB/dPDMS Composites

The CB/dPDMS composite was prepared through the evaporation-induced gelation process of the suspending solution of CB in the mixture of octamethylcyclotetrasiloxane (D_4, monomer), 1,1,1-tri(2-heptamethylcyclotetrasiloxane-yl-ethyl)-methylsilane ($triD_4$, crosslinker), triflic acid (catalyst), and toluene (solvent). A toluene solution was selected because CB could disperse well in it. In the solution, D_4 and $triD_4$ could undergo acid-catalyzed ring-opening copolymerization to form siloxane network clusters. In the presence of triflic acid, the siloxane was in an equilibrium state.[101] Therefore, with the evaporation of toluene, these siloxane clusters integrated together to form an elastic composite. Such evaporation-induced gelation process allowed us to prepare the composite to various shapes in different scales via facile casting or molding methods. The obtained composite is denoted as CB(*x*)/dPDMS(*y*) where *x* is the weight percentage (%) of CB in the composite and *y* is the weight concentration of crosslinker in dPDMS. **Figure 2a** displays a specimen of CB(1)/dPDMS(1) with a diameter of 5 cm prepared in a petri dish.

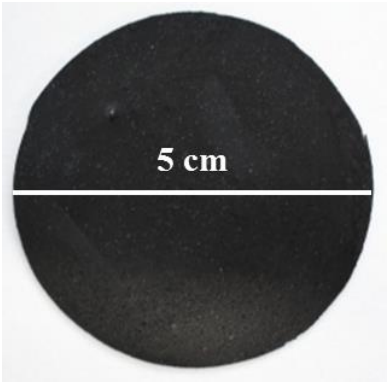

Figure 2. Photographs showing the as-prepared CB(1)/dPDMS(1) composites

3.2.2 Structure and Properties of CB/dPDMS Composites

Scanning electron microscopy (SEM) was used to study the morphology of the obtained composite. **Figure 3a** shows the cross-section of CB(1)/dPDMS(1) composites. A fractal structure was observed, in which the aggregates of CB particles were connected together to form networks in the dPDMS matrix. Similar fractural structures formed in all test samples with different CB contents (0.5-10 wt%, **Figure 3a**). We attributed the formation of such conductive networks to the synergic consequence of acid-induced aggregation of CB and solvent evaporation-induced gelation. CB particles could disperse well in the toluene solution without acid. Addition of acid into the solution not only trigger polymerization but also induce aggregation of CB particles, since CB particles would absorb acid molecules on their surface to increase surface hydrophilicity. The aggregation was accompanied with toluene evaporation and accumulative structures were then fixed in the gelation process. Here we expected the alternation of surface hydrophobicity, rather than the increase of polymer fraction, led to the aggregation. Control experiments were conducted to confirm this idea (**Figure 3b**). To a suspending solution of CB in the mixture of toluene and D_4, crosslinkable PDMS or acid was added. It was found that the addition of acid-induced fast sedimentation of CB but the addition of PDMS did not.

The conductivity (σ_e) of CB/dPDMS composites with different filler concentrations was measured (**Figure 3c**). An exponential relationship between the conductivity and the filler concentration was observed, which can be described by the equation (1)[162]:

$$\sigma_e \propto (x - x_c)^{n_e} \quad (1)$$

where x is the weight fraction of the filler, x_c is the critical weight fraction at the percolation threshold and n_e is the scaling exponent relating to the conductivity to the

weight fraction. Analysis of the data in **Figure 3c** using Eq. 1 yields a percolation threshold of 0.14 wt.% and an exponent n_e= 1.74. The exponent is very close to the theoretical value of three dimensional (3D) conductive networks (n_e= 2).[163] It was attributed to the formation of CB conductive networks within the polymer composites. Note that the critical fraction (x_c) is remarkably lower than previously reported values (3-10wt.% for CB/PDMS composites).[164] It could also be explained by the aggregated CB conductive network structure which made the polymer composites conductive even at a relatively low concentration.

Figure 3d shows the tensile E-modulus (Young's modulus) of the samples. The pristine dynamic PDMS exhibits an E-modulus of 230 ± 29 KPa. The addition of low loading CB (0.3-1 wt.%) into the matrices scarcely increases their E-modulus. Clear mechanical reinforcement was observed when the filler content was up to 2 wt.% and 5wt.% (285 ± 25 KPa and 462 ± 31 KPa, respectively). In addition, the modulus of CB/dPDMS could be remarkably tuned by varying the crosslinking degree of the dPDMS matrix (e.g. from 0.1 wt.% to 5 wt.%, **Figure 3e**).

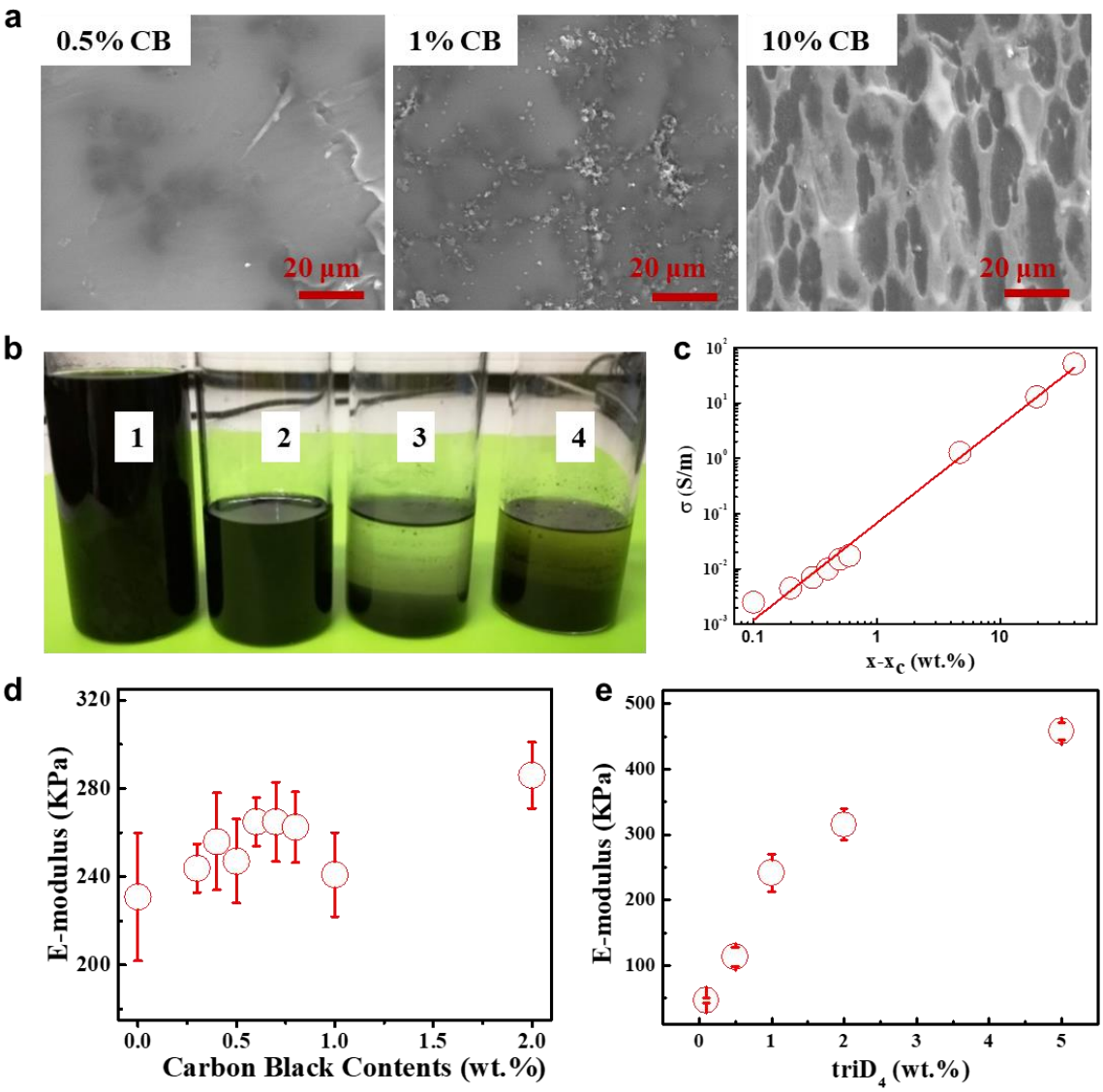

Figure 3. Structure and properties of CB/dPDMS composites. **a)** SEM images of cross-section of the CB(*x*)/dPDMS(1) composites showing a network of carbon black particles. **b)** Pictures showing the sedimentation rates of CB in the toluene/D_4/triflic acid (5g/1g/0.01g) mixture solution added with 1) linear PDMS polymers, 3) triflic acid, 4) D_4 monomer and triflic acid, 2) is the control sample. **c)** Electrical conductivity of CB/dPDMS(1) composites as a function of the parameter x-x_c, where x is the weight fraction and x_c is the electrical percolation threshold. **d)** E-modulus of CB(*x*)/dPDMS(1) composites with different CB contents. **e)** E-modulus (Young's modulus) of CB(1)/dPDMS(*y*) composites with different triD_4 contents.

3.2.3 Sensing properties of CB/dPDMS composites

The electrical resistance response of the CB/dPDMS composites to the force at the solid-state was investigated. It is known that the sensing property of the dynamic polymer composites is related to the viscoelastic property.[24] We thus assumed that CB content should be a good parameter to tune the sensing property since the viscoelastic property of the CB/dPDMS composites varied with it. Samples of CB(*x*)/dPDMS(1) where *x* ranges in 0-2 wt.%, were prepared for this study. The storage modulus (*G'*) is higher than loss modulus (*G"*) for all the samples in the tested frequency range of 0.0628-157 rad/s (**Figure 4a**), implying typical solid-like feature at the normal strain rates. In our test condition (strain amplitude: 0.1%-100%; frequency: 6.28 rad/s), the *G'* and *G"* of CB($x \leqslant 2$)/dPDMS(1) with different *x* display similar curves, i.e. stable in low amplitude and showing a shear-thinning in high amplitude (decrease in *G'* but increase in *G"*, **Figure 4b**). The similar curves of *G'* and *G"* suggested that the addition of CB in the range of < 2% has a negligible effect on the viscoelasticity of the polymer composites, though slightly increase of both *G'* and *G"* was observed.

The sensing property of CB(*x*)/dPDMS(1) was investigated. Electrical resistance (*R*) of as-prepared CB/dPDMS composites at a loading rate of 20 mm/min was collected to evaluate their response to strain. **Figure 4c** shows the relative resistance change, $\Delta R/R$, of the CB/dPDMS composites with strain. The CB(0.5)/dPDMS(1) and the CB(1)/dPDMS(1) display nearly the same $\Delta R/R$-ε curves, indicating that the CB contents less than 1% have a negligible effect on the sensing property of the CB/dPDMS composites. This could be attributed to the similar viscoelasticity of the samples with < 1% CB. In addition, the exponential variation of $\Delta R/R$ implies that the conductive network was broken during the stretching, as indicated in the graphene

putty.[24] When the CB content was further increased to 2 wt%, $\Delta R/R$ increased linearly with strain, showing a significantly different change from the CB (0.5 or 1)/dPDMS(1). The sensitivity can be quantitatively described by the gauge factor (GF, defined as GF = ($\Delta R/R$) /ε, where $\Delta R/R$ and ε are relative resistance change and applied strain, respectively). The GF of CB(2)/dPDMS(1) is about 2.13. This small GF indicates that the resistance change was attributed to geometry change of the sample, rather than the breaking of the conductive CB network under the strain. In other words, stretching could not break the connected CB network for the CB(2)/dPDMS composites. It might due to the strong CB network interaction made from high CB loading such that the CB network could resist the stretching.

The viscoelasticity and sensitivity of CB(*x*)/dPDMS(*y*) also varied with y (crosslinker content). Samples of CB(1)/dPDMS(y) where y is tuned from 0.1% to 5%, were prepared for this study. They all display the solid-like feature (*G'* > *G"*) in the tested frequency range of 0.0628-157 rad/s (**Figure 4d**). As shown in **Figure 4e**, the samples with various crosslinker display significantly different curves, especially those of *G"*, indicating that crosslinking degree was an efficient parameter to tune the viscoelastic property of the CB/dPDMS composites. The sensing property of the CB(1)/dPDMS(y) was also measured at the loading rate of 20 mm/min (**Figure 4f**). It was found that $\Delta R/R$ of CB(1)/dPDMS(y) with 0.1% ≤ y ≤ 2% increased exponentially with strain and the sensitivity increases with y. This phenomenon could be explained by the R-strain model, assuming that $\Delta R/R$ is the conflicting effect of the force-induced breaking of the conductive network and viscous polymer matrix-induced reforming of the CB network.[24] The force-induced breaking of the conductive particles is assumed to increase the resistance while rearrangement of the CB particle would decrease the

resistance. Since increasing crosslinking degree enhanced the solid feature of the samples (**Figure 4e**), the resistance change is more pronounced in CB(1)/dPDMS(y) with higher y. CB(1)/dPDMS(5) displays a linear increase of $\Delta R/R$ with a GF of 1.98 (**Figure 4f**), indicating that the connected CB network was not broken during stretching. Since CB(1)/dPDMS(5) behaved more like a good elastomer (low *G"*, **Figure 4e**), the unbroken CB network under stretching could be explained by one potential reason that the elastic polymer composites could not have the Payne's effect as the viscoelastic polymer composites, breaking of the particle interaction under stretching.[165]

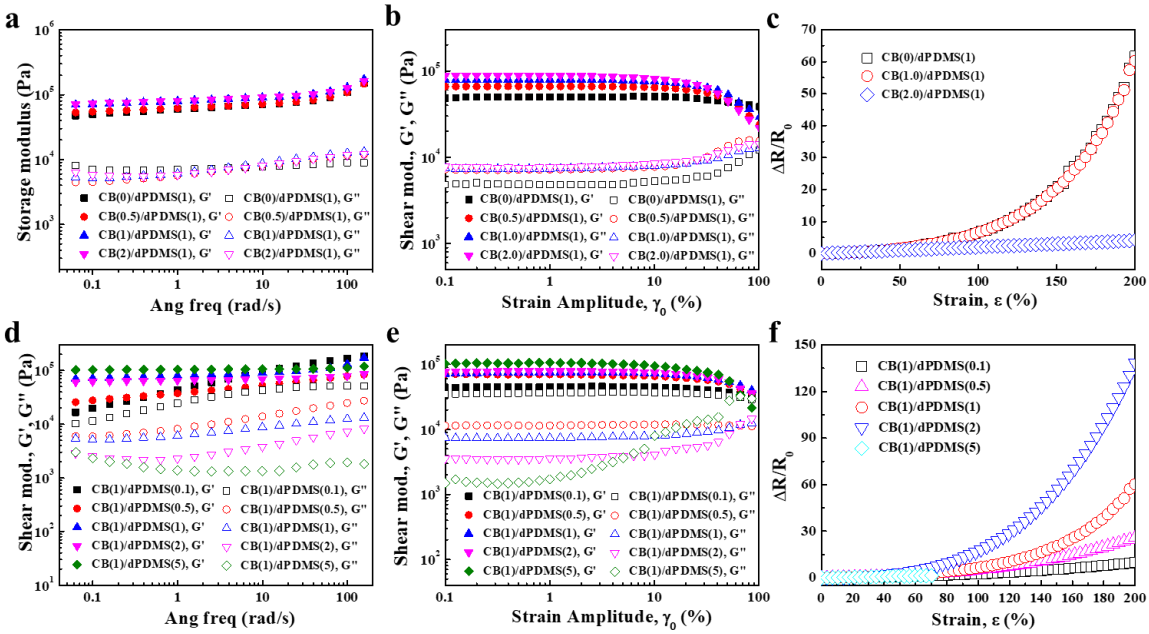

Figure 4. Mechanical and sensing properties of the CB/dPDMS composites. **a)** Storage modulus (G') and loss modulus (G") versus the angular frequency for the different CB(*x*)/dPDMS(1) composites with varying CB. **b)** *G'* and *G"* versus the oscillation strain amplitude for the CB(*x*)/dPDMS(1) composites with different CB (ω = 6.28 rad/s). **c)** Electrical response of the sensors, made from CB(*x*)/dPDMS(y) composites with different CB contents (Loading rate: 20 mm/min). **d)** Shear stroage (G') and loss (G") moduli of CB/dPDMS composites as a function of angular frequency with different CB contents. **e)** Shear stroage (*G'*) and loss (*G"*) moduli of CB(1)/dPDMS(*y*) composites as a

function of oscillation strain amplitude with different crosslinker contents (ω = 6.28 rad/s). **f)** Electrical response of the sensors, made from CB(1)/dPDMS(*y*) composites, versus the strain (Loading rate: 20 mm/min).

3.2.4 Tuning the Sensitivity of the CB/dPDMS Composites

CB(1)/dPDMS(1) was selected to demonstrate the modulation of sensitivity via mechanical treatment. We firstly checked the liquid-like feature of the sample at the low strain rates by rheological measurements starting from a frequency of 5×10^{-4} rad/s (**Figure 5a**). At the frequency lower than 8×10^{-4} rad/s, the loss modulus is higher than the storage modulus, implying a liquid-like state, while at the frequency of $>8\times10^{-4}$ rad/s, the sample shows a higher storage modulus, indicating a solid-like state. Such unique mechanical property of CB(1)/dPDMS(1) allows it to behave as a normal solid in the absence of stimuli so that they can maintain the original shapes but like a liquid under constant pressure to allow the redistribution of the CB particles (**Figure 5b**). Under the constant pressure, stress relaxation occurred in CB/dPDMS via chain exchange to induce permanent deformation. Stress relaxation measurement was conducted to study the reconfiguration rate of CB/dPDMS composite. As shown in **Figure 5c**, the stress was completely relaxed in 4.5 h, leading to permanent deformation. During this relaxation, redistribution of CB particles was expected. To confirm this, the resistance was tracked during the stress measurement (**Figure 5d**). The resistance jumped to a high value when the sample was stretched. In the process of stress relaxation with constant strain, the resistance gradually decreased. The jump was attributed to the disconnection of the CB network in straining while the decrease was assigned to the rearranging of CB particles to reform a new connecting structure. The rearrangement of the CB particles was also supported by SEM results in which

the morphology of CB network structure changed after the relaxation **(Figure 5e)**. Such change in resistance has been found in graphene putty and Ag flakes/PDMS-4,4′-methylenebis(phenyl urea) $(MPU)_{0.4}$-isophorone bisurea units $(IU)_{0.6}$ polymer composite,[24, 25] but high hysteresis effect is obversed in the material, making them not suitable to be used for the reconfigurable sensors.

The rearrangement of the CB network under a fixed strain was utilized to tune the sensitivity of the polymer composite. To demonstrate this concept, CB(1)/dPDMS(1) was stretched to different strains to create different arrangements of CB particles. Cyclic tensile stress-strain measurement was used to study the mechanical properties of the as-prepared and reconfigured composites at a high strain rate. Under a loading rate of 20 mm/min, small hysteresis loops were observed in the cyclic tensile test with a strain of 50% (black solid line in **Figure 5f**), implying a typical elastic behavior. Such an elastic feature at normal strain rates indicated that the CB/dPDMS composites could be a good candidate for tactile force sensors since mechanical hysteresis is undesired in sensing strain.[166] The same mechanical properties of the 150% strain-deformed samples (red short dot line in **Figure 5f**) suggested that the reconfigured CB(1)/dPDMS(1) composites could still be used as tactile force sensors. Here the reconfigured composites were denoted as n-rCB(*x*)/dPDMS (y) where n is the strain used in stress relaxation. The sensing property of the obtained materials were then collected at a loading rate of 20 mm/min, with an as-prepared CB/dPDMS sample as the control (**Figure 5g**). As expected, all the rCB/dPDMS display faster responsiveness to mechanical stimuli than the intact sample. Moreover, increasing the strain used for stress relaxation enhanced the sensitivity of the reconfigured CB/dPDMS composites. On the other hand, the sensing range also varied with the

strain (n in n-rCB/dPDMS).

Generally speaking, the sensitivity of the sensors increased when the fixed strains went up. Since the reconfiguration process does not affect on the mechanical property of the polymer composites (**Figure 5f**), there must be other reasons rather than the change of viscoelasticity that underlies the phenomenon. It is already reported in the literature that the distribution of interparticle connections can lead to different percolation exponents that would be intimately related to the sensitivity of the conductive composites upon strain.[163] The sufficient widely distributed interparticle connections could even show non-universal property, giving a percolation exponent greater than 2 in the three-dimensional (3D) network and the resulting resistance-strain curves could be logarithmically divergent, which has been demonstrated both theoretically and experimentally[167]. We attributed such tailorable sensor property to the on-demand redistribution of interparticle connections.[168] To demonstrate this, the R-strain model in the literature describing the resistance change versus strain for dynamic covalent polymer composites was applied in our case[159]. The resistance change versus the applied strain is as follows:

$$\frac{R}{R_0} = [(1 + \left(\frac{\varepsilon}{\varepsilon_c}\right)^{2m})^{-1} + k_2 t/N_0]^{-n_\varepsilon} (\varepsilon + 1)^2 \quad (2)$$

Where ε_c is the yield strain of the polymer composite, k_2 is the reforming constant due to particle arrangement within the viscous polymer matrix and N_0 is the initial number of interparticle connections per volume. In our case, it was assumed that the polymer composites were elastomers that the CB particles were not able to mobile at a normal strain rate. An approximate situation was made by setting $k_2 = 0$ in equation 2 to attain

$$\frac{R}{R_0} = [(1 + \left(\frac{\varepsilon}{\varepsilon_c}\right)^{2m})^{-1}]^{-n_\varepsilon} (\varepsilon + 1)^2 \quad (3)$$

By fitting the experimental data in **Figure 5g** with equation 3 (m = 0.7 and ε_c = 0.8), the fitting curves agreed well with the experiment data and we attained n_ε =1.2 for the as-prepared sensor and n_ε = 22.8, 31.8 and 45.9 for the 50%-rCB(1)/dPDMS(1), 100%-rCB(1)/dPDMS(1) and 150%-rCB(1)/dPDMS(1), respectively. Note that n_ε was the scaling exponent of connectivity while n_e was the scaling exponent of volume, but they both indicated the distribution of interparticle connections. Therefore, it was suggested that the distributions of the CB particles connections increased for the strain reconfigured CB/dPDMS composites, leading to the higher sensitivity of the sensors. Although the electrical resistance changes exponentially with the strain, the resistance change could be approximated as the linear change versus the strain when the deformation is sufficiently small. For our as-prepared CB(1)/dPDMS(1) composites and reconfigured materials, the resistance changes linearly within strain in the tested range (10%), as shown in **Figure 5h**. The gauge factor for the as-prepared CB(1)/dPDMS(1) composites is 1.4, and it jumps to 6.4, 30.2 or 51.5 after relaxation at a stretching state of 150%, 200% or 250%, respectively.

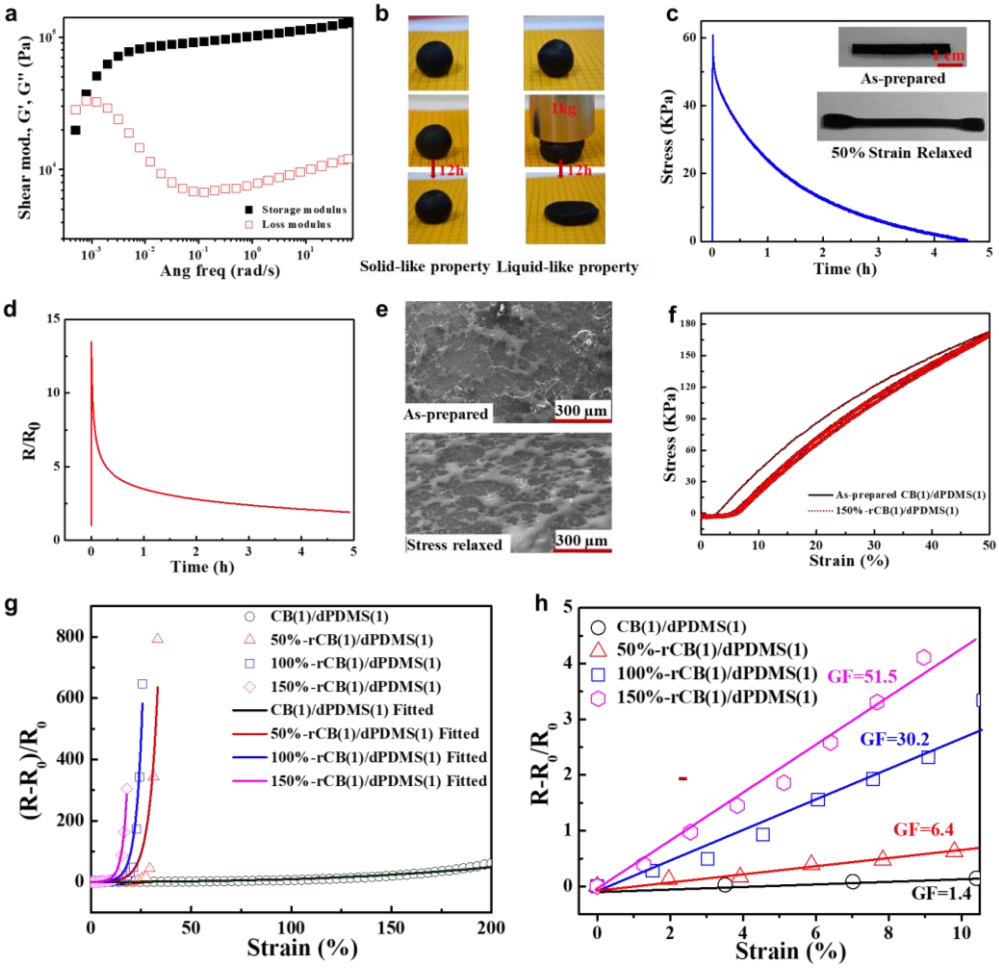

Figure 5. Mechano-tailorable sensitivities of the CB/dPDMS composites. **a)** Angular frequency dependence of storage modulus and loss modulus for the CB(1)/dPDMS(1). **b)** Pictures demonstrating the solid-like property in the absence of external stimuli and liquid-like property when there is a constant pressure. A CB(1)/dPDMS(1) was used. **c)** Stress relaxation of the CB(1)/dPDMS(1) at the fixed strain of 50%. Inset displays a CB(1)/dPDMS(1) sample before and after the stress-relaxation. **d)** Electrical resistance tracking of the CB(1)/dPDMS(1) at the fixed strain of 50%. **e)** SEM images of the cross-section for the as-prepared CB(1)/dPDMS(1) and 50%-rCB(1)/dPDMS(1). **f)** Cyclic stress-strain curves for the CB/dPDMS and 50%-strain reconfigured CB(1)/dPDMS(1) at the loading rate of 20 mm/min. **g)** Electrical resistance change versus strain of the sensors made from CB(1)/dPDMS(1) composites and the strain-reconfigured CB(1)/dPDMS(1) at a loading rate of 20 mm/min. The symbols are the experimental results and the solid lines are the simulated results. **h)** Gauge factors of the sensors made from CB(1)/dPDMS(1) composites and the strain-reconfigured CB(1)/dPDMS(1) composites within the small strain deformation (10%).

3.2.5 Self-healing of the CB/dPDMS Composites

Strong acid was used to initiate the ring-opening polymerization of the monomer and the ionic propagating species in resulted products retain activity after polymerization, inducing a dynamic equilibration of the siloxane matrix**.** It was assumed that such dynamic equilibration would bring about interesting self-healing at room temperature. To confirm this idea, the intact CB(1)/dPDMS(1) composites were tentatively cut by a knife and then stored in a sealed vial for observation. As shown in **Figure 6a**, the cut interfaces disappear after 24 hours, implying a recovery in the material's integration. Tensile measurements were used to quantitatively evaluate mechanical self-healing efficiency. The uniaxial tensile stress-strain curves of the healed samples agree well with the intact ones and a healing efficiency of 97 % was obtained, estimating by the rupturing energy **(Figure 6b)**. More than the recovery in mechanical properties, the electrical properties such as conductivity and sensing properties are also fully restored **(Figure 6c&d)**. The cut turns off the current of the sample under voltage (3V) which jumps back after healing. This restoration in current is reversible **(Figure 6c)**. A direct current-powered circuit connecting a light-emitting diode (LED) was further constructed to demonstrate the self-healing of electronic property **(**Inset in **Figure 6c).** The circuit was died out when being cut and was lit up again after being self-healed. Assembling the intact and self-healed composites to sensors and measure the R-strain curves at the speed of 20 mm/min, the sensing property of the self-healed sensor agrees well with the intact sensor, indicating a good recovery of the sensor properties **(Figure 6d)**.

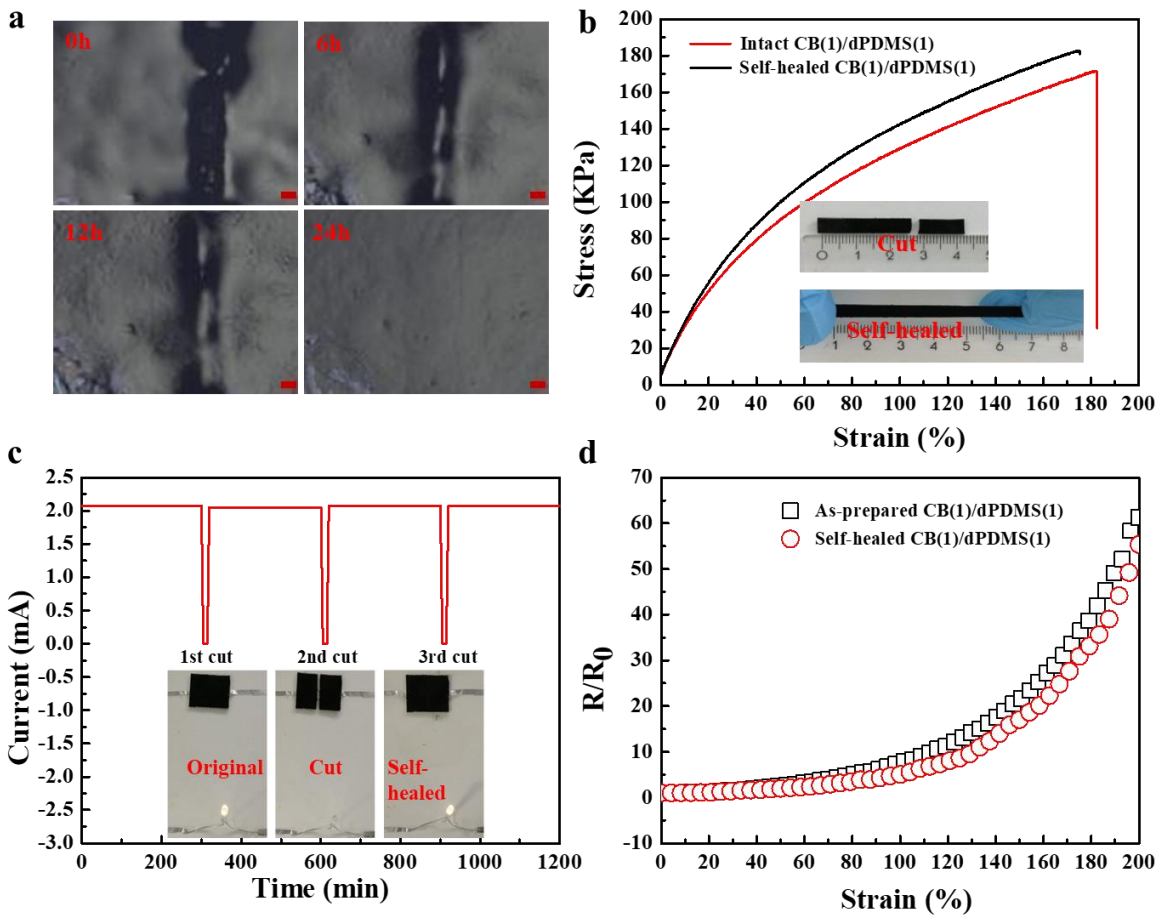

Figure 6. Self-healing of the CB/dPDMS composites. **a)** Optical images of the cut interface of the composites at different times. Scale bar: 100 μm. **b)** Stress-strain curves of the self-healed and intact specimens. **c)** The currents for the intact composites and the self-healed ones. The inset shows a circuit with a LED light to demonstrate the electronically self-healing of the CB/dPDMS composites. **d)** The sensor property for the intact sensors and the self-healed ones (20 mm/min). A CB(1)/dPDMS(1) was used for demonstration.

3.2.6 Recycling of the CB/dPDMS Composites

It is known that the polymer would depolymerize to oligomers if the polymer-oligomers equilibrium is moved to the oligomer directions (**Figure 7a**). In fact, the crosslinked materials could be dissolved for reprocessing in the presence of a good solvent for siloxane. The recyclability of the materials was demonstrated by subjecting the as-

prepared CB(1)/dPDMS(1) composites into toluene (**Figure 7b**). The composites were completely dissolved after stirring for 12h **(Figure 7b)**. Analyzing the dissolved solutions by gel permeation chromatography (GPC, **Figure 7c**) and gas chromatography-mass spectrometry (GC-MS, **Figure 7d**) revealed that the matrix had been completely converted into cyclic oligomers via depolymerization in the toluene solutions. To further confirm the acid-catalyzed depolymerization mechanism, a control experiment was conducted with well-defined PDMS (500 cSt) as a starting material. It was found that in the presence of triflic acid, the linear PDMS could also be converted into oligomers in 12h (checked by GC-MS and GPC, **Figure 7c and Figure 7d**).The contribution of CB particles to the depolymerization was demonstrated by a control experiment in which the PDMS oil (500 cSt) and PDMS elastomer (1 wt.% triD_4) did not contain any CB particle were dissolved in the toluene in the presence of triflic acid. Similar results were obtained, indicating that the presence of CB particles was not necessary for the depolymerization of polymers.

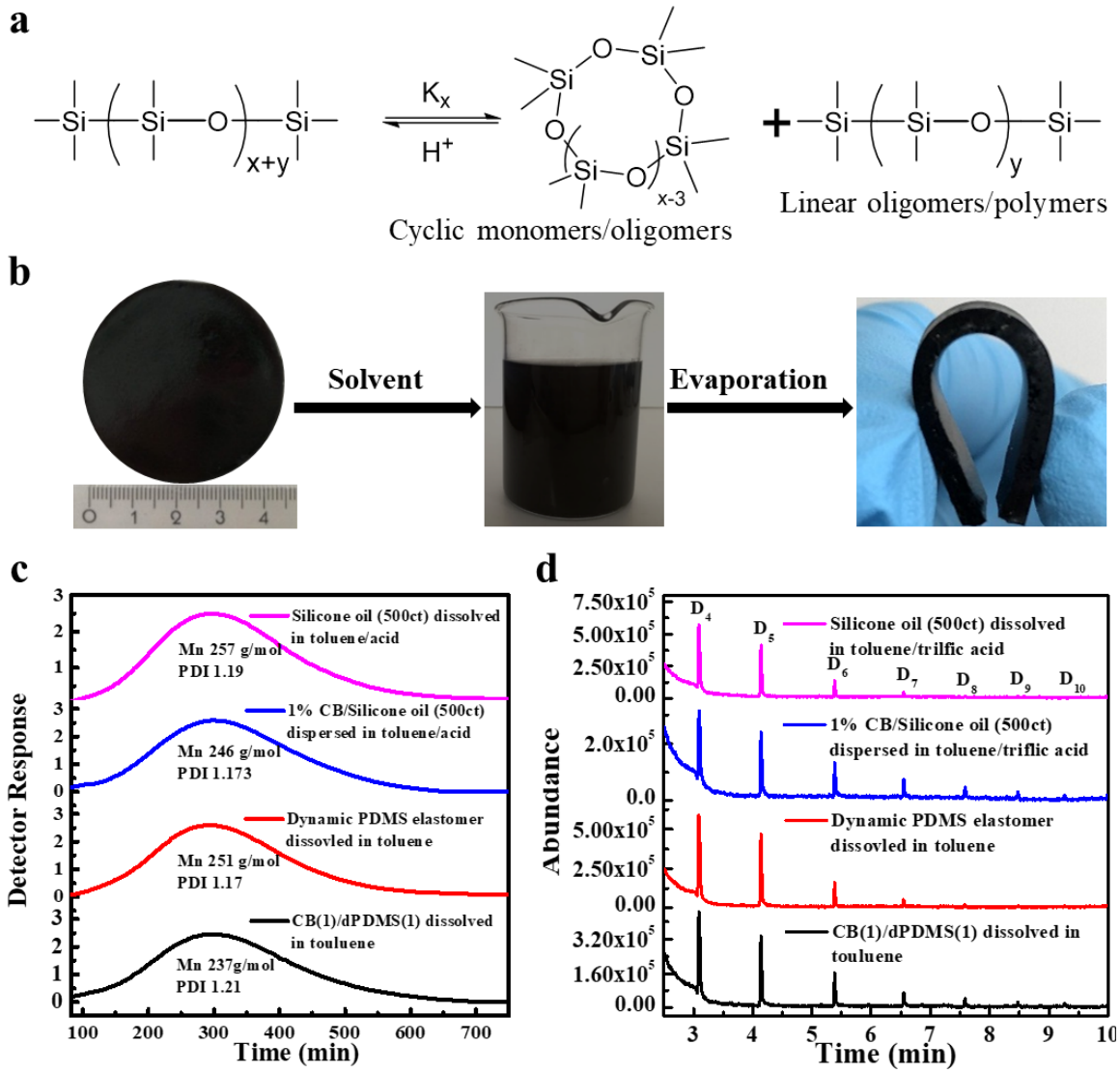

Figure 7. Recycling of the CB/dPDMS composites. **a)** Polymer-oligomer equilibrium in the acid-catalyzed dynamic PDMS. **b)** Reprocessing CB(1)/dPDMS(1) composites by dissolving them in toluene and the evaporation of toluene will rebuild the materials. **c)** GPC analysis of oligomers by dissolving CB(1)/dPDMS(1), dPDMS(1), 1%CB/silicone oli (500ct) and silicone oil (500ct) in toluene. **d)** GC-MS analysis of oligomers by dissolving CB/dPDMS, dPDMS (1), CB/Silicone oli (500ct) and silicone oil (500ct) in toluene.

3.2.7 Applications of the Tailorable Sensors

We demonstrated the tailorable sensing property of the CB/dPDMS composites via simple mechanical stretching. To this end, a CB(1)/dPDMS(1) stripe (3 mm

× 40 mm) was cut from the large size composites and assembled into circuits with a LED. For the as-prepared sensors, the illumination intensity of the LED reversibly decreased slightly when the stripe was stretched to 200% of its original length (**Figure8a**). Stretching the sensors to 150% for 24h stress relaxation in-situ increased the strain-sensitivity (**Figure 8b**). The illumination intensity decreased dramatically (totally die out), even the material was slightly stretched (25% strain, **Figure 8b**). The strain-induced switching was also reversible. Such in-situ modulation of sensitivity implied that our materials could be applied to sense a wide range of mechano-stimuli.

The sensing property of the materials was further tailored to accommodate customized wearable device applications. A flexible human motion detector was fabricated by connecting the assembled sensors to a daily bandage which was used to prevent direct contact with the skin (Inset in **Figure 8c**). A PDMS rubber glue (SH-78) was used to bind the assembled sensors and the bandage to avoid potential failure. After sticking the bandage onto the skin, the force sensors, the skin, and the bandage would behave as a single cohesive stretchable object, and therefore, the deformation of human-motion could be precisely monitored by the force sensors. Monitoring human tiny motion such as speaking requires high sensitivity. When the as-prepared CB(1)/dPDMS(1) tactile sensors were attached to the throat to monitor the speaking, no reliable signals was obtained since the low sensitivity of the sensor, as shown in **Figure 8c**. Instead of replacing the as-prepared sensor in the normal case, simply stretching the as-prepared sensors at a strain of 150% to allow a stress relaxation for 12h, the sample could re-use to detect the tiny motion to delivery reliable electrical signal

(**Figure 8d**). With this proof-of-concept demonstration, we envisioned that our post-tailorable strain-sensing materials could be used for preparing versatile sensors to alleviate the space usage. Such on-demand modulation could decrease the fabrication difficulties and cost, showing potential in preparing various flexible integrated circuits such as electronic skin, soft robotics and flexible prosthesis.

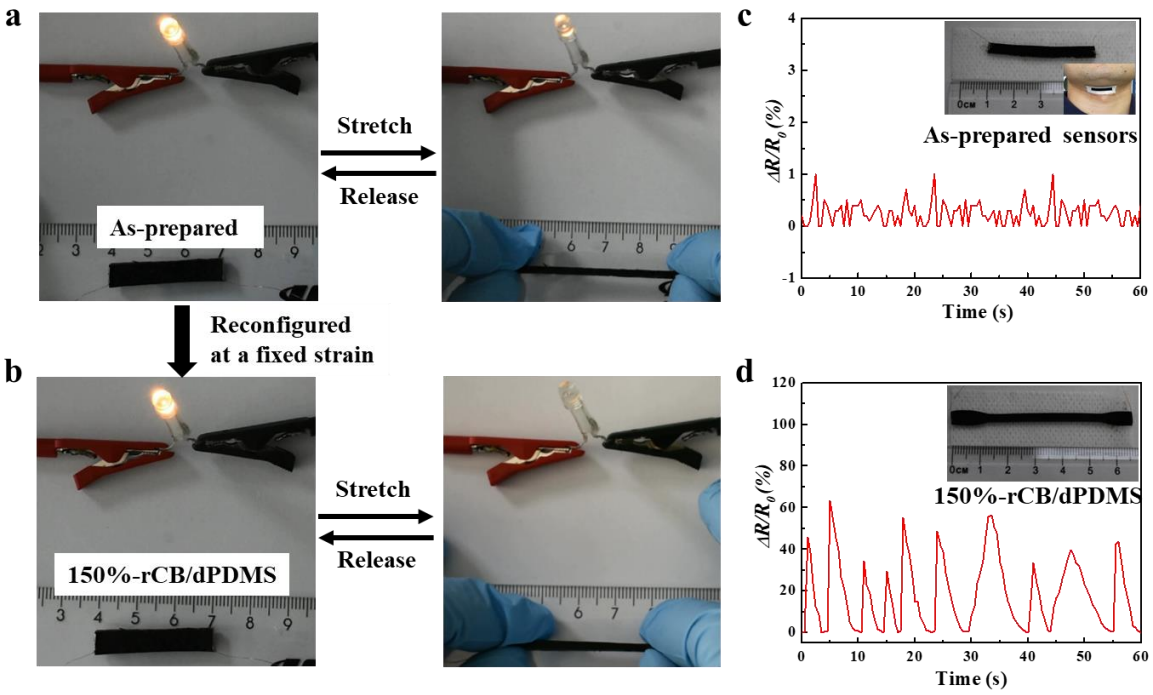

Figure 7. Application of tailorable tactile force sensors based on the CB/dPDMS composites. **a, b)** Demonstrating of different force-sensoring properties for the as-prepared CB(1)/dPDMS(1) and 150%-rCB(1)/dPDMS(1) composites. **c, d)** On-demanding tailorable force-sensoring property. The sensors that are not able to detect tiny motions could be reprocessed to be able to work by simple mechanical stretching and holding.

3.3 Conclusion

A facile strategy has been reported to post-tune the sensitivity of the conductive polymer composites using the mechano-treatment. The post-tunable sensor is

promising in reducing the sensor numbers for the flexible electronics that require different sensors to realize different functionalities. Though there are reported strategies that employ heating to post-tune the sensitivity of the sensing materials, it only works in thermoplastics, but not in the crosslinked rubbers. This is because heating induced post-tuning is realized by particle rearrangentment within the liquid phase thermoplastic polymers at elevated temperature. Whereas heating could not transform the crosslinked rubber into the liquid phase, therefore, particles could not redistribute and then the sensitivity remains unchanged. Our method is the first strategy that could post-tune the sensitivity of the crosslinked rubbers.

CB/dPDMS composites have been selected to demonstrate the feasibility to post-tune the sensitivity using the mechano-force. We have demonstrated that CB(1)/dPDMS(1) composites behave the liquid feature when the force angular frequency is lower than 8×10^{-4} rad/s, but behave the solid-feature when the angular frequency is higher than 8×10^{-4} rad/s. In the solid-state, the CB(1)/dPDMS(1) composites display a small hysteresis under the cyclic loading, indicating a potential candidate for the tactile force sensors. In the liquid state, the constant strain-induced particle rearrangement changes the distribution of the particles, thus altering the sensitivity of the polymer composites. Though this kind of “solid-liquid” viscoelasticity is assumed to be a general feature for dynamic covalent polymers, the application of the feature in the flexible electronics focuses on the study of the particle rearrangement under the strain, anti-impact and adaptive properties. This is the first example using this feature to post-tune the sensitivity.

We have proved that simply changing the constant strains, the obtained polymer composites display varying sensitivities. For example, the GF is 1.4 for the as-prepared CB(1)/dPDMS composites, and it increases to 6.4 when the fixed strain is 50%, and 30.2 for 100% fixed strain, and the 51.5 for the 150% fixed strain.

The CB/dPDMS composites exhibit self-healing and recycling properties. Both mechanical and electrical properties are well self-healed after the damage. The mechanical self-healing efficiency is 97% and the force-sensing property is almost unchanged for the self-heald samples compared to the intact one. The reycling of the CB/dPDMS composites has been demonstrated by dissolving the materials into the toluene.

3.4 Experiment Section

a. Materials

Octamethylcyclotetrasiloxane (D_4, 98%, Sigma-Aldrich), toluene (99.7, Sigma-Aldrich), triflic acid (Sigma-Aldrich) and conductive resin (Farnell) were used as purchased. Carbon black pearls 2000 (BP-2000) was offered by Cabot Corporation. D_4-based crosslinker (triD_4) was synthesized according to the method reported in **Chapter 2**.

b. Fabrication and Reconfiguration of CB/dPDMS Composites

For example, the mixture of 0.02g Carbon black powders and 2g D_4 monomer containing 1 wt.% crosslinker in 5 g toluene was subjected to ultrasonication for 30min, followed by addition of 20 μl triflic acid under stirring. The mixture was then put in the hood at room temperature to remove the solvent to get an elastic solid material without stirring. The sample was stored in a sealed glass bottle before use. The same process

was used to prepare the samples with different CB contents or formed under different conditions.

To reconfigure the CB/dPDMS composites, the materials were first stuck onto the two glass slides with the assistance of 502 glue (**Figure 8**), where samples were then stretched and fixed at different strains in a closed container for 24h.

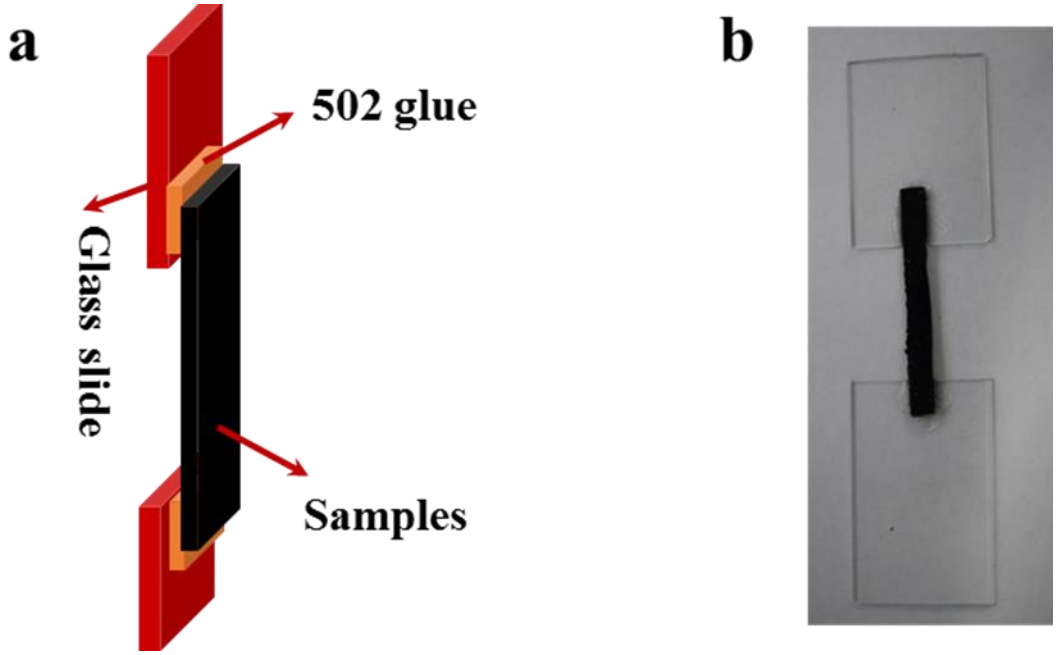

Figure 8. a) Schematic showing the method to stick CB/dPDMS composites onto the glass slides. **b)** The actual sample for sticking the samples onto the glass.

c. Recycle of Dynamic CB/dPDMS Composites

For example, a piece of CB/dPDMS film (2 g) was put into the mixture of 15 mL toluene containing 20 μl triflic acid. The mixture was stirred without heating for 12 hours. The composite was dissolved in half an hour, resulting in a suspending solution. The mixture solution was evaporated in the hood to remove the solvent and a new CB-PDMS composite was formed again.

d. Scanning Electron Microscopy (SEM) Observation

Scanning Electronic Microscope images were performed on an FEI Quanta 400 FEG-ESEM with an operating voltage of 10.0 kV. The CB/dPDMS composites were cut by knife and the cross-sections of the samples were subjected to the SEM without gold sputtering.

e. Rheological Characterizations

Rheological measurements were obtained using a TA instruments discovery hybrid rheometer with a PP8, 8 mm diameter parallel plate geometry with a rough surface. The dynamic modulus versus the oscillation strain rates was performed at the frequency of 1 Hz, while the dynamic modulus versus the oscillation strain rates was performed with a strain of 1%.

f. GC-MS and Chromatography Measurements

Gas chromatography-mass spectrometry was performed by GC-MS Shimadzu QP 2010 using ZB-5HT-Inferno columns. The number-average molecular weight (Mn) and polydispersity index were measured by Agilent HPC chromatography (GPC) system using a ZB-5HT-Inferno column with a series of silicone oils as standard samples. The concentration for GS-MS and GPC was 1mg/ml in toluene.

g. Mechanical Tests

Mechanical tensile-stress experiments were performed on a Zwick 1446 (Zwick/Roell, Germany) at room temperature at a strain speed of 20 mm/min. The initial gauge section is 20 mm. The specimens were 40 mm in length, 4 mm in width and 0.75 mm in thickness. The samples for the measurement of the E-modulus were stretched to break, and the E-modulus was calculated by the slope between the stress and the strain in the strain ranges of 5%-10%.

h. Electrical Measurements

All electrical measurements were performed on the samples with a length of 5 mm, a width of 30 mm, and a thickness of 0.75 mm, using two-point probe measurements. The resistance was tracked by the GDM-8255A (GW INSTEK). Conductive epoxy A and conductive epoxy B were first mixed homogeneously with a mass ratio of 1:1. Then the mixed composites were pasted onto the surfaces to eliminate the surface effect. Copper wires were used to connect the electrode and GDM-8255A.

The conductivity was calculated by $\sigma = L / (R * S)$, where σ is the conductivity, L is the length, S is the area of the cross-section and R is the electrical resistance.

Strain sensor measurements were performed on Zwick 1446 to apply loads to the sensor. The assembled sensors were stuck onto the glass sides and then the glass slides were subjected to the Zwick clamps (**Figure 9**). In this way, we avoid the effect of the force given by the Zwick clamps on the sensor property.

The resistance change at the fixed strains was also tracked by assembling the materials into the sensors and sticking the sensors onto the glasses. A parafilm was coated on the surfaces of the materials that were exposed to the air during the holding (**Figure 10**).

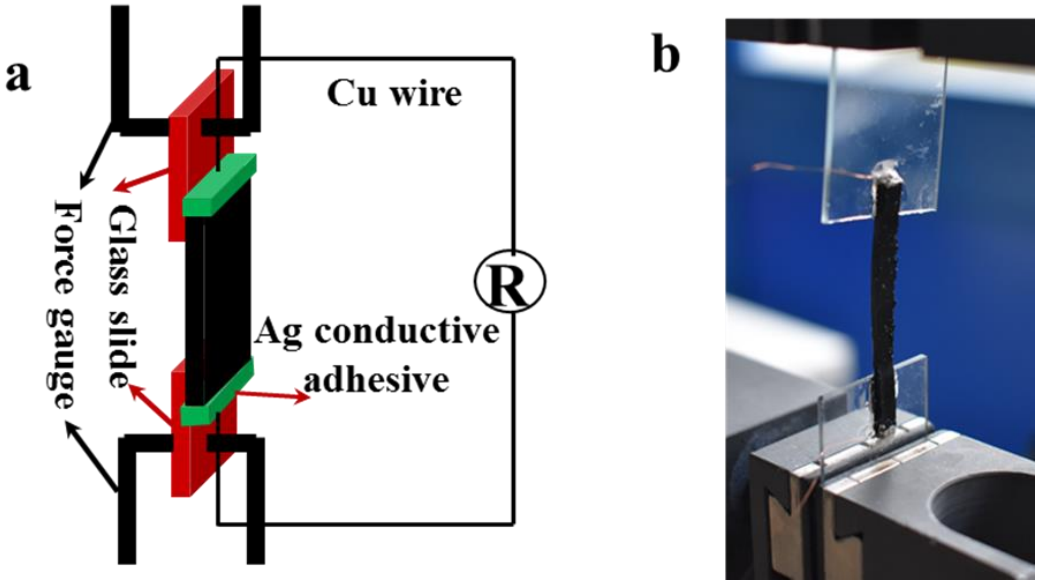

Figure 9. a) Schematic of the strain sensor measurement performed on Zwick. **b)** The actual sample picture.

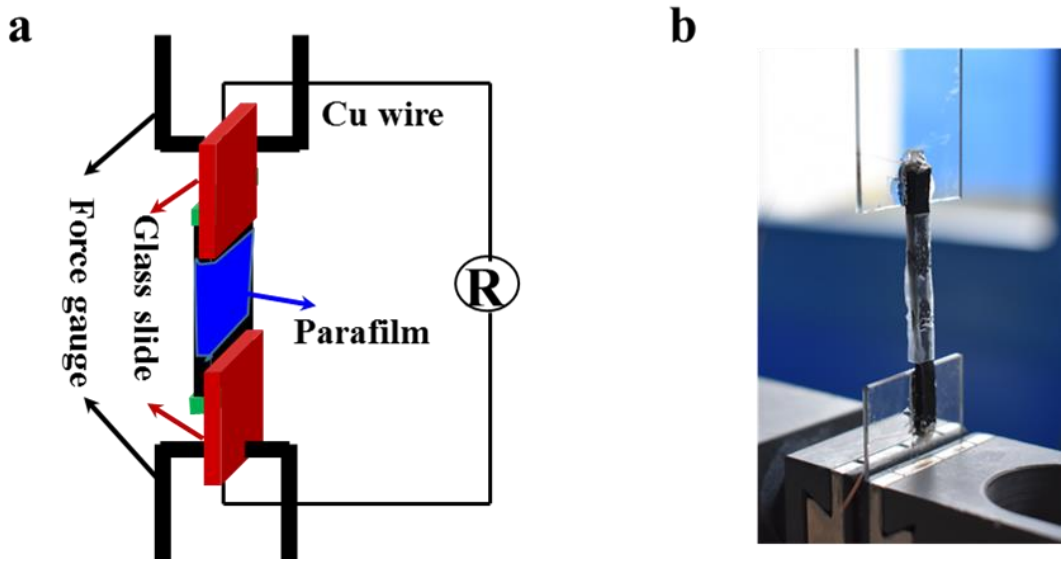

Figure 10. **a)** Schematic of the method for the resistance and force tracking during the material reconfiguration performed on Zwick. **b)** The actual sample picture.

I. R-strain model

On the one hand, the equilibrium number of interparticle connections per volume, N_1, can be interpreted as a function of the applied tensile strain $\mathcal{E}$, by applying the well-known Krauss model[169]

$$N_1 = \frac{N_0}{1+(\frac{\varepsilon}{\varepsilon_c})^{2m}} \quad (5)$$

Here, N_0 is the initial number of interparticle connections per volume, m is a constant related to the fractal structure of the network and ε_c is a constant which can be interpreted as the yield strain.

On the other hand, the viscous behavior of the polymer matrix enables the rearrangement of the filler particles, which additionally contributes to the interparticle connections. The number of interparticle connections per volume due to the rearrangement, N_2, increases linearly with time.

$N_2 = k_2 t = k_2 \varepsilon / \varepsilon_r$ (6)

where ε_r is strain rate, k_2 is the reforming constant because of the rearrangement. Then, at any given strain, the total number of interparticle connections per volume was given by $N = N_1 + N_2$. By analogy with percolation theory, the resistivity was given by

$\rho = (N - N_c)^{-n_\varepsilon}$ (7)

N_c is the threshold value when the first conductive path occurs and n_ε was a scaling exponent. When the filler loading was high enough, $N >> N_c$ and an approximation was made,

$\rho = (N)^{-n_\varepsilon} = (N_1 + N_2)^{-n_\varepsilon}$ (8)

Combining these equations gives

$$\rho = \frac{\rho_0}{[((1+\left(\frac{\varepsilon}{\varepsilon_c}\right)^{2m})^{-1}+\frac{\varepsilon}{\varepsilon_t}]^{n_\varepsilon}}$$ (9)

Where ρ_0 is the resistivity when there is no strain and $\varepsilon_t = \varepsilon_r N_0 / k_2$.

Combining the definition of resistance ($R = \rho L/S$) with the assumption that the volume remains constant under deformation ($S_0 L_0 = SL$) and the definition of strain ($\Delta L/L_0 = \varepsilon$) allows us to relate the material resistivity to the strain-dependent resistance:

$\rho = RS_0 L_0^{-1}(\varepsilon + 1)^2$ (10)

$$\frac{R}{R_0} = [(1 + \left(\frac{\varepsilon}{\varepsilon_c}\right)^{2m})^{-1} + k_2 t/N_0]^{-n_\varepsilon} (\varepsilon + 1)^2$$ (11)

Chapter 4

4. A Gas-flow Responsive Dynamic Covalent PDMS Composite

Abstract: Here, dynamic covalent polymer composites based on carbon black/dynamic polydimethylsiloxane (CB/dPDMS) were demonstrated to be gas-flow sensitive, regardless of the gas species. The composites were prepared via ring-opening polymerization of the mixture of D_4 and triD_4 with triflic acid as catalyst in the presence of carbon black. Obtained composites showed stress relaxation behavior after being stretched due to the exchange reaction of siloxane chains. It was found that the stress relaxation rate under a gas-flow condition is ~60 times faster than that under a sealed condition. The accelerated stress relaxation was attributed to the faster bond exchange reactions induced by the oligomer evaporation. This gas-flow responsiveness of CB/dPDMS could be applied to accelerate the self-healing process of materials (E-modulus ~1MPa) and to reshape the materials.

4.1 Introduction

Dynamic covalent polymer networks that could reconfigure in response to external stimuli,[14] have attained significant interest in various filed such as self-healing materials,[170] thermoset recycling,[24, 171, 172] photo-induced shape-shifting,[53, 54, 66, 173

and controlled degradation.[174-176] Different stimuli are used to modulate the reconfiguration of the dynamic network structures, including light, heat, pH, solvent, humidity, magnet etc.[31, 41, 48, 177-183] Recently, the application of gas as the external stimulus is gaining attention as an alternative strategy to trigger materials' response. For example, a polydimethylsiloxane (PDMS) elastomer crosslinked by electrostatic interactions between amide and carboxylic groups, amide and sodium hydrate-neutralized carboxyl cationic groups, has shown responsiveness to the presence of CO_2. The penetration of the CO_2 in the networked alters the sizes of the ionic aggregates by neutralizing carboxylic groups, which eventually affects the rearrangement rate of the dynamic polymer network.[184] Such responsiveness depends on the chemistry of the stimulus, rather than its phase state. In other words, an acid reagent is required for the rearrangement but not a gas, which limits their applications. Herein, a gas-flow enhanced stress-relaxation of dynamic covalent PDMS composite is reported. In this Chapter, the effect of the gas species and gas-flowing speed on the stress relaxation rate is described, and the possible mechanism for the gas-flow responsive elastomer is discussed. Finally, potential applications of this kind of gas-flow responsive elastomer are presented.

4.2 Results and Discussion

Acid-catalyzed carbon black/dynamic PDMS (CB/dPDMS) elastomer was prepared to demonstrate the gas-flow responsive behavior. CB/dPDMS elastomer was prepared by gelating carbon black (CB), octomethlycyclosiloxane (D_4, mononer), 1,1,1-tri(2-heptamethylcyclotetrasiloxane-yl-ethyl)-methylsilane ($triD_4$, crosslinker) mixture solution in the presence of triflic acid (catalyst). The obtained CB/dPDMS elastomers

were first stretched and fixed at a given strain, which was then subjected to different airflow environments, i.e., a sealed environment (**Figure 1a, & 1b**) or a gas-flowing environment (**Figure 1d, & 1e**). The Si-O bond exchange reaction would relax the stress, leading the stretched CB/dPDMS composites to have plastic deformation when they are released from the stretching. This is to say, when the stretched samples are released, they can not recover to the original length (L_0) like the normal elastomer, but come to a length (L) that is larger than L_0 because of the stress relaxation-induced plastic deformation.[102] The plastic deformation rate, defined by A/t, (where A is the plastic deformation ratio, $A = (L-L_0)/L_0 \times 100\%$, and t is the time) is used to quantitatively characterize the stress relaxation rate. Here, we expect that CB/dPDMS composites in the flowing environment display a faster plastic deformation rate (**Figure 1c**) than in the closed container (**Figure 1f**), i.e., the bond exchange rate in the flowing environment is faster than in the closed environment. Then the mechanism for this flowing gas-induced accelerated bond change reactions and the potential applications of this strategy will be described.

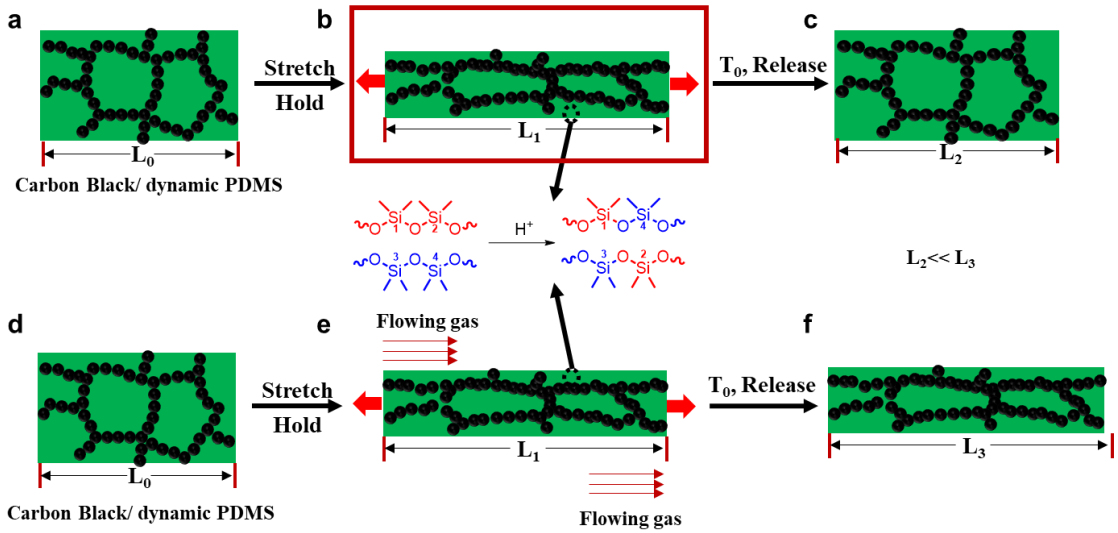

Figure 1. Different polymer chain exchange rates for the CB/dPDMS composites. **a)** In a closed container. **b)** In the flowing gas.

4.2.1 Effect of Flowing Gas and the Gas Species

The accelerating stress-relaxation behavior of the CB/dPDMS composites under the flowing gas was first confirmed. Since DMA does not allow the flowing of different gas species through the chamber with the controlling speed, a home-made chamber was prepared to flexibly control the airflow environment (**Figure 2a**). A sealed box was punched with two holes, one hole was used as the gas inlet with a flow meter to control the gas speed, and the other hole was used as the outlet. Different kinds of gas could be easily flowed by changing the flowing gas species and the flowing time could also be easily controlled by the flow meter. The CB/dPDMS composites containing 1% CB and 1% crosslinker (named as CB(1)/dPDMS(1)) were used for all the experiments if there is no otherwise statement. To put the fixed-strain stretched composites in the chamber, the elastomers were first stuck onto the two glass slides with the assistance of tapes, which could self-stuck onto the glass sides even the tapes were removed after 30min (**Figure 2b**). Then, the self-stuck composites could be easily fixed at a given strain by stretching and fixing the two glass slides onto the petri dish. Here, the stretchability of the glass bonded parts of the samples was ignored and the initial length (L_0) was measured as the distance between the two glass fronts. For better comparison, L_0 was set to14 mm for all the experiments of there is no statement. Specifically, CB(1)/dPDMS(1) elastomers were stretched to 150% L_0 in my experiment, denoted as the 50%-strained CB(1)/dPDMS(1). The 50%-strained composites were placed in the home-made chamber and N_2 was flowed. When the stretched samples were fully deformed, i.e, the plastic deformation ratio is 50%, the duration time (denoted as $t_{50\%}$) was recorded and it revealed the stress relaxation rate. The 50%-strained CB(1)/dPDMS(1) composites placed in the home-made chamber with two

pluggers to seal the inlet and outlet were used as the control experiments. As shown in **Figure 2c**, $t_{50\%}$ was 48h for the control sample and then it sharply decreased to 1.5h when the gas-flow rate was 1 LPM. Increasing the gas flow rate, and $t_{50\%}$ first dropped slightly and then became constant when the rate of flowing gas reached 15 LPM (**Inset in Figure 2c**). $t_{50\%}$ was only 50 min when the gas-flowing rate of 15 LPM, showing a rate of about 60 times faster compared to the control sample (48h). The sharp decrease of $t_{50\%}$ clearly demonstrated that the stress relaxation rate of the CB(1)/dPDMS(1) composites could be highly accelerated in the flowing gas compared in the closed container.

Next, we investigated whether the accelerated stress relaxation of the CB/dPDMS composites was gas-dependent. Three different gases (N_2, Ar, and Air) were selected. 50%-strain stretched CB(1)/dPDMS(1) composites were put in the chamber and three different gases were flowed through the home-made chamber at a flowing rate of 15 LPM (Liter per minute) for 40min, respectively. Then plastic deformation ratios under each gas were tracked, denoted as A_{40min}. Parallel to the sample explored to different gas flow speeds, a 50%-strain stretched CB(1)/dPDMS(1) was also placed in a closed home-made chamber by using two pluggers to seal the inlet and outlet to prevent any gas-flowing behavior for 40min, which was used as control. The results are listed in **Table 1**. A_{40min} is almost the same (about 36%) for all the samples that are exposed to the flowing gas, regardless of the gas species. This clearly demonstrated that accelerated stress relaxation is independent of the gas species. In addition, the control sample displayed a negligible plastic deformation ratio within 40min, which again proved that the flowing gas could accelerate the stress relaxation.

In parallel with the accelerated stress relaxation, the samples always lost weight when

incubated with the flowing gas (**Figure 2d, Table 1**), which was attributed to the evaporation of small molecules generated in the back-bite reaction of the living polymers, as discussed in **Chapter 2.** The weight loss rate represented the depolymerization rate. As shown in **Table 1,** the strained elastomer flowed by different gases at the same speed for 40min displayed nearly the same the weight loss ratios (*W* = lost weight/initial weight), i.e., about 5.5 wt.%, indicating that the depolymerization rates are also independent with the gas species. Since the gas species make no difference in accelerating the stress relaxation and in the depolymerization rate, N_2 was used as the flowing gas for all the experiment, unless otherwise specified. In order to find the relationship between the accelerated stress relaxation rates and the depolymerization rate of CB(1)/dPDMS(1) composites, the weight loss ratio of 50%-strained polymer composites at full relaxation (denoted as $W_{50\%}$) versus the gas-flowing rate was recorded (**Figure 2d**). As a control, the 50%-strained sample sealed in the closed home-made chamber was used. $W_{50\%}$ was negligible for the control sample (0.5 wt.%), but it jumped to 6.8 wt.% when the flowing rate was 1 LPM. This is reasonable since the samples sealed in the closed container would be stable, while the samples in the flowing gas would be depolymerized and that will decrease the weight triggered by the oligomer evaporation. Increasing the gas flow rates lead to a non-monotonic change of $W_{50\%}$. To be specific, $W_{50\%}$ decrease from 6.8% to 5.5 wt.% if the flowing rate was further increased to 15 LPM from 1 LPM, which was then followed by a raising trend (the weight loss reached 12.2 wt.% when the gas flowing rate was 50 LPM). The non-monotonic change of the weight loss versus the flow rate clearly indicated that the stress relaxation is not only related to the depolymerization. A more complicated mechanism might contribute to the

accelerated stress relaxation.

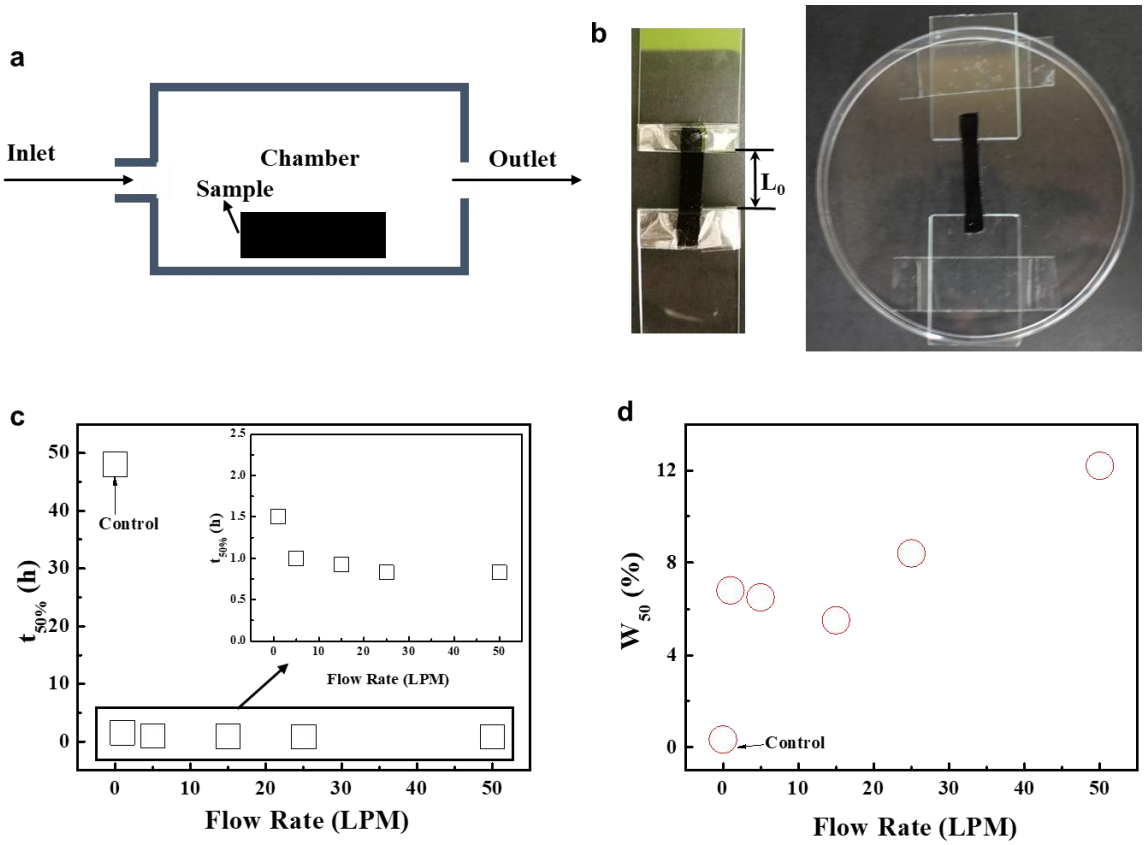

Figure 2. Effect of flow rates on the stress relaxation rate. **a)** Home-made chamber. **b)** Methods to fix the strained CB(1)/dPDMS(1) composites. **c)** $t_{50\%}$ as a function of the flowing rate. Inset displayed the $t_{50\%}$-flowing rate curves for the flow rate ≥ 1 LPM. **d)** W_{40min} as a function of the flowing gas rate.

Table 1. A_{40min} and $W_{50\%}$ of the CB(1)/dPDMS(1) composites exposed to different kinds of flowing gas (Flow rate: 15 LPM, duration time: 40min). A 50%-strain stretched CB(1)/dPDMS(1) composite sealed in the closed container was used as the control.

Gas species	Time (min)	Rate (LPM)	A_{40min}	$W_{50\%}$
N_2	40	15	36%	5.6
Ar	40	15	36%	5.8
Air	40	15	33%	5.4
Control	40	0	0.5%	0

4.2.2 Study of the Mechanism for the Accelerated Chain Exchange

As the gas is flowed though the stretched samples, many factors might contribute to the accelerated chain exchange rate. First, flowing gas could carry away the small molecules and the lose of the small molecules alters the energy of the CB(1)/dPDMS(1) composites, which might affect the polymer chain exchange rate. In addition, the escape of the small molecules also changes their contents in the polymer-oligomer equilibrium, which accelerates the depolymerization via the back-bite reaction. The effect of accelerated deplymerization on the bond exchange reaction could not be ignored. Moreover, as the acid-catalyzed bond exchange reaction is greatly affected by the water, the possible presence of water in the flowing gas also deserves attention. In the flowing parts, these possible effecting factors are discussed in detail, and the possible mechanism for the flowing gas-induced accelerated chain exchange was proposed in the end.

4.2.2.1 Effect of Evaporation

Dynamic Si-O bond exchange reaction is supposed to be a constant enthalpy and entropy process, but it needs the activation energy E_a to overcome the energy barrier (**Figure 3a**). Evaporation of D_4 could increase the entropy of the system, which might offer the driving force for the accelerated the chain exchange reaction by diminishing the entropy penalty of the bond exchange.[185, 186] Assuming the solvent evaporation of D_4 is the main contribution to the accelerated chain exchange reaction, then any other solvent evaporation should work as effectively as evaporating D_4. Therefore, the CB/dPDMS composites were swelled with 10 wt.% toluene and then stretched to 150%L_0, the toluene was evaporated in the home-made chamber with the flowing N_2

at the speed of 15 LPM. It was found that 10 wt.% toluene would be completely evaporated after 4min in the home-made chamber with 15 LPM flowing N_2 (**Figure 3b**). According to this kinetic, the sample was taken out from the home-made chamber after 4min and it was found that the plastic deformation ratio of the composites was negligible (0.5%), indicating that simple solvent evaporation could not accelerate the chain exchange reaction. In order to confirm if the evaporative toluene contributes less entropy as the same amount of D_4 due to the lower boiling points, the composites were swelled with 10 wt.% D_4 monomers. As soon as the D_4 monomers went inside the composites (no liquid on the surface), the composites were stretched to 150% L_0 and put in the home-made chamber, flowed with N_2 at the speed of 15 LPM. The swollen sample lost more weight than the as-prepared composites at the same time scale (**Figure 3c**), while the plastic deformation rate was the same as the as-prepared composites (**Figure 3d**). It indicated that enthalpy-entropy compensation induced by small molecule evaporation like D_4 was not the reason for the accelerated chain exchange reaction.

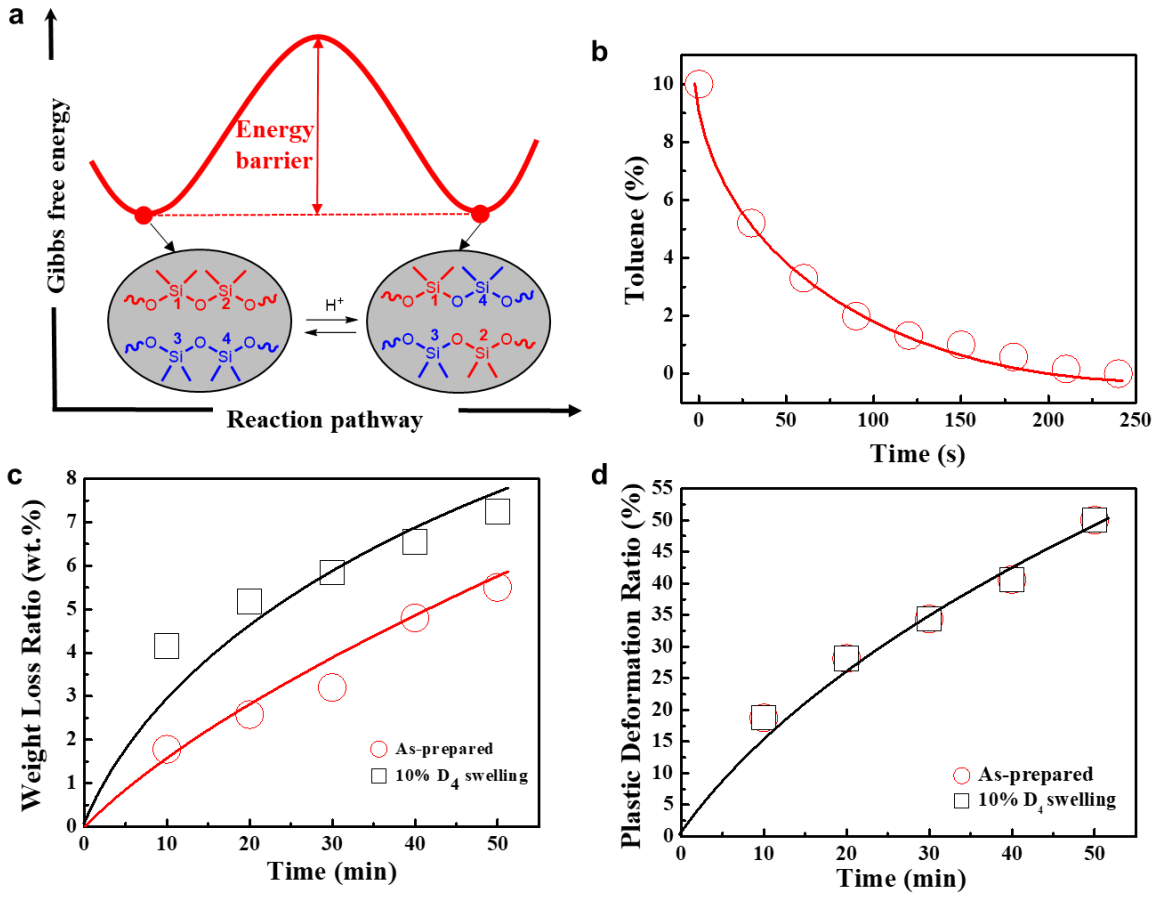

Figure 3. Effect of evaporation on the chain exchange kinetic. **a)** Energy barrier for the dynamic Si-O bonds. **b)** Evaporation kinetic of toluene within the CB(1)/dPDMS(1) composites. **c&d)** Weight loss and plastic deformations versus time for the as-prepared CB(1)/dPDMS(1) and 10% D_4 swelled CB(1)/dPDMS(1) composites in the gas flowing home-made chamber (N_2, 15LPM).

4.2.2.2 Effect of Small Molecules

It is common in dynamic polymers that the addition of small molecules could mediate the polymer chain rearrangement. For example, the presence of water in the polyimide dynamic polymer would switch the dynamic polymer network to rearrange the polymer network from a prevalent associative pathway to a dissociative pathway, affecting the stress relaxation greatly.[187-190] In the flowing gas, depolymerization occurred and generated small molecules (like D_4), altering the concentration. To check if the concentration variation of small molecules could accelerate the chain exchange

reaction, a control experiment in which the 10 wt.% D_4 swelled composites was sealed in the closed container was conducted. It was found that the plastic deformation rate is almost the same with the as-prepared CB(1)/dPDMS(1) composites sealed in the closed container (about 48 hours are needed to fully deform the stretching). In addition to the swollen sample, an experiment in which the CB(1)/dPDMS(1) composites was in-situ swollen was conducted to further study the contribution of small molecules to the relaxation. In this experiment, as-prepared CB(1)/dPDMS(1) composites were stretched with a strain of 50% and fixed in the N_2 flowing chamber. D_4 was dropped on the sample continuously (**Inset in Figure 4a**) during the relaxation. The plastic deformation rates were measured. The relaxation kinetics is almost the same as that without the addition of D_4 monomers (**Figure 4a**). This result indicated that the chain exchange reactions were not relevant to the presentation of small molecules.

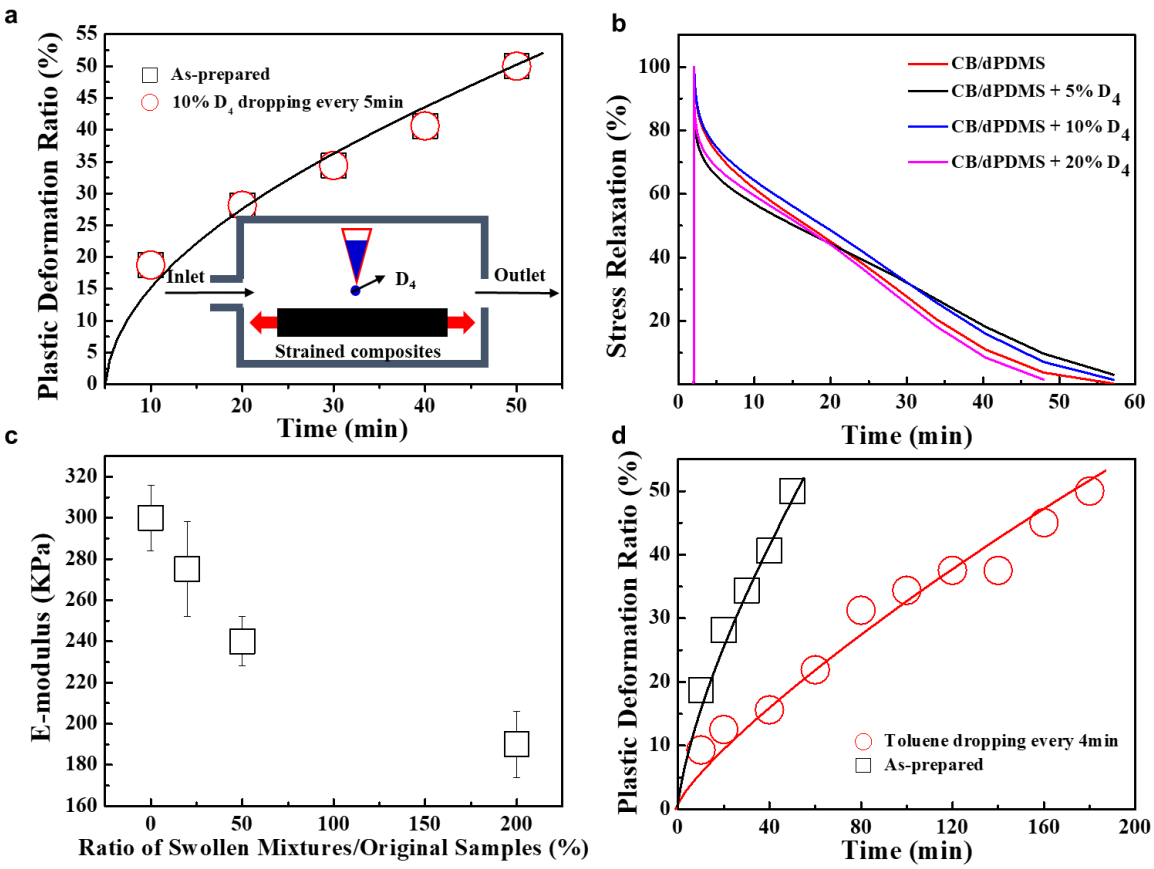

Figure 4. Effect of depolymerization and D_4 evaporation on the chain-exchange rate. **a)** The plastic deformation ratio of CB(1)/dPDMS(1) composites in-situ swollen by D_4. Inset shows detail performance of in-situ swelling D_4 onto the samples: dropping D_4 monomers onto the strained CB(1)/dPDMS(1) composites in the gas flowing home-made chamber (N_2, 15 LPM). **b)** Effect of D_4 swelling on the stress relaxation kinetics for the CB(1)/dPDMS(1) composites. **c)** E-modulus of the mixture solution (D_4+1% triD_4) swelled CB(1)/dPDMS(1) composites. **d)** Plastic deformation kinetics of the CB(1)/dPDMS(1) added with 10% toluene every 4min, in the home-made chamber with the gas-flowing (N_2, 15 LPM).

4.2.2.3 Effect of Depolymerization

As mentioned above, weight loss always occurred together with the accelerated chain exchange reactions. This is attributed to the accelerated polymer depolymerization induced by the flowing gas since flowing gas could take the oligomers away, moving the polymer-oligomers equilibrium towards the cyclic oligomers side.[102, 191] With more

oligomers evaporated by the gas flow, more polymers are depolymerized into oligomers. It is reasonable to assume that the depolymerization is the main factor for accelerating the chain exchange. In order to demonstrate the assumption, D_4 monomers were swollen in the CB(1)/dPDMS(1) composites. The addition of D_4 monomers is expected to slow down the depolymerization. Experiments with different amounts of D_4 monomers (5%, 10% and 20% of the initial weight of the sample) were performed. After the D_4 monomers diffused inside the composites (the droplets disappeared from the surface), stress relaxation of the composites was analyzed by DMA. Since these experiments were performed in DMA, the composites were not stuck onto the glass slides. As shown in **Figure 5b**, all the samples display similar relaxation curves and they all achieved full relaxation state in ~55 min. It suggested that the swelling of D_4 does not affect the chain exchange rate. The possible reasons for this phenomenon could be either that the swelled D_4 was converted into polymers immediately after entrapped into the composites and therefore could not restrict the depolymerization, or that the accelerated chain exchange rate has nothing to do with the depolymerization. In order to distinguish the two possible reasons, E-moduli of the swollen composites were measured. Swelling with D_4 is expected to decrease the cross-linking density of the polymer and, therefore, a mixture containing D_4 monomer and 1 wt.% triD_4 was used to maintain the cross-linking density. If the provided monomers would not be converted into polymers, a decrease of the modulus of the swollen sample is expected since the monomers would act as plasticizers and soften the materials. If the swollen monomers were converted into polymers, E-modulus was supposed to have a negligible decrease. As soon as the droplets of monomer solution disappeared from the surface of the composites, these were subjected to the tensile

tests. It was found that the E-modulus decreased with the amount of swollen mixture solutions (**Figure 4c**). The decrease in modulus suggested that the monomers were not fully polymerized. Therefore, the addition of D_4 should restrict depolymerization. Since the sample with restricted depolymerization displayed the same stress relaxation rate as the as-prepared composites, depolymerization itself might not be the reason for the accelerated chain exchange. This assumption was also supported by the experiment of the in-situ addition of the D_4 monomer (**Figure 4a**).

The performed experiments suggest that the accelerated chain exchange reactions have nothing to do with the depolymerization, but are related to the evaporation of the D_4 monomers. In order to confirm that the accelerated chain exchange is related to the D_4 evaporation, toluene was swelled into the composites continuously to prevent the evaporation of D_4 monomer. According to the toluene evaporation kinetic (**Figure 3b**), 10% toluene was fully evaporated within 4min. That is to say, D_4 evaporation after 4min would not be affected and this short-time disruption of the D_4 evaporation might have a negligible effect on the plastic deformation kinetics. In order to prevent the D_4 evaporation continuoulsy, 10% toluene was in-situ added into the CB/dPDMS every 4min. The plastic deformation kinetics of the composites were measured with the addition of toluene. It was found that the plastic deformation was much slower than the as-prepared composites (**Figure 4d**), which is due to the much slower evaporation rate of D_4 in the presence of toluene because of Raoult's law. However, the addition of toluene cannot prevent D_4 evaporation completely. To fully prevent the evaporation of D_4, a series of water droplets were added onto the strained composites and then gas was flowed into the chamber, it was found that the composites did not lose the weight at all, showing negligible plastic deformations within the experiment time scale.

The addition of toluene and the presence of water droplets clearly demonstrated the accelerated chain exchange kinetic is related to the D_4 evaporation.

4.2.2.4 Effect of Water

Acid-catalyzed rearrangement of Si-O bonds in polydimethylsiloxane involves an equilibrium reaction in which coordination of the acid proton to the siloxane oxygen is followed by cleavage of the siloxane bond with the formation of a silanol group and a silyl ester group (**reaction 1**). The condensation of the silanol groups may reform siloxane linkages with the forming of water molecules (**reaction 2**). The formed water molecules could, in turn, react with the silyl ester to give the acid and the silanol groups (**reaction 3**). The rate of attainment of equilibrium in such a system depends on the effective concentrations in the siloxane phase of silanol and silyl ester end groups, water and acid.[96] The possible presence of water in the flowing gas would disturb the equilibrium to some extent, which was confirmed by the accelerated stress relaxation rate in the wet N_2. The phenomenon was attributed to the scission of the siloxane bond with the subsequent formation of silanols which are free to condense again in the relaxed state.[192] Therefore, it should be clarified that the accelerated chain exchange reaction in our experiments could also be induced by water. To confirm this, the flowing gas was dried by passing through the drying columns containing NaOH particles and $CaCl_2$ particles in sequence. However, a similar relaxation rate was observed, indicating that the water plays a negligible role in our system (**Figure 5b**).

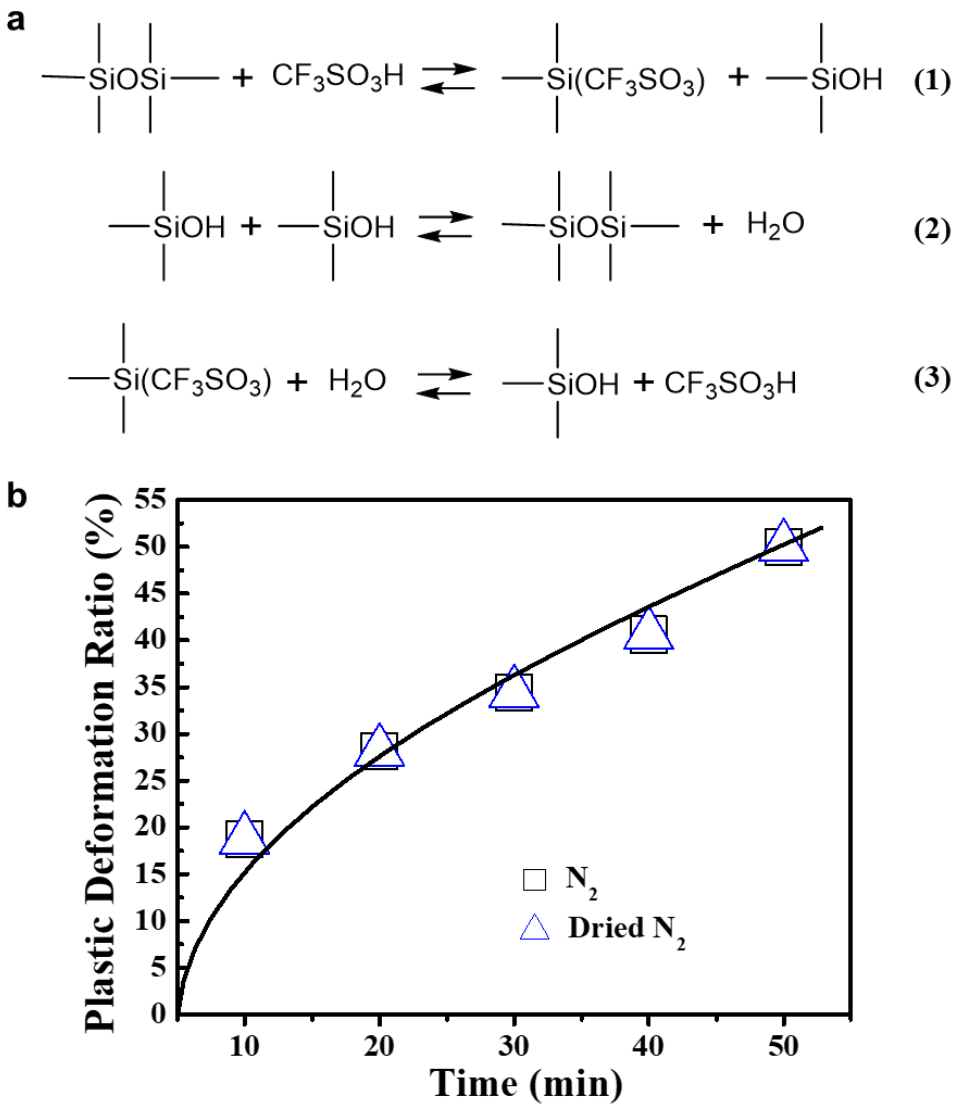

Figure 5. a) Acid-catalyzed Si-O rearrangement. **b)** Plastic deformation kinetics for the CB(1)/dPDMS(1) under the N_2 and dried N_2

4.2.2.5. Proposed Mechanism

The described experiments confirmed that the accelerated chain exchange reaction was related to the D_4 evaporation. The potential mechanism for the accelerated chain exchange reactions induced by D_4 evaporation is proposed. **Figure 6** shows the main reactions occurring in the acid-activated ring-opening polymerization of D_4 with trifluoromethanesulfonic acid as an initiator/catalyst. The initiation of the

polymerization starts from the electrophilic attack of the proton of trifluoromethanesulfonic acid on a siloxane ring oxygen and the opening of the ring, resulting in a cationic species that can either directly attack cyclic monomers to propagate (propagation) or undergo end-group condensation to increase the molecular weight. Both propagation and condensation pathways lead to chain growth without consuming the cationic species. A backbiting reaction would lead to the reformation of the cyclic monomers and the decrease in the molecular weight of the polymer chains. This reaction also does not lead to the deactivation of the cationic species. There are two kinds of termination reactions of the propagating silyl cations: with a counterion to form a silylester or with water to release a proton. This proton can initiate polymerization again while the ester chain can undergo condensation to extend or react with water to reform the trifluoromethanesulfonic acid.[96, 100, 101]

The kinetics of all the main reactions are related to the acid reactivity. Therefore, it is reasonable to assume that the evaporation of D_4 may cause an increase in the acid reactivity, which in turn accelerates the chain exchange reaction. For example, the evaporation of D_4 could possibly enhance the movement of the acid in the PDMS. The D_4 evaporation might take away the acid on the surface, giving an acid gradient between the inside materials and surface materials (**Figure 7a**). The inside acid would move to the surface via the silyl-cation transfer mechanism (**Figure 7b**), accelerating the acid movement.[191, 193, 194] The increased acid movement would enhance the acid reactivity, accelerating the depolymerization and chain exchange reactions and softening the materials. Another possible mechanism is that the evaporation of D_4 might change the polymeric acid structure that influences the reactivity. The reactivity of acid in the chain exchange reactions is related to its ability to transfer protons:

transfer to the siloxane bond or to the end group. A hydrogen-bond polymeric complex involving several H_2O molecules functions better as a proton donor than the single acid molecule because the incipient charge is delocalized over the entire complex, e.g. structure 1 (**Figure 8**). Since the polymeric acid-water complexes may be destroyed by competitive acid monomer interaction, a decrease in monomer concentration induced by evaporation may cause an increase in reaction rates. Though these assumptions could explain some of the experiments, further strong data are still necessary to prove them.

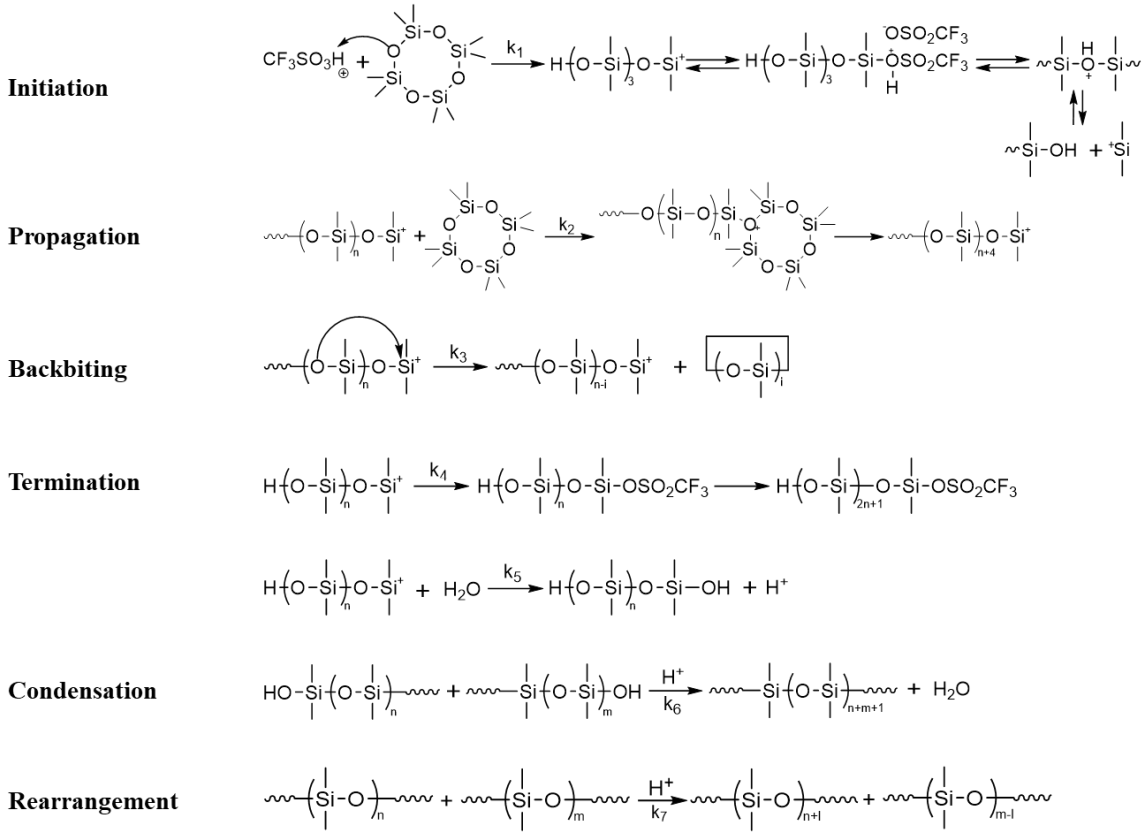

Figure 6. Acid-activated polymerization of D_4 and related reactions.

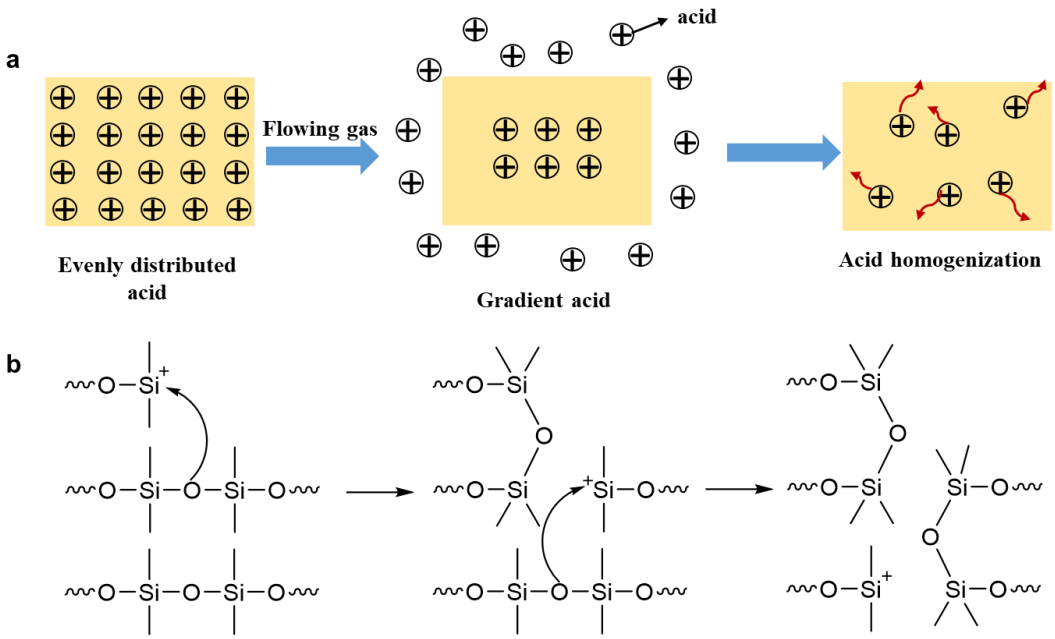

Figure 7. a) Scheme showing the evaporation enhanced acid movement mechanism**. b)** Silyl-cation transfer mechanism.

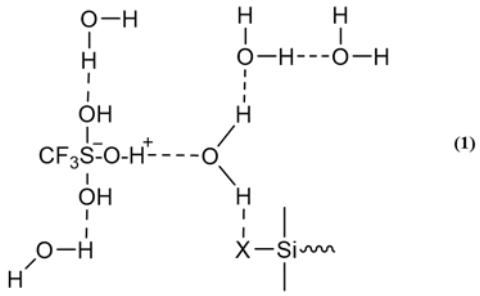

Figure 8. Structure of a hydrogen-bond polymeric complex.

4.2.3 Applications of the Gas-flow Responsive Dynamic Covalent Polymers

4.2.3.1 Self-healing Materials

The acceleration of the self-healing efficiency by a flowing gas was demonstrated. CB/dPDMS composites containing 10 wt.% cross-links were prepared. Then, a tentative experiment was conducted to study the self-healing ability of the composite under different conditions. For better comparison, an as-prepared composite was cut into two pieces. One piece was cut and self-healed in a closed container, as the control

experiment. The control experiment was designed to study the intrinsic self-healing ability of the composite. In contrast, the other piece was cut and self-healed in the container with continual N_2 flow at a speed of 5 LPM for 3h. Then the self-healing ability in the closed container and in the flowing gas was checked by the optical microscopy and the mechanical tests. From the optical images, it was found that the cracks were still visible for the composites placed in the closed container while the cracks on the composites at the flowing gas disappeared at the time scale of 3h, indicating that the sample explored to gas flow self-healed more efficiently than that in the closed container (**Figure 9a**). Mechanical tests displayed that the E-modulus of the CB/dPDMS composites with a 10% cross-link is about 1MPa. The sample stored in the closed container did not self-heal into an integrated piece that can suffer the mechanical tests. The self-healing efficiency of the composites self-healed at the flowing gas is about 58% according to the rupture energy, clearly demonstrating that the higher chain exchange rate of the materials in the flowing gas (**Figure 9b**).

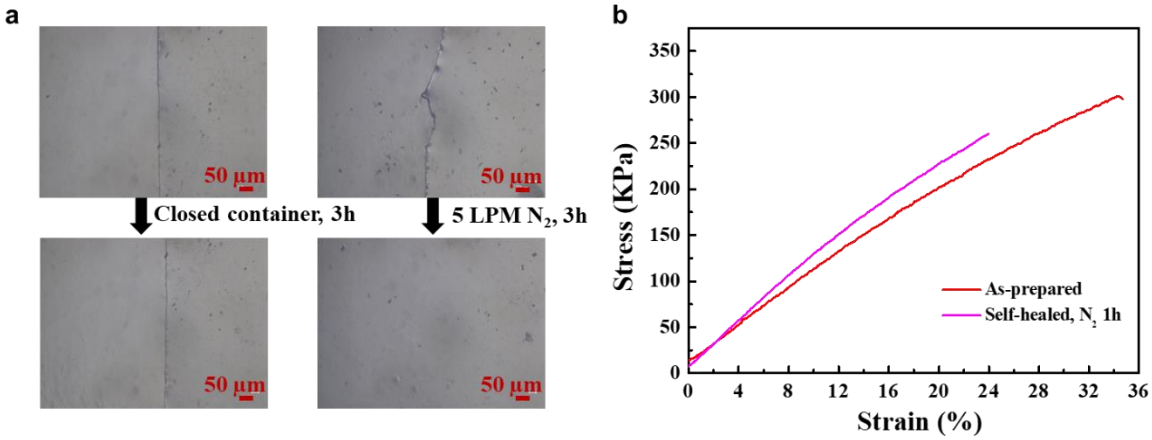

Figure 9. Self-healing of the stiff CB/dPDMS composites. **a)** Optical images of the cut interface self-healed in the closed container and in the presence of flowing gas (N_2, 5 LPM), respectively. **b)** Stress-strain curves for the intact samples and the composites self-healed in the flowing gas for 3h at the speed of 5 LPM (CB/dPDMS composites containing 10% triD_4).

4.2.3.2 Gas-flow Induced Shape-shifting Materials

Manupulating the internal stress distribution could flexibly actuate the materials, as shown in the photo-induced shape-shifting materials.[53] The different stress relaxation of the composites in the flowing gas presents opportunities for manipulating internal stress distribution in the polymer network, reshaping the materials into a complex structure. For example, introducing out-of-plane gradient internal stress within the pre-strained samples by depolymerization on one side would reshape the materials when they are removed from the strained state to redistribute the internal stress. To be more specific, creating the out-of-plane non-uniform stress distribution involved the gradient evaporation of D_4 across the thickness of the composite sample, as shown in the schematic diagram (**Fig. 10a)**. The composites were first stretched, and then one side of the surface was covered by a mask (paper) and the other surface was exposed to the flowing gas. In this way, stress relaxation should occur faster on the unmasked side of the film and this would lead to gradient stress across the sample. When the sample relaxes from the strained state, it will bend to the masked side to redistribute the stress evenly throughout the samples. The bending angle would depend on the internal gradient stress which could be controlled by simply changing the gas flowing time. This hypothesis was tested by exposing the 50%-strain pre-stretched CB(1)/dPDMS(1) composites to the flowing N_2 for different duration time, with one surface masked by the paper. The size of the CB(1)/dPDMS(1) was 40 mm *4 mm *1 mm (length * width * thickness), L_0 was 30mm and N_2 flowing speed was 15 LPM. **Figure 10b** displayed that the materials bent to the masked side and the angle of curvature first increased and then decreased with increasing gas-flowing time (**Figure 10c**), indicating flowing on one side by masking the other side could reshape the

materials into a complex structure. Instead simply curvature the materials, alternatingly masking the pre-stretched samples on both sides and subsequent stress relaxation in the flowing gas allowed us to obtain more complex shapes. For example, attaching a series of 5 mm wide paper strips to alternating sides of a sample (the paper strips did not overlap each other), and subsequently flowed in the 15 LPM flowing N_2 for 10min produced a wave-shaped sample (**Figure 10d**).

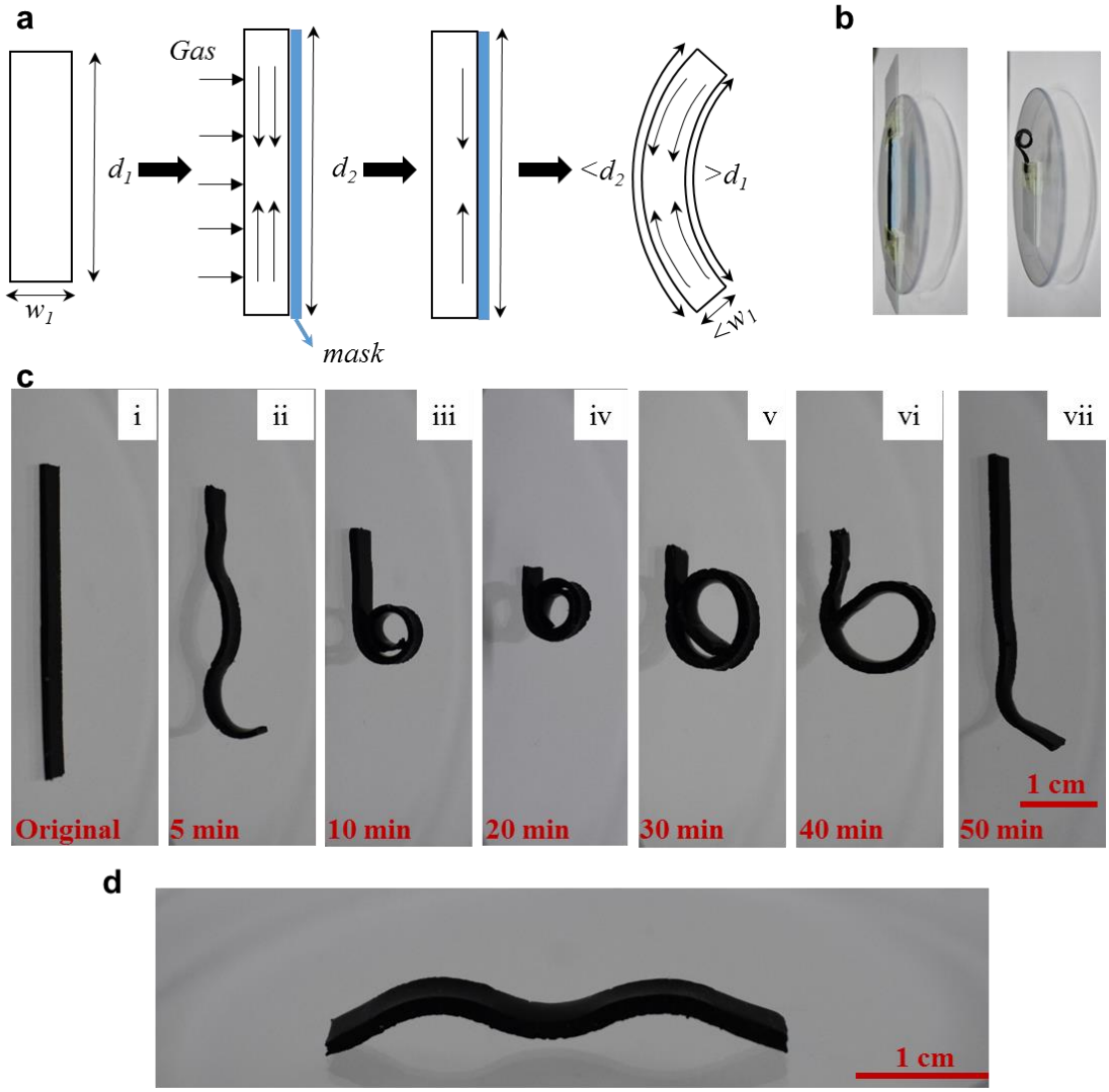

Figure 10 Gas flow-induced shape-shifting. a) Schematic diagram of the introduction of stress and subsequent actuation in the CB(1)/dPDMS(1) composites. **b)** The left picture shows the sample will be put in the home-made chamber to allow the gas-flow to pass through one side only; the right picture shows the sample will bend to the masked side after gradient stress was introduced. **c)** Gas-flowed induced actuation as seen in a 50% strain pre-stressed CB(1)/dPDMS(1) composites (sizes 40 mm in length, 4 mm in width and 1mm in thickness), for different times: i) 0 min, ii) 5 min, iii) 10 min, iv) 20 min, v) 30 min, vi) 40 min, vii) 50 min, viii) 60 min. **d)** A sample gas-flowed on both sides through periodic masks (5 mm in width) for 10 min while at a tensile strain of 50%. (Gas flow: N_2, 15 LPM)

4.3 Conclusion

In this chapter, a gas flow-enhanced relaxation of dynamic polymer composite has been described. Unlike the CO_2-accelerated chain exchange PDMS system that requires the gas to be able to react with the carboxylic groups, our system is independent of the gas species. Any flowing gas such as N_2, Ar, and air is able to be used as the stimuli. This gives flexible choices for the gas and broadens the fields of the gas-responsive materials. In addition, our system is responsive to the flowing gas in contrast to the “static” gas in the CO_2 accelerating PDMS system. The acceleration kinetics are associated with the gas speed, which could be sped up by nearly 60-fold compared to 10-fold in the CO_2 system.

Oligomer evaporation has been proved to be the reason for the accelerated stress relaxation. Neither the solvent, nor small molecules, water, or depolymerization alone are able to accelerate stress relaxation. The acid reactivity is assumed to increase during the oligomer evaporation by fostering silyl-cation transfer kinetics or changing the polymeric acid structure. However, the exact mechanism is still unclear, and it could be interesting since it is a new finding in the acid-catalyzed PDMS. It might offer a fresh new perspective to understand the cationic ring-opening polymerization of cyclic monomers.

The flowing gas-enhanced stress relaxation behavior has been exploited to the self-healing materials. CB(1)/dPDMS(10) composites have shown a 58% self-healing efficiency under the flowing gas in contrast to the 0% self-healing efficiency in the closed container.

The flowing gas-enhanced stress relaxation behavior has also been used to manipulate the stress distribution within the polymer composites to attain 3D complex

shapes by controlling the oligomer evaporation. A curled polymer composite has obtained when the oligomer evaporated from one surface to the other surface and a wave-shape polymer composite has been prepared when the alternative evaporation on both sides was performed. Gas flow-induced actuation has several advantages over commonly used thermally induced shape-shifting or photoinduced actuation techniques. First, the lack of a need for temperature rise and light is important for many applications. For example, when the materials are combined with other components to form a product, heating would probably damage other components while light could not reach the responsive materials if they are buried inside the product. Additionally, pattering could be utilized in both the shape formation and release, enabling arbitrary actuation patterns that are not attainable via the thermal-induced shape memory materials. Though the patterning technique is attainable to the photoinduced shape-shifting materials and the photoinduced actuation has the advantages in the resolution control and actuation speed over the flowing gas-induced actuation, photoinduced actuation requires the materials to be transparent so that light can penetrate the materials. And this requires the special polymer design and limits the application of photoinduced actuation. And to this point, our flowing gas-induced actuation is preferable.

4.4 Experiment Section

a. Materials and Methods

Octamethylcyclotetrasiloxane (D_4, 98%, Gelest), NaOH (Sigma-Aldrich) and $CaCl_2$, toluene (99.7, Sigma-Aldrich), trifluoromethanesulfonic acid (99%, Sigma-Aldrich), conductive epoxy resin (Farnell) were all used as purchased. Carbon black pearls

2000 was provided by Carbot Corporation for free, aiming to the experimental research. The synthesis of 1,1,1-tri(2-heptamethylcyclotetrasiloxane-yl-ethyl)-methylsilane (triD$_4$) has already been reported in **Chapter 2**.

b. Fabrication of CB/dPDMS Composites

For example, the mixture of 0.02g carbon black (CB) powders and 2g D$_4$ monomer containing 1 wt.% crosslinker was subjected to ultrasonication for 30 min, followed by adding 20 μl triflic acid. The obtained mixture was stored for 12h before being used for further experiments. The same process was used to prepare the samples with different triD$_4$ contents. In our experiments, CB/dPDMS composites were cut into strips with the sizes about 27mm*4mm*1mm (length, width, and thickness) for all measurements, if there was no special statement.

c. Fabrication of Home-made Chamber

Figure 12 showed the image of the home-made chamber. A PET box was with one inlet and one outlet was connected to the gas bottle via a flowmeter to control the gas rate. This chamber was used with different gas species, such as the N_2, air, and Ar.

Figure 11. Home-made chamber to control the gas flow

Chapter 5

5. Conclusions and Outlooks

The dynamic nature of acid-catalyzed silicone rubber has been investigated in 1950s but it has not been utilized to prepare dynamic functional soft materials yet. This thesis focuses on the exploration of acid-catalyzed silicone rubbers as matrices for the preparation of various dynamic polymer composite.

This thesis has concluded the basic term of dynamic covalent elastomer and discussed the state of the art of material systems based on the acid-catalyzed dynamic PDMS. Especially, the equilibrium of acid-catalyzed silicone has been stated in detail (**Chapter 1**). Such equilibrium nature has been amplified from the molecular level to material ones by applying the concept of growth to design the materials (**Chapter 2**). Here a novel inspiration from Planarian has been introduced and led to the creation of a kind of self-growing and self-degrowing polymeric composites that could either increase the size by incorporating nutrients or decrease by releasing nutrients. It has been demonstrated that self-growing and self-degrowing polymeric composites can flexibly control their size, structure, shape, mechanical property, and hydrophobicity. On the other hand, this thesis also has explored the application of dynamic silicone composites on tactile force sensors (**Chapter 3**). It has been found

that the CB/dPDMS composites show post-tunable sensitivity by shifting the equilibrium state of dynamic silicone composites. My results have proved that the conductive nanoparticles have been rearranged during stretching-induced equilibrium shifting (relaxation). In the last part of this thesis, a surprise flowing gas-enhanced relaxation behavior of acid-catalyzed silicone composites has been shown for the first time (**Chapter 4**). The stress can be relaxed 60 times faster in the flowing gas than in the closed container. And the experiments have demonstrated that flowing gas-enhanced relaxation behaviour is independent on the gas species and associate with acid reactivity. The main contributions are presented as follows:

- This Thesis offers new methods to prepare polymeric materials. The self-growing and self-degrowing strategy in **Chapter 2** provides a fundamentally new approach to prepare polymeric materials, distinguished from the synthetic objects that are produced through completely different strategies, i.e. molding, assembling, printing, tailoring etc. And the mechano-stretching method in **Chapter 3** also provides a facile method to post-tune the sensitivity of the polymer composites, which is normally not attainable in the covalent polymer composites.
- This Thesis displays novel functional polymer material of CB/dPDMS composites. The flowing gas-enhanced stress relaxation behaviour means that flowing gas could be used as the stimuli to trigger the materials (**Chapter 4**). The flowing gas-responsive material enriches the stimuli-responsive materials society that normally exploits the light, heat,

pH, humidity, electrical or magnetic field as the stimuli to trigger the materials.

- This Thesis spurs the understanding of the cationic polymerization of cyclic siloxanes. The enhanced acid reactivity under the flowing gas implies that the flowing gas offers a stimulus to activate the acid. This is not reported in the literature and will be interesting for the chemist, especially those concentrate on the dynamic Si-O bonds. Though the mechanism is still unclear, it definitely benefits the investigation of the cationic polymerization of cyclic siloxanes.

Generally speaking, three different functional materials based on the acid-catalyzed dynamic PDMS were proposed for the applications in different fields. Beyond the materials science, the Thesis is also attractive to the chemical communities. For further development, our concentration will be focused on the following points

- Since the Thesis offers fundamentally new material synthesis methods, it is reasonable to expand these methods to other material systems. Also, the strong acid used in the dynamic PDMS system limits the applications in various fields, especially in the biological system. The development of the bio-compatible material system would diverse the applications.
- The mechanism that is responsible for the flowing gas-accelerated stress relaxation kinetics will be figured out. The mechanism would be interesting to the basic chemistry and could also be used for designing new functional materials.

List of scientific contributions

Articles

1. **X. Zhou**, G. Ma, H. Zhao, J. Cui, Self-Forming Interlocking Interfaces on the Immiscible Polymer Bilayers via Gelation-Mediated Phase Separation. **Macromolecular Rapid Communications**, 2017, 38, 1700206.
2. H. Zhao, P. Lizbeth, **X. Zhou**, X. Deng, J. Cui, Multi-Stimuli Responsive Liquid-Release in Dynamic Polymer Coatings for Controlling Surface Slipperiness and Transparency, **Advanced Materials Interfaces,** 2019, 6, 1901028.
3. **X. Zhou**, X. Zhang, H. Zhao, B. P. Krishnan, J. Cui, Self-healable and recyclable tactile force sensors with post-tunable sensitivity, **submitted to Advanced Functional Materials.**
4. Y. Zheng, M. Dehghanydahaj, M. Aizenberg, Y. Yao, Y. Hu, **X. Zhou**, J. Aizenberg, J. Cui, Self-growing Polymeric Materials with on-demand Evolution of Shape and Properties, **to be submitted**.
5. **X. Zhou**, B. P. Krishnan, H.Zhao, J. Cui, A Bio-inspired Self-adaptive, Self-growing and Degrowing Elastomer with Programmable Bulk Properties, **to be submitted.**
6. **X. Zhou**, H. Zhao, J. Cui, A Gas-flow Responsive Dynamic Covalent Polymer Composite, **to be submitted.**

Participation in exercises

7. "The 5th International Symposium of Flexible and Stretchable Electronics", at Southern University of Science and Technology, 2019, Shenzhen, China

Curriculum Vitae

Name: Xiaozhuang Zhou

Sex: Male

Date of Birth: 15 October 1990

Nationality: P. R. China

Tel: +49 (0) 1795594029

E-mail: Xiaozhuang.Zhou@leibniz-inm.de

Address: INM-Leibniz Institute for New Materials

Campus D2 2, 66123 Saarbrücken, Germany

Education and Research Experience

07/2016-05/2020, INM-Leibniz Institute for New Materials, Saarbrücken, Germany

Ph.D in Chemical Science

Advisor: Dr. Jiaxi Cui, Prof. Dr. Aránzazu del Campo, Prof. Gerhard Wenz

11/2015-06/2016, Karlsruher Institute of Technology, Karlsruher, Germany

Ph.D in Institute for Applied Materials

Advisor: Prof. Dr. Hans Jürgen Seifert, Dr. Martin Steinbrück

09/2012-07/2015, Wuhan University of Technology, Wuhan, China

Master Student in Materials Science

Advisor: Prof. Lianmeng Zhang, Member of Chinese Engieering Academy

09/2007-07/2011, Chang'an University, Xi'an, China.

Bachelor in Biological Engineering

Patent

L. Zhang, X. Zhou, K. Yu, Q. Shen, G. Luo, M. Li, C. Wang, S. Liu, One Novel Method to Fabricate W-Cu Gradient Materials by Tape-Casting (**Authorized**, Granted No. CN103317140B)

Selected Award

2015-2019 Chinese Scholarship Council

2014 All-round Good Student for the College

2013 Master National Scholarship

Selected Conference Presentation

1. The 5th International Symposium of Flexible and Stretchable Electronics 2019, Shenzhen, China

2. EERA JPNM Stakeholders Workshop 2016, Rome, Italy

Contacts of References

1. Dr. Jiaxi Cui; E-mail: jiaxi.cui@leibniz-inm.de

INM–Leibniz Institute for New Materials, Campus D2 2, Saarbrücken 66123, Germany

2. Prof. Lianmeng Zhang; Tel.: +86 027 87168606; E-mail: lmzhang@whut.edu.cn

State Key Lab of Advanced Technology for Materials Synthesis and Processing, Wuhan University of Technology, Wuhan 430070, China.

3. Prof. Zhengyi Fu: Tel:+86 0 27-87662983; E-mail: zyfu@whut.edu.cn

Director of State Key Lab of Advanced Technology for Materials Synthesis and Processing, Wuhan University of Technology, Wuhan 430070, China.

Reference

1. Warrick, E.; Pierce, O.; Polmanteer, K.; Saam, J., Silicone elastomer developments 1967–1977. *Rubber chemistry and Technology* **1979,** *52* (3), 437-525.

2. Shit, S. C.; Shah, P., A review on silicone rubber. *National Academy Science Letters* **2013,** *36* (4), 355-365.

3. Cherney, E.; Gorur, R., RTV silicone rubber coatings for outdoor insulators. *IEEE Transactions on Dielectrics and Electrical Insulation* **1999,** *6* (5), 605-611.

4. Martins, P.; Natal Jorge, R.; Ferreira, A., A comparative study of several material models for prediction of hyperelastic properties: Application to silicone - rubber and soft tissues. *Strain* **2006,** *42* (3), 135-147.

5. Lewis, F., The science and technology of silicone rubber. *Rubber Chemistry and Technology* **1962,** *35* (5), 1222-1275.

6. Zhou, H.; Wang, H.; Niu, H.; Gestos, A.; Wang, X.; Lin, T., Fluoroalkyl silane modified silicone rubber/nanoparticle composite: a super durable, robust superhydrophobic fabric coating. *Advanced Materials* **2012,** *24* (18), 2409-2412.

7. Vondráček, P.; Doležel, B., Biostability of medical elastomers: a review. *Biomaterials* **1984,** *5* (4), 209-214.

8. Minami, A.; Iwasaki, N.; Kutsumi, K.; Suenaga, N.; Yasuda, K., A long-term follow-up of silicone-rubber interposition arthroplasty for osteoarthritis of the thumb carpometacarpal joint. *Hand Surgery* **2005,** *10* (01), 77-82.

9. Brookes, P.; Livingston, A., Aqueous-aqueous extraction of organic pollutants through tubular silicone rubber membranes. *Journal of Membrane Science* **1995,** *104* (1-2), 119-137.

10. Abbasi, F.; Mirzadeh, H.; Katbab, A. A., Bulk and surface modification of silicone rubber for biomedical applications. *Polymer International* **2002,** *51* (10), 882-888.

11. Zou, W.; Dong, J.; Luo, Y.; Zhao, Q.; Xie, T., Dynamic covalent polymer networks: from old chemistry to modern day innovations. *Advanced Materials* **2017,** *29* (14), 1606100.

12. Rahimi, A.; García, J. M., Chemical recycling of waste plastics for new materials production. *Nature Reviews Chemistry* **2017,** *1* (6), 1-11.

13. Chakma, P.; Konkolewicz, D., Dynamic covalent bonds in polymeric materials. *Angewandte Chemie International Edition* **2019,** *58* (29), 9682-9695.

14. Winne, J. M.; Leibler, L.; Du Prez, F. E., Dynamic covalent chemistry in polymer networks: a mechanistic perspective. *Polymer Chemistry* **2019,** *10* (45), 6091-6108.

15. Denissen, W.; Winne, J. M.; Du Prez, F. E., Vitrimers: permanent organic networks with glass-like fluidity. *Chemical Science* **2016,** *7* (1), 30-38.

16. Jin, Y.; Yu, C.; Denman, R. J.; Zhang, W., Recent advances in dynamic covalent chemistry. *Chemical Society Reviews* **2013,** *42* (16), 6634-6654.

17. Mark, H.; Tobolsky, A., *Physical Chemistry of High Polymeric Systems*. Interscience: New York, 1940.

18. Imbernon, L.; Oikonomou, E.; Norvez, S.; Leibler, L., Chemically crosslinked yet reprocessable epoxidized natural rubber via thermo-activated disulfide rearrangements. *Polymer Chemistry* **2015,** *6* (23), 4271-4278.

19. Otsuka, H.; Nagano, S.; Kobashi, Y.; Maeda, T.; Takahara, A., A dynamic covalent polymer driven by disulfide metathesis under photoirradiation. *Chemical Communications* **2010,** *46* (7), 1150-1152.

20. Fairbanks, B. D.; Singh, S. P.; Bowman, C. N.; Anseth, K. S., Photodegradable, photoadaptable hydrogels via radical-mediated disulfide fragmentation reaction. *Macromolecules* **2011,** *44* (8), 2444-2450.

21. Scott, T. F.; Schneider, A. D.; Cook, W. D.; Bowman, C. N., Photoinduced plasticity in cross-linked polymers. *Science* **2005,** *308* (5728), 1615-1617.

22. Amamoto, Y.; Kamada, J.; Otsuka, H.; Takahara, A.; Matyjaszewski, K., Repeatable photoinduced self-healing of covalently cross-linked polymers through reshuffling of trithiocarbonate units. *Angewandte Chemie International Edition* **2011,** *50* (7), 1660-1663.

23. Amamoto, Y.; Otsuka, H.; Takahara, A.; Matyjaszewski, K., Self-healing of covalently cross-linked polymers by reshuffling thiuram disulfide moieties in air under visible light. *Advanced Materials* **2012,** *24* (29), 3975-3980.

24. Montarnal, D.; Capelot, M.; Tournilhac, F.; Leibler, L., Silica-like malleable materials from permanent organic networks. *Science* **2011,** *334* (6058), 965-968.

25. Brutman, J. P.; Delgado, P. A.; Hillmyer, M. A., Polylactide vitrimers. *ACS Macro Letters* **2014,** *3* (7), 607-610.

26. Zhao, Q.; Zou, W.; Luo, Y.; Xie, T., Shape memory polymer network with thermally distinct elasticity and plasticity. *Science Advances* **2016,** *2* (1), e1501297.

27. Blank, W. J.; He, Z.; Picci, M., Catalysis of the epoxy-carboxyl reaction. *Journal of Coatings Technology* **2002,** *74* (926), 33-41.

28. Delahaye, M.; Winne, J. M.; Du Prez, F. E., Internal Catalysis in Covalent Adaptable Networks: Phthalate Monoester Transesterification As a Versatile Dynamic Cross-Linking Chemistry. *Journal of the American Chemical Society* **2019,** *141* (38), 15277-15287.

29. Fortman, D. J.; Brutman, J. P.; Cramer, C. J.; Hillmyer, M. A.; Dichtel, W. R., Mechanically activated, catalyst-free polyhydroxyurethane vitrimers. *Journal of the American Chemical Society* **2015,** *137* (44), 14019-14022.

30. Zheng, N.; Fang, Z.; Zou, W.; Zhao, Q.; Xie, T., Thermoset shape‐memory polyurethane with intrinsic plasticity enabled by transcarbamoylation. *Angewandte Chemie International Edition* **2016,** *55* (38), 11421-11425.

31. Neal, J. A.; Mozhdehi, D.; Guan, Z., Enhancing mechanical performance of a covalent self-healing material by sacrificial noncovalent bonds. *Journal of the American Chemical Society* **2015,** *137* (14), 4846-4850.

32. Lu, Y.-X.; Guan, Z., Olefin metathesis for effective polymer healing via dynamic exchange of strong carbon–carbon double bonds. *Journal of the American Chemical Society* **2012,** *134* (34), 14226-14231.

33. Guerre, M.; Taplan, C.; Nicolaÿ, R.; Winne, J. M.; Du Prez, F. E., Fluorinated vitrimer elastomers with a dual temperature response. *Journal of the American Chemical Society* **2018,** *140* (41), 13272-13284.

34. Denissen, W.; De Baere, I.; Van Paepegem, W.; Leibler, L.; Winne, J.; Du Prez, F. E., Vinylogous urea vitrimers and their application in fiber reinforced composites. *Macromolecules* **2018,** *51* (5), 2054-2064.

35. Denissen, W.; Droesbeke, M.; NicolaÿR.; Leibler, L.; Winne, J. M.; Du Prez, F. E., Chemical control of the viscoelastic properties of vinylogous urethane vitrimers. *Nature Communications* **2017,** *8* (1), 1-7.

36. Denissen, W.; Rivero, G.; NicolaÿR.; Leibler, L.; Winne, J. M.; Du Prez, F. E., Vinylogous urethane vitrimers. *Advanced Functional Materials* **2015,** *25* (16), 2451-2457.

37. Obadia, M. M.; Mudraboyina, B. P.; Serghei, A.; Montarnal, D.; Drockenmuller, E., Reprocessing and recycling of highly cross-linked ion-conducting networks through transalkylation exchanges of C–N bonds. *Journal of the American Chemical Society* **2015,** *137* (18), 6078-6083.

38. Nicolaou, K. C.; Snyder, S. A.; Montagnon, T.; Vassilikogiannakis, G., The Diels–Alder reaction in total synthesis. *Angewandte Chemie International Edition* **2002,** *41* (10), 1668-1698.

39. Xu, F.; Xiao, X.; Hoye, T. R., Photochemical Hexadehydro-Diels–Alder Reaction. *Journal of the American Chemical Society* **2017,** *139* (25), 8400-8403.

40. Aragones, A. C.; Haworth, N. L.; Darwish, N.; Ciampi, S.; Bloomfield, N. J.; Wallace, G. G.; Diez-Perez, I.; Coote, M. L., Electrostatic catalysis of a Diels–Alder reaction. *Nature* **2016,** *531* (7592), 88-91.

41. Chen, X.; Dam, M. A.; Ono, K.; Mal, A.; Shen, H.; Nutt, S. R.; Sheran, K.; Wudl, F., A thermally re-mendable cross-linked polymeric material. *Science* **2002,** *295* (5560), 1698-1702.

42. Radl, S.; Kreimer, M.; Griesser, T.; Oesterreicher, A.; Moser, A.; Kern, W.; Schloegl, S., New strategies towards reversible and mendable epoxy based materials employing [4πs+ 4πs] photocycloaddition and thermal cycloreversion of pendant anthracene groups. *Polymer* **2015,** *80*, 76-87.

43. Nguyen, L.-T. T.; Nguyen, H. T.; Truong, T. T., Thermally mendable material based on a furyl-telechelic semicrystalline polymer and a maleimide crosslinker. *Journal of Polymer Research* **2015,** *22* (9), 186.

44. Gaina, C.; Ursache, O.; Gaina, V., Re-mendable polyurethanes. *Polymer-Plastics Technology and Engineering* **2011,** *50* (7), 712-718.

45. Toncelli, C.; Bouwhuis, S.; Broekhuis, A. A.; Picchioni, F., Cyclopentadiene-functionalized polyketone as self-cross-linking thermo-reversible thermoset with increased softening temperature. *Journal of Applied Polymer Science* **2016,** *133* (4).

46. Foster, R. A.; Willis, M. C., Tandem inverse-electron-demand hetero-/retro-Diels–Alder reactions for aromatic nitrogen heterocycle synthesis. *Chemical Society Reviews* **2013,** *42* (1), 63-76.

47. Billiet, S.; De Bruycker, K.; Driessen, F.; Goossens, H.; Van Speybroeck, V.; Winne, J. M.; Du Prez, F. E., Triazolinediones enable ultrafast and reversible click chemistry for the design of dynamic polymer systems. *Nature Chemistry* **2014,** *6* (9), 815.

48. Ying, H.; Zhang, Y.; Cheng, J., Dynamic urea bond for the design of reversible and self-healing polymers. *Nature Communications* **2014,** *5* (1), 1-9.

49. Zhang, Y.; Ying, H.; Hart, K. R.; Wu, Y.; Hsu, A. J.; Coppola, A. M.; Kim, T. A.; Yang, K.; Sottos, N. R.; White, S. R., Malleable and recyclable poly (urea - urethane) thermosets bearing hindered urea bonds. *Advanced Materials* **2016,** *28* (35), 7646-7651.

50. Cremaldi, J. C.; Bhushan, B., Bioinspired self-healing materials: lessons from nature. *Beilstein Journal of Nanotechnology* **2018,** *9* (1), 907-935.

51. White, S. R.; Sottos, N. R.; Geubelle, P. H.; Moore, J. S.; Kessler, M. R.; Sriram, S.; Brown, E. N.; Viswanathan, S., Autonomic healing of polymer composites. *Nature* **2001,** *409* (6822), 794-797.

52. Chung, C.-M.; Roh, Y.-S.; Cho, S.-Y.; Kim, J.-G., Crack healing in polymeric materials via photochemical [2+ 2] cycloaddition. *Chemistry of Materials* **2004,** *16* (21), 3982-3984.

53. Scott, T. F.; Draughon, R. B.; Bowman, C. N., Actuation in crosslinked polymers via photoinduced stress relaxation. *Advanced Materials* **2006,** *18* (16), 2128-2132.

54. Kloxin, C. J.; Scott, T. F.; Park, H. Y.; Bowman, C. N., Mechanophotopatterning on a photoresponsive elastomer. *Advanced Materials* **2011,** *23* (17), 1977-1981.

55. Mu, X.; Sowan, N.; Tumbic, J. A.; Bowman, C. N.; Mather, P. T.; Qi, H. J., Photo-induced bending in a light-activated polymer laminated composite. *Soft Matter* **2015,** *11* (13), 2673-2682.

56. Zhang, G.; Zhao, Q.; Yang, L.; Zou, W.; Xi, X.; Xie, T., Exploring dynamic equilibrium of Diels–Alder reaction for solid state plasticity in remoldable shape memory polymer network. *ACS Macro Letters* **2016,** *5* (7), 805-808.

57. Yang, Z.; Wang, Q.; Wang, T., Dual-triggered and thermally reconfigurable shape memory graphene-vitrimer composites. *ACS Applied Materials and Interfaces* **2016,** *8* (33), 21691-21699.

58. Pei, Z.; Yang, Y.; Chen, Q.; Wei, Y.; Ji, Y., Regional shape control of strategically assembled multishape memory vitrimers. *Advanced Materials* **2016,** *28* (1), 156-160.

59. Li, Y.; Rios, O.; Keum, J. K.; Chen, J.; Kessler, M. R., Photoresponsive liquid crystalline epoxy networks with shape memory behavior and dynamic ester bonds. *ACS Applied Materials and Interfaces* **2016,** *8* (24), 15750-15757.

60. Lawton, M. I.; Tillman, K. R.; Mohammed, H. S.; Kuang, W.; Shipp, D. A.; Mather, P. T., Anhydride-based reconfigurable shape memory elastomers. *ACS Macro Letters* **2016,** *5* (2), 203-207.

61. Behl, M.; Lendlein, A., Shape-memory polymers. *Kirk-Othmer Encyclopedia of Chemical Technology* **2000**, 1-16.

62. Zheng, N.; Hou, J.; Xu, Y.; Fang, Z.; Zou, W.; Zhao, Q.; Xie, T., Catalyst-free thermoset polyurethane with permanent shape reconfigurability and highly tunable triple-shape memory performance. *ACS Macro Letters* **2017,** *6* (4), 326-330.

63. Ohm, C.; Brehmer, M.; Zentel, R., Liquid crystalline elastomers as actuators and sensors. *Advanced Materials* **2010,** *22* (31), 3366-3387.

64. Wermter, H.; Finkelmann, H., Liquid crystalline elastomers as artificial muscles. *e-Polymers* **2001,** *1* (1).

65. Küpfer, J.; Finkelmann, H., Nematic liquid single crystal elastomers. *Die Makromolekulare Chemie, Rapid Communications* **1991,** *12* (12), 717-726.

66. Pei, Z.; Yang, Y.; Chen, Q.; Terentjev, E. M.; Wei, Y.; Ji, Y., Mouldable liquid-crystalline elastomer actuators with exchangeable covalent bonds. *Nature Materials* **2014,** *13* (1), 36-41.

67. Yang, Y.; Pei, Z.; Li, Z.; Wei, Y.; Ji, Y., Making and remaking dynamic 3D structures by shining light on flat liquid crystalline vitrimer films without a mold. *Journal of the American Chemical Society* **2016,** *138* (7), 2118-2121.

68. Ube, T.; Kawasaki, K.; Ikeda, T., Photomobile liquid - crystalline elastomers with rearrangeable networks. *Advanced Materials* **2016,** *28* (37), 8212-8217.

69. Ishida, K.; Yoshie, N., Two-way conversion between hard and soft properties of semicrystalline cross-linked polymer. *Macromolecules* **2008,** *41* (13), 4753-4757.

70. Ishida, K.; Nishiyama, Y.; Michimura, Y.; Oya, N.; Yoshie, N., Hard-Soft Conversion in Network Polymers: Effect of Molecular Weight of Crystallizable Prepolymer. *Macromolecules* **2010,** *43* (2), 1011-1015.

71. Ishida, K.; Weibel, V.; Yoshie, N., Substituent effect on structure and physical properties of semicrystalline Diels–Alder network polymers. *Polymer* **2011,** *52* (13), 2877-2882.

72. Chow, C.-F.; Fujii, S.; Lehn, J.-M., Crystallization-driven constitutional changes of dynamic polymers in response to neat/solution conditions. *Chemical Communications* **2007,** (42), 4363-4365.

73. Ono, T.; Fujii, S.; Nobori, T.; Lehn, J.-M., Optodynamers: expression of color and fluorescence at the interface between two films of different dynamic polymers. *Chemical Communications* **2007,** (42), 4360-4362.

74. Costanzo, P. J.; Beyer, F. L., Thermally driven assembly of nanoparticles in polymer matrices. *Macromolecules* **2007,** *40* (11), 3996-4001.

75. Costanzo, P. J.; Beyer, F. L., Thermoresponsive, optically active films based on Diels–Alder chemistry. *Chemistry of Materials* **2007,** *19* (25), 6168-6173.

76. Singh, N.; Hui, D.; Singh, R.; Ahuja, I.; Feo, L.; Fraternali, F., Recycling of plastic solid waste: A state of art review and future applications. *Composites Part B: Engineering* **2017,** *115*, 409-422.

77. Morris, J., Recycling versus incineration: an energy conservation analysis. *Journal of Hazardous Materials* **1996,** *47* (1-3), 277-293.

78. Marco, I. d.; Caballero, B.; Torres, A.; Laresgoiti, M. F.; Chomon, M. J.; Cabrero, M. A., Recycling polymeric wastes by means of pyrolysis. *Journal of Chemical Technology and Biotechnology* **2002,** *77* (7), 817-824.

79. Xu, P.; Li, J., Chemical recycling of carbon fibre/epoxy composites in a mixed solution of peroxide hydrogen and N, N-dimethylformamide. *Composites Science and Technology* **2013,** *82*, 54-59.

80. Dang, W.; Kubouchi, M.; Yamamoto, S.; Sembokuya, H.; Tsuda, K., An approach to chemical recycling of epoxy resin cured with amine using nitric acid. *Polymer* **2002,** *43* (10), 2953-2958.

81. Tian, Q.; Yuan, Y. C.; Rong, M. Z.; Zhang, M. Q., A thermally remendable epoxy resin. *Journal of Materials Chemistry* **2009,** *19* (9), 1289-1296.

82. Takahashi, A.; Ohishi, T.; Goseki, R.; Otsuka, H., Degradable epoxy resins prepared from diepoxide monomer with dynamic covalent disulfide linkage. *Polymer* **2016,** *82*, 319-326.

83. Mcelhanon, J. R.; Russick, E. M.; Wheeler, D. R.; Loy, D. A.; Aubert, J. H., Removable foams based on an epoxy resin incorporating reversible Diels–Alder adducts. *Journal of Applied Polymer Science* **2002,** *85* (7), 1496-1502.

84. Buchwalter, S. L.; Kosbar, L. L., Cleavable epoxy resins: Design for disassembly of a thermoset. *Journal of Polymer Science Part A: Polymer Chemistry* **1996,** *34* (2), 249-260.

85. Zia, K. M.; Bhatti, H. N.; Bhatti, I. A., Methods for polyurethane and polyurethane composites, recycling and recovery: A review. *Reactive and Functional Polymers* **2007,** *67* (8), 675-692.

86. Hashimoto, T.; Umehara, A.; Urushisaki, M.; Kodaira, T., Synthesis of a new degradable polyurethane elastomer containing polyacetal soft segments. *Journal of Polymer Science Part A: Polymer Chemistry* **2004,** *42* (11), 2766-2773.

87. Endo, T.; Suzuki, T.; Sanda, F.; Takata, T., A novel approach for the chemical recycling of polymeric materials: the network polymer⇄ bifunctional monomer reversible system. *Macromolecules* **1996,** *29* (9), 3315-3316.

88. Endo, T.; Sanda, F., A novel approach for the chemical 'recycling'of polymeric materials equilibrium polymerization system of spiro orthoesters. *Reactive and Functional Polymers* **1997,** *33* (2-3), 241-245.

89. Kojima, M.; Ogawa, K.; Mizoshima, H.; Tosaka, M.; Kohjiya, S.; Ikeda, Y., Devulcanization of sulfur-cured isoprene rubber in supercritical carbon dioxide. *Rubber Chemistry and Technology* **2003,** *76* (4), 957-968.

90. Kojima, M.; Tosaka, M.; Ikeda, Y., Chemical recycling of sulfur-cured natural rubber using supercritical carbon dioxide. *Green Chemistry* **2004,** *6* (2), 84-89.

91. Myhre, M.; Saiwari, S.; Dierkes, W.; Noordermeer, J., Rubber recycling: chemistry, processing, and applications. *Rubber Chemistry and Technology* **2012,** *85* (3), 408-449.

92. Kojima, M.; Tosaka, M.; Ikeda, Y.; Kohjiya, S., Devulcanization of carbon black filled natural rubber using supercritical carbon dioxide. *Journal of Applied Polymer Science* **2005,** *95* (1), 137-143.

93. Buese, M. A.; Chang, P.-S., Highly functionalized polycyclosiloxanes and their polymerization into thermally reversible living rubbers. US Patent 5,298,589: March 29, 1994.

94. Treptow, R. S., Le Châtelier's principle applied to the temperature dependence of solubility. *Journal of Chemical Education* **1984,** *61* (6), 499.

95. Campbell, J. A., Le Châtelier's principle, temperature effects, and entropy. *Journal of Chemical Education* **1985,** *62* (3), 231.

96. Chojnowski, J., Kinetically controlled siloxane ring-opening polymerization. *Journal of Inorganic Organometallic Polymers* **1991,** *1* (3), 299-323.

97. Chojnowski, J.; Wilczek, L., Mechanism of the Polymerization of Hexamethylcyclotrisiloxane (D3) in the Presence of a Strong Protonic Acid. *Makromolekulare Chemie* **1979,** *180* (1), 117-130.

98. Chojnowski, J.; Rubinsztajn, S.; Wilczek, L., Acid-catalyzed condensation of model hydroxyl-terminated dimethylsiloxane oligomers-cyclization vs. linear condensation: intra-inter catalysis. *Macromolecules* **1987,** *20* (10), 2345-2355.

99. Sigwalt, P.; Masure, M.; Moreau, M.; Bischoff, R. In *Mechanism of formation of cyclic species in cationic ring-opening polymerization of cyclodimethylsiloxanes*, Makromolekulare Chemie. Macromolecular Symposia, Wiley Online Library: 1993; pp 147-166.

100. Hurd, D. T., On the mechanism of the acid-catalyzed rearrangement of siloxane linkages in organopolysiloxanes. *Journal of the American Chemical Society* **1955,** *77* (11), 2998-3001.

101. Kantor, S. W.; Grubb, W. T.; Osthoff, R. C., The mechanism of the acid-and base-catalyzed equilibration of siloxanes. *Journal of the American Chemical Society* **1954,** *76* (20), 5190-5197.

102. Zheng, P.; McCarthy, T., A surprise from 1954: siloxane equilibration is a simple, robust, and obvious polymer self-healing mechanism. *Journal of the American Chemical Society* **2012,** *134* (4), 2024-2027.

103. Schmolke, W.; Perner, N.; Seiffert, S., Dynamically cross-linked polydimethylsiloxane networks with ambient-temperature self-healing. *Macromolecules* **2015,** *48* (24), 8781-8788.

104. de Sousa, N.; Adell, T., Detection of Cell Death in Planarians. *BIO-PROTOCOL* **2018,** *8* (19).

105. Tu, K. C.; Pearson, B. J.; Alvarado, A. S., TORC1 is required to balance cell proliferation and cell death in planarians. *Developmental Biology* **2012,** *365* (2), 458-469.

106. Rink, J. C., Stem cell systems and regeneration in planaria. *Development Genes and Evolution* **2013,** *223* (1-2), 67-84.

107. Akl, W.; Baz, A., Multi-cell active acoustic metamaterial with programmable bulk modulus. *Journal of Intelligent Material Systems and Structures* **2010,** *21* (5), 541-556.

108. Bathe, M.; Rothemund, P. W., DNA nanotechnology: A foundation for programmable nanoscale materials. *MRS Bulletin* **2017,** *42* (12), 882-888.

109. Sanner, N.; Huot, N.; Audouard, E.; Larat, C.; Huignard, J.-P., Direct ultrafast laser micro-structuring of materials using programmable beam shaping. *Optics and Lasers in Engineering* **2007,** *45* (6), 737-741.

110. Knight, A. S.; Zhou, E. Y.; Francis, M. B.; Zuckermann, R. N., Sequence programmable peptoid polymers for diverse materials applications. *Advanced Materials* **2015,** *27* (38), 5665-5691.

111. Bui, H.; Onodera, C.; Kidwell, C.; Tan, Y.; Graugnard, E.; Kuang, W.; Lee, J.; Knowlton, W. B.; Yurke, B.; Hughes, W. L., Programmable periodicity of quantum dot arrays with DNA origami nanotubes. *Nano Letters* **2010,** *10* (9), 3367-3372.

112. Fan, X.; Chung, J. Y.; Lim, Y. X.; Li, Z.; Loh, X. J., Review of adaptive programmable materials and their bioapplications. *ACS Applied Materials and Interfaces* **2016,** *8* (49), 33351-33370.

113. Ware, T. H.; McConney, M. E.; Wie, J. J.; Tondiglia, V. P.; White, T. J., Voxelated liquid crystal elastomers. *Science* **2015,** *347* (6225), 982-984.

114. White, T. J.; Broer, D. J., Programmable and adaptive mechanics with liquid crystal polymer networks and elastomers. *Nature Materials* **2015,** *14* (11), 1087-1098.

115. Yakacki, C.; Saed, M.; Nair, D.; Gong, T.; Reed, S.; Bowman, C., Tailorable and programmable liquid-crystalline elastomers using a two-stage thiol–acrylate reaction. *Rsc Advances* **2015,** *5* (25), 18997-19001.

116. Wu, Z. L.; Moshe, M.; Greener, J.; Therien-Aubin, H.; Nie, Z.; Sharon, E.; Kumacheva, E., Three-dimensional shape transformations of hydrogel sheets induced by small-scale modulation of internal stresses. *Nature Communications* **2013,** *4* (1), 1-7.

117. Shang, J.; Le, X.; Zhang, J.; Chen, T.; Theato, P., Trends in polymeric shape memory hydrogels and hydrogel actuators. *Polymer Chemistry* **2019,** *10* (9), 1036-1055.

118. Korde, J. M.; Balasubramanian, K., Naturally biomimicked smart shape memory hydrogels for biomedical functions. *Chemical Engineering Journal* **2019**, 122430.

119. Mishra, A.; Korlepara, D. B.; Kumar, M.; Jain, A.; Jonnalagadda, N.; Bejagam, K. K.; Balasubramanian, S.; George, S., Biomimetic temporal self-assembly via fuel-driven controlled supramolecular polymerization. *Nature Communications* **2018,** *9* (1), 1-9.

120. Oohora, K.; Burazerovic, S.; Onoda, A.; Wilson, Y. M.; Ward, T. R.; Hayashi, T., Chemically programmed supramolecular assembly of hemoprotein and streptavidin with alternating alignment. *Angewandte Chemie International Edition* **2012,** *51* (16), 3818-3821.

121. Zhang, W.; Ochi, K.; Fujiki, M.; Naito, M.; Ishikawa, M.; Kaneto, K. i.; Takashima, W.; Saeki, A.; Seki, S., Programmed High-Hole-Mobility Supramolecular Polymers from Disk-Shaped Molecules. *Advanced Functional Materials* **2010,** *20* (22), 3941-3947.

122. Zheng, Y.; Dehghanydahaj, M.; Aizenberg, M.; Yao, Y.; Hu, Y.; Aizenberg, J.; Cui, J., Self-growing polymeric materials with on-demand evolution of shape and properties. *Unpulished*.

123. de Sousa, N.; Adell, T. J. B.-P., Detection of Cell Death in Planarians. *BIO-PROTOCOL* **2018,** *8* (19).

124. Bennardi, D. O.; Romanelli, G. P.; Autino, J. C.; Pizzio, L. R., Trifluoromethanesulfonic acid supported on carbon used as catalysts in the synthesis of flavones and chromones. *Catalysis Communications* **2009,** *10* (5), 576-581.

125. Bely, A. E.; Nyberg, K. G., Evolution of animal regeneration: re-emergence of a field. *Trends in Ecology Evolution* **2010,** *25* (3), 161-170.

126. Reddien, P. W.; Alvarado, A. S., Fundamentals of planarian regeneration. *Annual Review of Cell and Developmental Biology* **2004,** *20*, 725-757.

127. Mizuno, H.; Tobita, M.; Uysal, A. C., Concise review: adipose‐derived stem cells as a novel tool for future regenerative medicine. *Stem Cells* **2012,** *30* (5), 804-810.

128. Dai, X.; Sun, N.; Nielsen, S. O.; Stogin, B. B.; Wang, J.; Yang, S.; Wong, T.-S., Hydrophilic directional slippery rough surfaces for water harvesting. *Science Advances* **2018,** *4* (3), eaaq0919.

129. Liu, M.; Wang, S.; Jiang, L., Nature-inspired superwettability systems. *Nature Reviews Materials* **2017,** *2* (7), 1-17.

130. Assender, H.; Bliznyuk, V.; Porfyrakis, K., How surface topography relates to materials' properties. *Science* **2002,** *297* (5583), 973-976.

131. Ma, Y.; Ma, S.; Wu, Y.; Pei, X.; Gorb, S. N.; Wang, Z.; Liu, W.; Zhou, F., Remote control over underwater dynamic attachment/detachment and locomotion. *Advanced Materials* **2018,** *30* (30), 1801595.

132. Mertaniemi, H.; Jokinen, V.; Sainiemi, L.; Franssila, S.; Marmur, A.; Ikkala, O.; Ras, R. H., Superhydrophobic tracks for low-friction, guided transport of water droplets. *Advanced Materials* **2011,** *23* (26), 2911-2914.

133. Yang, Y.; Li, X.; Zheng, X.; Chen, Z.; Zhou, Q.; Chen, Y., 3D-printed biomimetic super-hydrophobic structure for microdroplet manipulation and oil/water separation. *Advanced Materials* **2018,** *30* (9), 1704912.

134. Kota, A. K.; Kwon, G.; Choi, W.; Mabry, J. M.; Tuteja, A., Hygro-responsive membranes for effective oil-water separation. *Nature Communications* **2012,** *3* (1), 1-8.

135. Zhao, Z.; Li, C.; Dong, Z.; Yang, Y.; Zhang, L.; Zhuo, S.; Zhou, X.; Xu, Y.; Jiang, L.; Liu, M., Adaptive superamphiphilic organohydrogels with reconfigurable surface topography for programming unidirectional liquid transport. *Advanced Functional Materials* **2019,** *29* (16), 1807858.

136. Ilievski, F.; Mazzeo, A. D.; Shepherd, R. F.; Chen, X.; Whitesides, G. M., Soft robotics for chemists. *Angewandte Chemie International Edition* **2011,** *50* (8), 1890-1895.

137. Nghiem, B. T.; Sando, I. C.; Gillespie, R. B.; McLaughlin, B. L.; Gerling, G. J.; Langhals, N. B.; Urbanchek, M. G.; Cederna, P. S., Providing a sense of touch to prosthetic hands. *Plastic and Reconstructive Surgery* **2015,** *135* (6), 1652-1663.

138. Antfolk, C.; D'alonzo, M.; Rosén, B.; Lundborg, G.; Sebelius, F.; Cipriani, C., Sensory feedback in upper limb prosthetics. *Expert Review of Medical Devices* **2013,** *10* (1), 45-54.

139. Son, D.; Lee, J.; Qiao, S.; Ghaffari, R.; Kim, J.; Lee, J. E.; Song, C.; Kim, S. J.; Lee, D. J.; Jun, S. W.; Yang, S.; Park, M.; Shin, J.; Do, K.; Lee, M.; Kang, K.; Hwang, C. S.; Lu, N.; Hyeon, T.; Kim, D.-H., Multifunctional wearable devices for diagnosis and therapy of movement disorders. *Nature Nanotechnology* **2014,** *9* (5), 397.

140. Webb, R. C.; Ma, Y.; Krishnan, S.; Li, Y.; Yoon, S.; Guo, X.; Feng, X.; Shi, Y.; Seidel, M.; Cho, N. H.; Kurniawan, J.; Ahad, J.; Sheth, N.; Kim, J.; Taylor VI, J. G.; Darlington, T.; Chang, K.; Huang, W.; Ayers, J.; Gruebele, A.; Pielak, R. M.; Slepian, M. J.; Huang, Y.; Gorbach, A. M.; Rogers, J. A., Epidermal devices for noninvasive, precise,

and continuous mapping of macrovascular and microvascular blood flow. *Science Advances* **2015,** *1* (9), e1500701.

141. Choi, S.; Park, J.; Hyun, W.; Kim, J.; Kim, J.; Lee, Y. B.; Song, C.; Hwang, H. J.; Kim, J. H.; Hyeon, T.; Kim, D.-H., Stretchable heater using ligand-exchanged silver nanowire nanocomposite for wearable articular thermotherapy. *ACS Nano* **2015,** *9* (6), 6626-6633.

142. Dahiya, R. S.; Metta, G.; Valle, M.; Sandini, G., Tactile sensing-from humans to humanoids. *IEEE Transactions on Robotics* **2009,** *26* (1), 1-20.

143. Johansson, R. S.; Flanagan, J. R., Coding and use of tactile signals from the fingertips in object manipulation tasks. *Nature Reviews Neuroscience* **2009,** *10* (5), 345-359.

144. Abraira, V. E.; Ginty, D. D., The sensory neurons of touch. *Neuron* **2013,** *79* (4), 618-639.

145. Lin, L.; Liu, S.; Zhang, Q.; Li, X.; Ji, M.; Deng, H.; Fu, Q., Towards tunable sensitivity of electrical property to strain for conductive polymer composites based on thermoplastic elastomer. *ACS Applied Materials and Interfaces* **2013,** *5* (12), 5815-5824.

146. Jeon, J.-Y.; Ha, T.-J., Waterproof electronic-bandage with tunable sensitivity for wearable strain sensors. *ACS Applied Materials and Interfaces* **2016,** *8* (4), 2866-2871.

147. Hu, Y.; Zhao, T.; Zhu, P.; Zhang, Y.; Liang, X.; Sun, R.; Wong, C.-P., A low-cost, printable, and stretchable strain sensor based on highly conductive elastic composites with tunable sensitivity for human motion monitoring. *Nano Research* **2018,** *11* (4), 1938-1955.

148. Tao, L.-Q.; Wang, D.-Y.; Tian, H.; Ju, Z.-Y.; Liu, Y.; Pang, Y.; Chen, Y.-Q.; Yang, Y.; Ren, T.-L., Self-adapted and tunable graphene strain sensors for detecting both subtle and large human motions. *Nanoscale* **2017,** *9* (24), 8266-8273.

149. Hwang, J.; Jang, J.; Hong, K.; Kim, K. N.; Han, J. H.; Shin, K.; Park, C. E., Poly (3-hexylthiophene) wrapped carbon nanotube/poly (dimethylsiloxane) composites for use in finger-sensing piezoresistive pressure sensors. *Carbon* **2011,** *49* (1), 106-110.

150. Wang, Z.; Liu, X.; Shen, X.; Han, N. M.; Wu, Y.; Zheng, Q.; Jia, J.; Wang, N.; Kim, J. K., An Ultralight Graphene Honeycomb Sandwich for Stretchable Light - Emitting Displays. *Advanced Functional Materials* **2018,** *28* (19), 1707043.

151. Mannsfeld, S. C.; Tee, B. C.; Stoltenberg, R. M.; Chen, C. V. H.; Barman, S.; Muir, B. V.; Sokolov, A. N.; Reese, C.; Bao, Z., Highly sensitive flexible pressure sensors with microstructured rubber dielectric layers. *Nature Materials* **2010,** *9* (10), 859-864.

152. Tee, B. C. K.; Chortos, A.; Dunn, R. R.; Schwartz, G.; Eason, E.; Bao, Z., Tunable flexible pressure sensors using microstructured elastomer geometries for intuitive electronics. *Advanced Functional Materials* **2014,** *24* (34), 5427-5434.

153. Wang, Z.; Zhang, Q.; Yue, Y.; Xu, J.; Xu, W.; Sun, X.; Chen, Y.; Jiang, J.; Liu, Y., 3D printed graphene/polydimethylsiloxane composite for stretchable strain sensor with tunable sensitivity. *Nanotechnology* **2019,** *30* (34), 345501.

154. Zeng, X.; Wang, Z.; Zhang, H.; Yang, W.; Xiang, L.; Zhao, Z.; Peng, L.-M.; Hu, Y., Tunable, ultrasensitive, and flexible pressure sensors based on wrinkled microstructures for electronic skins. *ACS Applied Materials and Interfaces* **2019,** *11* (23), 21218-21226.

155. Tee, B. C.; Wang, C.; Allen, R.; Bao, Z., An electrically and mechanically self-healing composite with pressure-and flexion-sensitive properties for electronic skin applications. *Nature Nanotechnology* **2012,** *7* (12), 825.

156. Zou, Z.; Zhu, C.; Li, Y.; Lei, X.; Zhang, W.; Xiao, J., Rehealable, fully recyclable, and malleable electronic skin enabled by dynamic covalent thermoset nanocomposite. *Science Advances* **2018,** *4* (2), eaaq0508.

157. Lei, Z. Q.; Xie, P.; Rong, M. Z.; Zhang, M. Q., Catalyst-free dynamic exchange of aromatic Schiff base bonds and its application to self-healing and remolding of crosslinked polymers. *Journal of Materials Chemistry A* **2015,** *3* (39), 19662-19668.

158. Xia, N. N.; Xiong, X. M.; Wang, J.; Rong, M. Z.; Zhang, M. Q., A seawater triggered dynamic coordinate bond and its application for underwater self-healing and reclaiming of lipophilic polymer. *Chemical Science* **2016,** *7* (4), 2736-2742.

159. Boland, C. S.; Khan, U.; Ryan, G.; Barwich, S.; Charifou, R.; Harvey, A.; Backes, C.; Li, Z.; Ferreira, M. S.; Möbius, M. E., Sensitive electromechanical sensors using viscoelastic graphene-polymer nanocomposites. *Science* **2016,** *354* (6317), 1257-1260.

160. Kim, S. H.; Seo, H.; Kang, J.; Hong, J.; Seong, D.; Kim, H.-J.; Kim, J.; Mun, J.; Youn, I.; Kim, J.; Kim, Y.-C.; Seok, H.-K.; Lee, C.; Tok, J. B. H.; Bao, Z.; Son, D., An ultrastretchable and self-healable nanocomposite conductor enabled by autonomously percolative electrical pathways. *ACS Nano* **2019,** *13* (6), 6531-6539.

161. Wu, Q.; Xiong, H.; Peng, Y.; Yang, Y.; Kang, J.; Huang, G.; Ren, X.; Wu, J., Highly Stretchable and Self-Healing "Solid-Liquid" Elastomer with Strain-Rate Sensing Capability. *ACS Applied Materials and Interfaces* **2019,** *11* (21), 19534-19540.

162. Li, J.; Ma, P. C.; Chow, W. S.; To, C. K.; Tang, B. Z.; Kim, J. K., Correlations between percolation threshold, dispersion state, and aspect ratio of carbon nanotubes. *Advanced Functional Materials* **2007,** *17* (16), 3207-3215.

163. Kogut, P. M.; Straley, J. P., Distribution-induced non-universality of the percolation conductivity exponents. *Journal of Physics C: Solid State Physics* **1979,** *12* (11), 2151.

164. Shang, S.; Yue, Y.; Wang, X., Piezoresistive strain sensing of carbon black/silicone composites above percolation threshold. *Review of Scientific Instruments* **2016,** *87* (12), 123910.

165. Cassagnau, P., Payne effect and shear elasticity of silica-filled polymers in concentrated solutions and in molten state. *Polymer* **2003,** *44* (8), 2455-2462.

166. Yang, T.; Xie, D.; Li, Z.; Zhu, H., Recent advances in wearable tactile sensors: Materials, sensing mechanisms, and device performance. *Materials Science and Engineering: R: Reports* **2017,** *115*, 1-37.

167. Cipriano, B. H.; Kota, A. K.; Gershon, A. L.; Laskowski, C. J.; Kashiwagi, T.; Bruck, H. A.; Raghavan, S. R., Conductivity enhancement of carbon nanotube and nanofiber-based polymer nanocomposites by melt annealing. *Polymer* **2008,** *49* (22), 4846-4851.

168. Bilotti, E.; Zhang, H.; Deng, H.; Zhang, R.; Fu, Q.; Peijs, T., Controlling the dynamic percolation of carbon nanotube based conductive polymer composites by addition of secondary nanofillers: the effect on electrical conductivity and tuneable sensing behaviour. *Composites Science Technology* **2013,** *74*, 85-90.

169. Kraus, G. In *Mechanical losses in carbon-black-filled rubbers*, Journal of Applied Polymer Science: Applied Polymer Symposium, 1984; pp 75-92.

170. Salehuddina, S. M. F.; Hawajia, M. H.; Md, A. S.; Khana, B.; Mana, S. H. C.; Alib, W. K. W.; Baharulrazia, N., A Review of Recent Developments: Self-Healing Approaches for Polymeric Materials. *Chemcial Engineering Transactions* **2019,** *72*.

171. Krishnakumar, B.; Sanka, R. P.; Binder, W. H.; Parthasarthy, V.; Rana, S.; Karak, N., Vitrimers: Associative Dynamic Covalent Adaptive Networks in Thermoset Polymers. *Chemical Engineering Journal* **2019**, 123820.

172. Jehanno, C.; Sardon, H., Dynamic polymer network points the way to truly recyclable plastics. *Nature* **2019,** *568*, 467-468.

173. Long, K. N.; Dunn, M. L.; Scott, T. F.; Turpin, L. P.; Qi, H. J., Light-induced stress relief to improve flaw tolerance in network polymers. *Journal of Applied Physics* **2010,** *107* (5), 053519.

174. Johnson, L. M.; Ledet, E.; Huffman, N. D.; Swarner, S. L.; Shepherd, S. D.; Durham, P. G.; Rothrock, G. D., Controlled degradation of disulfide-based epoxy thermosets for extreme environments. *Polymer* **2015,** *64*, 84-92.

175. DiLauro, A. M.; Robbins, J. S.; Phillips, S. T., Reproducible and scalable synthesis of end-cap-functionalized depolymerizable poly (phthalaldehydes). *Macromolecules* **2013,** *46* (8), 2963-2968.

176. Fukuda, K.; Shimoda, M.; Sukegawa, M.; Nobori, T.; Lehn, J.-M., Doubly degradable dynamers: dynamic covalent polymers based on reversible imine connections and biodegradable polyester units. *Green Chemistry* **2012,** *14* (10), 2907-2911.

177. Chen, X.; Wudl, F.; Mal, A. K.; Shen, H.; Nutt, S. R., New thermally remendable highly cross-linked polymeric materials. *Macromolecules* **2003,** *36* (6), 1802-1807.

178. Burattini, S.; Greenland, B. W.; Merino, D. H.; Weng, W.; Seppala, J.; Colquhoun, H. M.; Hayes, W.; Mackay, M. E.; Hamley, I. W.; Rowan, S., A healable supramolecular polymer blend based on aromatic π-π stacking and hydrogen-bonding interactions. *Journal of the American Chemical Society* **2010,** *132* (34), 12051-12058.

179. Yoshie, N.; Watanabe, M.; Araki, H.; Ishida, K., Thermo-responsive mending of polymers crosslinked by thermally reversible covalent bond: Polymers from bisfuranic terminated poly (ethylene adipate) and tris-maleimide. *Polymer Degradation and Stability* **2010,** *95* (5), 826-829.

180. Burnworth, M.; Tang, L.; Kumpfer, J. R.; Duncan, A. J.; Beyer, F. L.; Fiore, G. L.; Rowan, S. J.; Weder, C., Optically healable supramolecular polymers. *Nature* **2011,** *472* (7343), 334-337.

181. Canadell, J.; Goossens, H.; Klumperman, B., Self-healing materials based on disulfide links. *Macromolecules* **2011,** *44* (8), 2536-2541.

182. Ji, S.; Cao, W.; Yu, Y.; Xu, H., Visible-light-induced self-healing diselenide-containing polyurethane elastomer. *Advanced Materials* **2015,** *27* (47), 7740-7745.

183. Lai, J.-C.; Li, L.; Wang, D.-P.; Zhang, M.-H.; Mo, S.-R.; Wang, X.; Zeng, K.-Y.; Li, C.-H.; Jiang, Q.; You, X.-Z., A rigid and healable polymer cross-linked by weak but abundant Zn (II)-carboxylate interactions. *Nature Communications* **2018,** *9* (1), 1-9.

184. Miwa, Y.; Taira, K.; Kurachi, J.; Udagawa, T.; Kutsumizu, S., A gas-plastic elastomer that quickly self-heals damage with the aid of CO 2 gas. *Nature Communications* **2019,** *10* (1), 1-6.

185. Page, M. I.; Jencks, W. P., Entropic contributions to rate accelerations in enzymic and intramolecular reactions and the chelate effect. *Proceedings of the National Academy of Sciences* **1971,** *68* (8), 1678-1683.

186. Åqvist, J.; Kazemi, M.; Isaksen, G. V.; Brandsdal, B. O., Entropy and enzyme catalysis. *Accounts of Chemical Research* **2017,** *50* (2), 199-207.

187. Belowich, M. E.; Stoddart, J. F., Dynamic imine chemistry. *Chemical Society Reviews* **2012,** *41* (6), 2003-2024.

188. Taynton, P.; Yu, K.; Shoemaker, R. K.; Jin, Y.; Qi, H. J.; Zhang, W., Heat-or Water-Driven Malleability in a Highly Recyclable Covalent Network Polymer. *Advanced Materials* **2014,** *26* (23), 3938-3942.

189. Kissounko, D. A.; Taynton, P.; Kaffer, C., New material: vitrimers promise to impact composites. *Reinforced Plastics* **2018,** *62* (3), 162-166.

190. Chakma, P.; Digby, Z. A.; Shulman, M. P.; Kuhn, L. R.; Morley, C. N.; Sparks, J. L.; Konkolewicz, D., Anilinium salts in polymer networks for materials with mechanical stability and mild thermally induced dynamic properties. *ACS Macro Letters* **2019,** *8* (2), 95-100.

191. Chang, P. S.; Buese, M. A., Silicone networks prepared via a living percolation mechanism: postgelation structure for networks with a variety of junction functionalities. *Journal of the American Chemical Society* **1993,** *115* (24), 11475-11484.

192. Osthoff, R.; Bueche, A.; Grubb, W., Chemical stress-relaxation of polydimethylsiloxane elastomers1. *Journal of the American Chemical Society* **1954,** *76* (18), 4659-4663.

193. Sigwalt, P.; Gobin, C.; Nicol, P.; Moreau, M.; Masure, M. In *Inhibiting or cocatalytic effect of water and other additives on cationic polymerization of cyclodimethylsiloxanes*, Makromolekulare Chemie. Macromolecular Symposia, Wiley Online Library: 1991; pp 229-240.